AQUEOUS FLUORIDE BIOSORPTION USING CALCIUM-SPIKED AND NON-SPIKED *Moringa oleifera* SEED POWDER: INFLUENCE OF DOSAGE, PARTICLE SIZE, AND PROCESS PARAMETERS

GEOFFREY CHAVAREGI

A THESIS SUBMITTED TO THE SCHOOL OF SCIENCE IN PARTIAL FULFILMENT OF THE REQUIREMENTS FOR THE CONFERMENT OF DOCTOR OF PHILOSOPHY IN CHEMISTRY OF THE UNIVERSITY OF ELDORET,

KENYA

2025

DECLARATION

Declaration by the Candidate

This thesis is my original work and has never been presented for the award of an academic degree in any other university and should not be copied, or reproduced in any format without written authority from the author and/or University of Eldoret.

_____ Date_____

Geoffrey Chavaregi

SSCI/CHE/P/001/20

Approval by the Supervisors

This thesis is submitted with our approval as the university supervisors.

_____ Date_____

Prof. John Kituyi Lusweti

School of Science

Department of Chemistry and Biochemistry

University of Eldoret, Kenya

_____ Date_____

Prof. Pius Keronei Kipkemboi

School of Science

Department of Chemistry and Biochemistry

University of Eldoret, Kenya

DEDICATION

To my dear wife, Nancy,who has silently watched me leave home time and again, wondering why her husband chooses the quiet corridors of learning over the warmth of home.

To my sons, Carsten, Ayden, and my daughter Lexie, whose innocent eyes have often asked without words, “Where does Daddy go, and why does he stay away so long?”

And to my youngest son, Roden,too small to understand, yet whose tiny hands remind me every day of the home I leave behind in pursuit of this dream.

ACKNOWLEDGEMENTS

I give glory to Almighty God for granting me the strength, grace, and wisdom to undertake and complete this study. This academic journey would not have been possible without divine providence, and I remain deeply grateful for the opportunities and guidance bestowed upon me throughout the process.

I am profoundly thankful to my dear wife, Nancy, whose unwavering encouragement, patience, and sacrifices provided the moral support I needed to persevere through challenging moments. To my beloved children, Carsten, Ayden, Lexie, and Roden, your love, understanding, and enthusiasm have been an incredible source of motivation. Thank you for enduring my long hours of study and research with grace and cheer.

My sincere and heartfelt appreciation goes to my supervisors, Prof. J. Lusweti and Prof. P. Kipkemboi. Your tireless guidance, insightful feedback, and continuous encouragement were invaluable in shaping and refining this thesis. Your commitment to academic excellence has inspired me and enriched my intellectual growth in countless ways.

I also extend my gratitude to the technical staff of the Department of Chemistry and Biochemistry, University of Eldoret, for their technical support during sample analysis. Your professionalism, timely assistance, and dedication ensured the smooth execution of the experimental phase of this research.

Special thanks are due to my fellow postgraduate students at the University of Eldoret for their camaraderie, stimulating discussions, and constructive peer reviews. Your academic insights and moral support significantly contributed to the success of this work.

To everyone who contributed directly or indirectly to this study, your support is deeply appreciated. May God richly bless you.

ABSTRACT

Excessive fluoride concentrations in drinking water pose serious public health risks, including dental and skeletal fluorosis, particularly in rural, semi-arid and arid regions of developing countries where groundwater is the primary source of potable water. Traditional defluoridation methods remain costly, chemically intensive, or environmentally unsustainable, prompting the search for low-cost, eco-friendly alternatives. *Moringa oleifera* seed powder (MOSP) has emerged as a promising biosorbent, though its native adsorption capacity remains limited. This study aimed to enhance fluoride removal efficiency by modifying MOSP with calcium (Ca-MOSP) and to evaluate the influence of key process parameters including adsorbent dosage,particle size,pH,contact time, temperature and initial fluoride concentration; adsorption equilibrium behaviour, kinetic rates, and thermodynamic properties. Batch experiments were conducted under controlled laboratory conditions using both calcium-spiked and non-spiked MOSP to assess the effect of dosage, particle size, contact time, pH, temperature, and initial fluoride concentration. The biosorption performance was analysed using Langmuir and Freundlich isotherm models, pseudo-first-order and pseudo-second-order kinetics, and thermodynamic parameters such as enthalpy (ΔH°), entropy (ΔS°), and Gibbs free energy (ΔG°). Results showed that calcium spiking significantly improved fluoride removal efficiency, with Ca-MOSP achieving over 90% removal under optimal conditions (2 g/50 mL dosage, 40 mesh size, pH 7-, and 120-minute contact time), compared to 78% for the non-spiked powder. Finer particle sizes led to increased surface area and binding site availability, while increased dosage improved performance up to a saturation threshold. Adsorption was found to be pH-dependent, with neutral pH offering the best removal efficiencies for both biosorbent types. The adsorption isotherm data fitted best with the Langmuir model, suggesting monolayer adsorption on homogeneous surfaces. Ca-MOSP exhibited a higher maximum adsorption capacity (q_e = 4.98 mg/g) and affinity constant (K_l = 0.442 L/mg) than the non-spiked variant. Kinetic data followed the pseudo-second-order model, indicating chemisorption as the dominant uptake mechanism, with high R^2 values (>0.99) and strong agreement between experimental and theoretical adsorption capacities. Thermodynamic analysis confirmed that biosorption was endothermic (ΔH° = +28.45 kJ/mol for Ca-MOSP), spontaneous (ΔG° < 0), and associated with an increase in system randomness (ΔS° = +85.6 J/mol·K). Thus, calcium-modified *Moringa oleifera* seed powder offers a significantly enhanced, sustainable, and low-cost alternative for fluoride remediation in drinking water. The findings support its potential for practical application in areas with fluoride endemism, particularly in rural and resource-limited settings. Recommendations include adopting Ca-MOSP in decentralised treatment systems and optimising operational conditions for field deployment. Future research should explore regeneration potential, competing ion effects, and long-term performance in continuous-flow and field-scale systems.

TABLE OF CONTENTS

LIST OF TABLES

LIST OF FIGURES

LIST OF ACRONYMS AND ABBREVIATIONS

AlDE	Aluminium modified *Dicerocaryum eriocarpum*
FT-IR	Fourier Transform Infrared spectrometer
HCl	Hydrochloric acid
ISE	Ion-selective electrode
MgDE	Magnesium modified *Dicerocaryum eriocarpum*
MOSP	*Moringa oleifera* powder
NaOH	Sodium hydroxide
NH_4^+	Ammonium
NO_3^-	Nitrate
Pty (Ltd)	Proprietary Limited
SEM-EDX	Scanning Electron Microscope - Energy Dispersive X-ray spectroscopy
TD	Thermal degradation
WHO	World Health Organisation
XRF	X-ray Fluorescence
XRD	X-ray Diffraction

CHAPTER ONE

1.0 INTRODUCTION

Fluoride is a naturally occurring element commonly found in the earth's crust, mainly in minerals such as fluorspar, cryolite, rock phosphate, and apatite (Prabhu *et al*., 2023). Natural geochemical processes like weathering and leaching make fluoride to dissolve from these minerals and enter groundwater, sometimes accumulating to levels above safe limits for drinking water. Geothermal actions and extended water–rock interactions, in many regions,further increase fluoride levels by releasing fluoride-rich minerals into aquifers (Chaudhuri *et al*., 2024). Fluoride concentrations in groundwater vary widely but often exceed the WHO guideline of 1.5 mg/L, with some areas reportedly having levels as high as 10–20 mg/L, especially where water movement is slow and evaporation rates are high. Other areas have reported values of up to 26 mg/L in some regions (Asmamaw *et al*., 2025).

In addition, human activities such as phosphate fertiliser use and emissions from industries like aluminium smelting and coal combustion contribute more fluoride to soils and water bodies (Lodh *et al*., 2025). Fluoride is highly stable and does not readily breakdown, therefore it can remain dissolved in aquifers for long periods, explaining the widespread occurrence of high fluoride levels in many regions, mostly in parts of the Rift Valley, India, and other semi-arid areas (Chowdareddy *et al*., 2023).

In trace amounts (≤1.5 mg/L), fluoride is helps in strengthening bones and teeth, as it helps form fluorapatite [$Ca_{10}(PO_4)_6F_2$], a compound more resistant to acid than

hydroxyapatite [$Ca_{10}(PO_4)_6(OH)_2$], thus protecting against tooth decay (Lubojanski *et al*., 2023; Prabhu *et al*., 2023). However, when taken in excess, fluoride's strong affinity for calcium leads to excessive deposition in bones and teeth, resulting in conditions like dental fluorosis, that is characterized by white streaks, pitting, and weakened enamel and skeletal fluorosis, whichleads to abnormal bone hardening, joint pain, stiffness, and even deformities (Rajak *et al*., 2023). In Excess, fluoride can also interfere with enzyme activity by forming strong bonds and complexes that inhibit proteins such as Na^+/K^+-ATPase, affecting nerve signals, cellular energy balance, and metabolic functions (Waugh, 2019; MDPI review, 2025). Recent research links long-term fluoride exposure to oxidative stress due to reactive oxygen species (ROS) production, which damages organs like the liver, kidneys, thyroid, and reproductive system (Turner *et al*., 2025).

Around the world, excessive fluoride contamination is a significant health issue, affecting both developing and developed regions. Approximately 200 million people around the globe are exposed to fluoride levels that exceed the World Health Organisation's recommended limit for safe drinking water (WHO, 2024). These regions include large parts of India, China, Sri Lanka, Turkey, the Middle East, and extensive areas across Africa (Chaudhuri *et al*., 2024). In India, for example, more than 17 states including Chhattisgarh, Kerala, Delhi, Haryana, and Jharkhand regularly report dangerously elevated groundwater fluoride levels that contribute to widespread cases of dental and skeletal fluorosis, osteoporosis, neurological disorders, parathyroid gland impairment, and emerging concerns over male infertility and thyroid and kidney dysfunction (Duvva *et al*., 2022; Baboo *et al*., 2022; Rajak *et al*., 2023). Studies carried out in rural and

peri-urban areas show that children and women are particularly most affected due to their dependence on untreated groundwater for daily consumption and food preparation (Baboo *et al*., 2022)). in the developed countries,too, this problem occurs. Industrial effluent, fertiliser runoff, and poorly managed waste from aluminum smelting and coal combustion have created localized fluoride hotspots in groundwater and surface water sources (FDAH, 2025). In places with intensive agriculture, overuse of phosphate fertilisers has also been linked to rising fluoride concentrations in shallow aquifers and streams, adding further stress to drinking water safety. With urban populations expanding and industrial activities increasing, the need for cost-effective, reliable defluoridation methods becomes even more critical to safeguard public health on a global scale.

Across Africa, fluoride contamination remains a big environmental and public health burden, especially in the Rift Valley of East Africa's , where volcanic geology and geothermal activity have increased fluoride concentrations in groundwater (Bianchini *et al*., 2025). Studies done in Ethiopia's Rift Valley have reported fluoride levels of 20–26 mg/L, far exceeding the WHO guideline (Bianchini *et al*., 2025). Such high fluoride concentration spots exist in northern Tanzania, some areas in Uganda, Sudan, Algeria, and northern Nigeria, where the rural populace depend a lot on untreated boreholes and shallow wells (Wambu *et al*., 2022; Chaudhuri *et al*., 2024). Surveys done in Ethiopia's Ziway and Shashemene regions continue to record high cases of dental and skeletal fluorosis in children, which leads to less school attendance and hence limits productivity (Asmamaw *et al*., 2025). In Tanzania, rural villages report joint pain and mottled teeth which are linked to daily consumption of high-fluoride water (Chaudhuri *et al*., 2024).

Lack of access to affordable defluoridation technologies and safe piped water means that millions remain exposed to health risks, highlighting the urgent need for cheaper , locally adaptable solutions.

In Kenya, the Rift Valley is one of Africa's most fluoride-endemic zones, where unique geological conditions and active geothermal processes naturally elevate fluoride levels in groundwater. Shallow wells and Boreholes used for domestic water supply regularly report fluoride concentrations of up to 20 mg/L, which surpass the WHO guideline of 1.5 mg/L for safe water for human consumption (Kenyan Rift Data, 2025). Endemic fluorosis remains a problem in counties such as Nakuru, Baringo, Kajiado, Elgeyo Marakwet and Samburu, where rural communities generally depend on groundwater for drinking, cooking, and for livestock (Wambu *et al*., 2022). In these places, visible signs of dental fluorosis among children and skeletal fluorosis in adults continue to be documented through community health surveys and local hospital reports. In spite of the government efforts to expand piped safe water networks and urban water treatment systems, significant fractions of the rural population still rely on untreated groundwater due to limited financial resources, poor public infrastructure, and the dispersed nature of settlements (Wambu *et al*., 2022). Seasonal droughts and poor rainfall patterns complicate more the dependence on the wells and boreholes that have high fluoride concentrations. This clearly indicates that there is the urgent need for practical, cost-effective, and locally adaptable defluoridation technologies that can be easily maintained by communities with minimal technical expertise and financial burden.

The Most commonly used fluoride removal methods such as ion exchange, precipitation–coagulation, membrane filtration, reverse osmosis, electrodialysis, and electrolytic defluoridation are technically proven and have shown high removal efficiencies under controlled laboratory and large scale conditions (Tolkou *et al*., 2021; Wan *et al*., 2023; Devasthali *et al*., 2024; Mousazadeh *et al*., 2021; Malalagama *et al*., 2022). Nonetheless, translating these techniques into sustainable community-scale solutions has proven challenging, especially in rural and low-income contexts. The systems typically require significant upfront capital investment for installation, reliable access to electricity or pressure pumps, skilled operators for routine monitoring and maintenance, and availability of replacement parts and consumables, all of which pose practical and financial barriers for households already facing economic constraints.

Additional to high operational and maintenance costs, most of these technologies generate hazardous wastes, brine concentrate, or spent media that must be safely handled, stored, or disposed of to prevent secondary environmental contamination (Smith *et al*., 2020). Insufficient local technical know-how, unreliable supply chains for spare parts, and seasonal variations in water quality further complicate regular operation (Kumar *et al*., 2021). These limitations have increased the push for affordable, robust, and community-friendly defluoridation methods that can be deployed with limited infrastructure and are easily adaptable to local conditions (Perez *et al*., 2023). As a result, researchers and policymakers are increasingly focusing on natural, low-cost biosorbents that harness locally available materials, require simple treatment steps, and minimise

waste, offering more sustainable and practical pathways for reducing excessive fluoride levels in drinking water at the household and community scale.

Moringa oleifera (MO) seeds are most favourable due their sustainability, local availability, and proven higher biosorption efficiency (Aboagye *et al*., 2021; Taiwo *et al*., 2020). The seeds of Moringa are very rich in functional including carboxyl, hydroxyl, and amino groups, which enable effective ion binding by surface complexation and ion exchange processes (Gomes *et al*., 2022). Fluoride ions interrract with active sites strongly, making the seeds to act as an environmentally friendly and biodegradable biosorbent material. Recent studies show that when MO seeds are modified by spiking them with calcium ions, their adsorption performance is greatly improved by creating additional active sites that bind fluoride forming insoluble complexes, thereby enhancing removal efficiency even at higher concentrations of the contaminants (Khader *et al*., 2022; Nguyen *et al*., 2024).

Fourier transform infrared spectroscopy (FTIR) and Scanning electron microscopy (SEM) have confirmed the presence and effectiveness of these active sites while revealing the seeds highly porous surface structure and diverse functional groups (Chowdareddy *et al*., 2023). Moringa tree parts like the leaves and the bark, have also demonstrated valuable adsorption properties, thanks to their lignocellulosic matrix, which provides large surface areas and a robust framework for pollutant adsorption. This versatility and bioactivity makes *Moringa oleifera be* described as a “multipurpose tree,” that is valued not only for its coagulant and anti oxidant capabilities but also for its

unique interparticle bridging and flocculation mechanisms that promote the aggregation and removal of suspended contaminants. Moringa oleifera has also proven that it's effective in biosorbing heavy metals and other emerging pollutants as an accessible, low-cost alternative to the synthetic or chemical adsorbents. This makes it a promising alternative for communities in fluoride-endemic regions where conventional treatments remain unaffordable (Oluwasanya *et al*., 2023).

Though there is laboratory evidence, there are knowledge gaps concerning how calcium modification influences the adsorption isotherms, kinetics, and thermodynamics of *Moringa oleifera* seeds when applied under varied and unpredictable real-life situations (Gai & Deng, 2021; Smith *et al*., 2025). When these parameters are well understood, it is easy to determine how well the biosorbent would interract with fluoride ions over time, how equilibrium isestablished, and how factors like reaction spontaneity and energy changes affect performance at larger scales. Factors of operation such as solution pH, contact time, ambient temperature, adsorbent dosage, particle size, and initial fluoride concentration controlled the speed and capacity of fluoride uptake as well as influencing the feasibility and repeatability of applying this method at household or community levels where water chemistry can vary seasonally or even daily (Khader *et al*., 2022). For instance, variations in groundwater pH can change the surface charge of the adsorbent and the ionisation state of fluoride, while temperature changes can shift the thermodynamic favourability of the reaction. Similarly, the optimising the dosage and particle size must ensure that there is balance of maximum fluoride removal with minimal resource input and manageable regeneration or disposal. These knowledge gaps

indicate that there is the need for more detailed experimental research that will bridge laboratory work with real field experience so as to generate design and operation models that can be relied on for cost-effective, scalable, and community-friendly biosorption systems.

Addressing these gaps, the present study investigated the comparative fluoride removal performance of calcium-spiked and non-spiked *Moringa oleifera* seed powder under systematically varied operational conditions. Specifically, it explored how key process variables such as pH, contact time, adsorbent dosage, particle size, initial fluoride concentration, and temperature jointly influence the adsorption isotherms, kinetics, and thermodynamics governing fluoride removal. By providing new data and mechanistic insights, this research aims to refine practical guidelines for preparing, modifying, and deploying *Moringa* seed biosorbents at household and community levels in some fluoride prone rural Kenya and similar fluoride-endemic regions (Smith *et al*., 2025). The findings are expected to inform policymakers, community water managers, and local innovators about cost-effective and adaptable defluoridation strategies, ultimately contributing to safer drinking water and improved public health in vulnerable areas where conventional water treatment remains out of reach.

1.2 Statement of the problem

Fluoride contamination in drinking water has emerged as a critical public health problem in Kenya, particularly in regions with naturally high geochemical fluoride levels that frequently exceed the WHO-recommended limit of 1.5 mg/L (WHO, 2017; Kiptoo,

2024). Prolonged consumption of such water leads to dental and skeletal fluorosis, contributing to severe health and socioeconomic challenges, including school absenteeism, reduced productivity, and long-term disabilities (Nelima *et al*., 2023). Rural communities in the Rift Valley, including Baringo, Nakuru, and Kajiado counties, face the greatest risk, with some boreholes and shallow wells recording concentrations up to 20 mg/L, over ten times the guideline, while relying heavily on untreated groundwater due to financial and infrastructural limitations (Wambu *et al*., 2022). Conventional defluoridation technologies, including reverse osmosis, ion exchange, and activated alumina, though effective, remain costly in terms of acquisition and running of the equipment , energy-intensive, and maintenance-demanding, producing waste streams that require specialised handling. These constraints make them unsuitable for sustained application in relatively poor rural settings (Khatkar & Nagpal, 2024; Tolkou *et al*., 2021). as a consequence, there is a pressing need for affordable, locally available, and eco-friendly defluoridation solutions that can function with minimal technicalities. Biosorption, an environmentally friendly method that employs the use of plant-based biomaterials to remove fluoride, offering a promising alternative. *Moringa oleifera* seeds, particularly, have shown potential because of their natural adsorptive and coagulative properties (Al-Jadabi *et al*., 2023). However, when unmodified, the seeds exhibit limited efficiency in fluoride removal but with chemical modifications, such as calcium spiking, their ion-binding capacity is enhanced (Shrestha, 2021). in spite of the encouraging laboratory findings, critical knowledge gaps remain regarding the chemical mechanisms through which calcium spiking alters surface functional groups and fluoride adsorption pathways under diverse operational conditions. Addressing this knowledge gap is vital.

An investigation of adsorption isotherms, kinetics, and thermodynamic behaviour of calcium-spiked *Moringa oleifera* seed powder can well reveal how process variables pH, contact time, particle size, dosage, initial fluoride concentration, and temperature affect biosorption efficiency (Gai & Deng, 2021). This study clarifies these mechanisms and identifies optimal biosorption conditions, aiming to generate evidence to inform scalable, community-based, and low-cost defluoridation strategies for rural Kenya and other fluoride-endemic regions.

1.3 Objectives

1.3.1 Broad Objective

To evaluate the effectiveness of chemically modified (calcium-spiked) *Moringa oleifera* seed powder in removing fluoride from aqueous solutions under varying conditions relevant for community-level defluoridation in fluoride-endemic regions.

1.3.2 Specific Objectives

i. To determine the fluoride removal efficiency of calcium-spiked and non-spiked *Moringa oleifera* seed powder.
ii. To determine the effect of key process parameters, including biosorbent dosage and particle size, on fluoride biosorption performance.
iii. To determine how solution pH, contact time, temperature, and initial fluoride concentration influence the adsorption capacity of calcium-spiked versus non-spiked *Moringa oleifera* seed powder.
iv. To establish the adsorption isotherms and kinetic models that describe the

biosorption of fluoride ions by spiked and non-spiked *Moringa oleifera* seed powder, with emphasis on understanding the underlying chemical mechanisms.

v. To determine the thermodynamic parameters (enthalpy, entropy, and Gibbs free energy changes) of fluoride biosorption by calcium-spiked and non-spiked *Moringa oleifera* seed powder.

1.4 Null Hypotheses

H_{01}: There is no significant difference in the fluoride removal efficiency between calcium-spiked *Moringa oleifera* seed powder and non-spiked *Moringa oleifera* seed powder.

H_{02}: Adsorbent dosage and particle size have no significant effect on the fluoride removal efficiency of Moringa *oleifera* seed powder.

H_{03}: Process parameters (pH, contact time, temperature, adsorbent dosage, and initial fluoride concentration) do not have a significant influence on the fluoride removal efficiency of calcium-spiked and non-spiked *Moringa oleifera* seed powder.

H_{04}: The biosorption of fluoride by powdered *Moringa oleifera* seeds and calcium-spiked powdered Moringa *oleifera* seeds does not follow any specific adsorption isotherm or kinetic model.

H_{05}: There are no significant differences in the thermodynamic parameters (enthalpy, entropy, and Gibbs free energy changes) of fluoride biosorption between calcium-spiked and non-spiked *Moringa oleifera* seed powder.

1.5 Justification of the study

Firstly, fluoride contamination remains a severe and persistent public health problem in many parts of Kenya, especially in the Rift Valley counties, where natural geochemical processes elevate fluoride levels in groundwater far above the WHO guideline of 1.5 mg/L. Excessive exposure to fluoride causes dental and skeletal fluorosis, which impairs health, limits levels of production thus straining rural livelihoods. Conventional defluoridation technologies, including reverse osmosis and ion exchange, are often un-affordable, technically demanding, and unsustainable for widespread use in low-income communities. This study is therefore justified as it explores an affordable, locally available, and community-friendly biosorption solution using *Moringa oleifera* seeds which is naturally abundant and easily accessible in Kenya.

Secondly, when *Moringa oleifera* seed powder is used as a biosorbent, it represents a practical innovation when enhanced through chemical modification. Spiking with Calcium increases the fluoride removal capacity by introducing additional active binding sites. This spiking improves the efficiency beyond that of unmodified seeds. For the best results, the study systematically examines the underlying chemical processes of the adsorption process, focusing on critical factors like adsorbent dosage, particle size, pH, contact time, initial fluoride concentration, and temperature. Data generated from the adsorption isotherms, kinetics, and thermodynamic provides essential scientific evidence for designing practical, cost-effective water treatment systems that rural communities can benefit from.

Thirdly, this research supports Kenya's national goal of ensuring safe drinking water for all as is enshrined in the water act of 2024, Africa water vision 2063 and policy(AWVP2063) and the UN sustainable development goals (SDGs), by contributing a sustainable, low-cost, and environmentally friendly technology that can be scaled up or adapted for local use. The findings will guide the development of community-based defluoridation units, reduce dependence on imported technologies, and strengthen local capacity for water treatment innovation. Moreover, the knowledge produced will fill critical gaps in the literature on biosorption chemistry and expand the practical application of plant-based adsorbents for fluoride removal, directly benefiting communities most affected by endemic fluorosis.

1.6. Significance of the study

This study makes an important scientific contribution to the understanding of how plant-based biosorbents can be chemically modified to improve the removal of fluoride ions from contaminated water. By investigating the adsorption behaviour, isotherms, kinetics, and thermodynamic parameters of calcium-spiked *Moringa oleifera* seed powder, the research deepens the knowledge of adsorption chemistry and surface interaction mechanisms, which are fundamental for designing effective, low-cost water treatment technologies. These insights will add to the growing field of green chemistry solutions for water purification, which is vital as communities worldwide seek affordable and sustainable alternatives to conventional, often expensive and energy-intensive methods like reverse osmosis and ion exchange.

By generating locally relevant evidence on how to optimise dosage, particle size, pH, contact time, and initial fluoride concentration for maximum fluoride removal, the research provides practical knowledge that stakeholders, including policy makers, Non-governmental organisations (NGOs), and rural water service providers, can apply in scaling up community-level defluoridation systems.

1.7. Scope of the Study

This study is limited to investigating the removal of fluoride ions from aqueous solutions using chemically modified *Moringa oleifera* seed powder, specifically focusing on the effectiveness of calcium-spiked and non-spiked seed powders under controlled laboratory conditions. The research examines the influence of key operational parameters, including adsorbent dosage, particle size, initial fluoride concentration, solution pH, contact time, and temperature, on the biosorption process.

The study further explores the adsorption isotherms, kinetics, and thermodynamic properties to understand the mechanisms that govern the interaction between fluoride ions and the biosorbent material. The scope does not extend to field trials or pilot-scale implementation but generates essential baseline data needed to inform the design and development of community-level defluoridation systems in fluoride-endemic regions of Kenya.

Geographically, the study focuses on fluoride contamination challenges relevant to Kenya's Rift Valley counties such as Nakuru, Baringo, Kajiado, Elgeyo Marakwet, and Samburu, where excessive natural fluoride levels in groundwater pose significant public

health risks. However, the findings have broader applicability to other fluoride-affected regions with similar geochemical and socio-economic contexts.

The research confines itself to laboratory-scale synthetic water samples to maintain controlled experimental conditions. It does not investigate the removal of other co-occurring contaminants or the regeneration and reuse potential of the spent biosorbent, which may be addressed in future studies. This scope ensures that the study remains focused on demonstrating the fundamental adsorption capacity and chemical performance of calcium-spiked *Moringa oleifera* seeds as a low-cost, locally available biosorbent for potential community-level application.

CHAPTER TWO

2.0 LITERATURE REVIEW

2.1 Introduction

Access to clean drinking water is a basic human right and a critical factor for public health and socio-economic development. Yet millions of people globally are affected by groundwater contaminated with naturally occurring or anthropogenically introduced fluoride. The unique chemical properties of fluoride ions, including their small ionic radius, high electronegativity, and affinity for calcium-rich minerals, make fluoride both beneficial and harmful depending on its concentration. Understanding the chemistry behind fluoride occurrence, transport, and removal is, therefore, essential for designing sustainable defluoridation strategies. This literature review synthesises global, regional, and local perspectives on fluoride contamination and removal, and sets the stage for investigating calcium-spiked *Moringa oleifera* seeds as a locally viable biosorbent.

2.2 Background on Fluoride Contamination

Fluoride is among the most common ions naturally occurring in groundwater worldwide, mainly due to the geochemical weathering of fluoride-bearing minerals such as fluorspar (CaF_2), cryolite (Na_3AlF_6), and apatite [$Ca_5(PO_4)_3F$]. As rainwater infiltrates rock formations rich in these minerals, chemical dissolution processes release fluoride ions into aquifers (Prabhu *et al.*, 2023). Regions characterised by prolonged water–rock interaction, high evaporation rates, and limited aquifer recharge often develop naturally high fluoride concentrations that exceed the WHO recommended limit of 1.5 mg/L (WHO, 2024). Where calcium ions are scarce, fluoride persists in solution because

insufficient precipitation as insoluble calcium fluoride (CaF_2) occurs (Chowdhury *et al.*, 2024). While this general pattern is well documented, many regional hydrogeological variations remain under-explored, and differences in mineralogy that affect fluoride release rates are not always quantified in many studies.

Beyond natural geochemical sources, anthropogenic activities increase fluoride contamination in many parts of the world. Intensive use of phosphate fertilisers, emissions from aluminium smelters, ceramic and glass manufacturing, and fly ash deposition from coal burning all add extra fluoride to soils and groundwater (Lodh *et al.*, 2025). The chemical mobility of fluoride ions in the subsurface strongly depends on local conditions, especially pH, ionic strength, and competing ions, which determine whether fluoride remains dissolved or precipitates out. However, the evidence base often does not distinguish between point-source discharges and diffuse agricultural runoff, nor does it adequately quantify how anthropogenic sources compare to natural loading in specific contexts.

Globally, fluoride contamination of drinking water has become an urgent environmental and public health challenge, with an estimated 200 million people exposed to concentrations above safe limits in over 100 countries (Yadav *et al.*, 2023). The global burden is concentrated in parts of Asia, Africa, and Europe where high-grade metamorphic rocks, geothermal activity, or volcanic geology naturally enrich aquifers with fluoride. Figure 2.1 illustrates the widespread distribution of these high-fluoride zones worldwide, showing that countries such as India, China, Bangladesh, Iran, Mexico,

and regions of Eastern Europe frequently report levels well above safe thresholds (Solanki *et al.*, 2022; Mannzhi, 2022). Yet, the broad global perspective still lacks recent and comparable national monitoring data for some under-reported regions, and further clarity is needed to separate natural geogenic hotspots from those where contamination is amplified by poor waste management or fertiliser overuse.

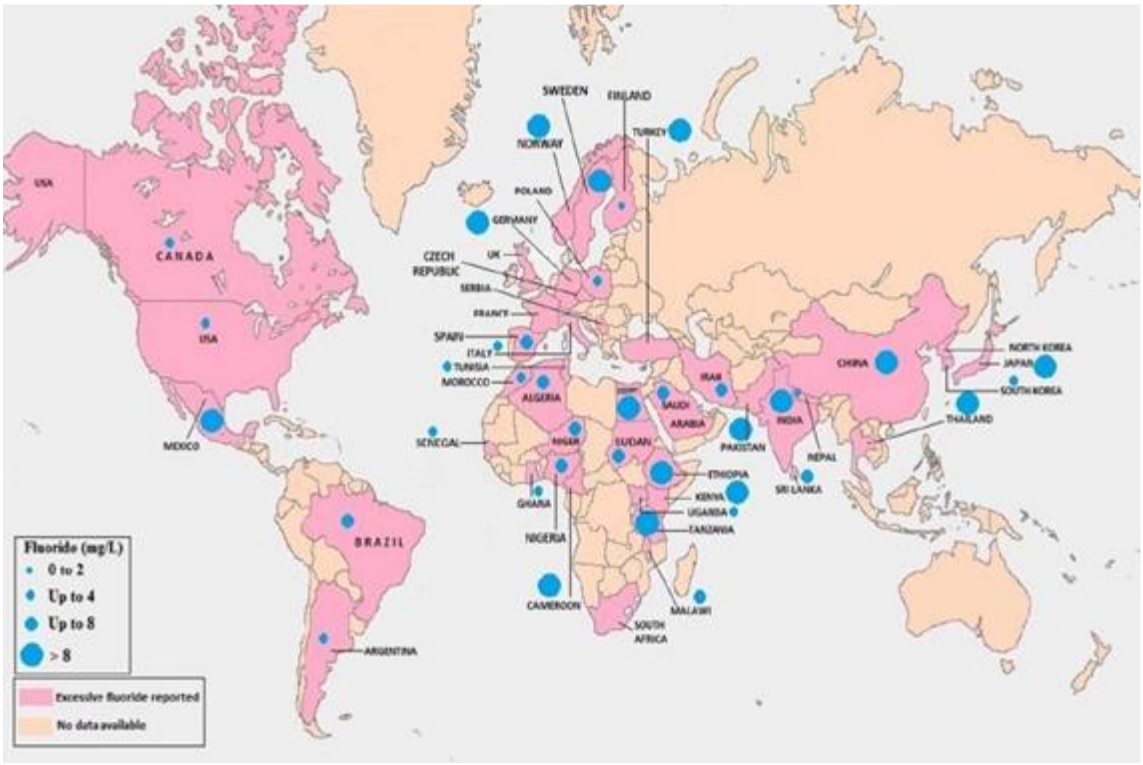

Figure 2.1: Fluoride concentrations across the globe

Source: Yadav *et al*. (2023)

India remains among the worst-affected nations, with more than 20 states facing chronic fluoride contamination of groundwater and an estimated 65 million people exposed to unsafe levels (Kisku & Sahu, 2020). In China, the problem is similarly widespread in arid northern provinces and near volcanic belts (Mannzhi, 2022). Elevated fluoride levels have also been recorded in parts of Europe, such as Sweden and Moldova, where local geochemical conditions naturally increase groundwater fluoride (Mazukhina *et al.*, 2024). Such evidence demonstrates that fluoride contamination is not confined to the Global South but is a broader hydrogeological phenomenon. However, these country-level reports rarely provide consistent cross-country comparative data on severity or treatment capacity, and little is known about how variations in local governance affect whether high fluoride levels persist untreated.

Across Africa, fluoride contamination is largely concentrated within the East African Rift Valley, a major geological feature stretching from Malawi through Tanzania and Kenya to Ethiopia and Eritrea (Bianchini *et al.*, 2020). The Rift's volcanic and geothermal activity, combined with extended water–rock contact and strong evaporation, naturally concentrates fluoride ions in aquifers. For example, boreholes in Ethiopia's Rift Valley frequently record concentrations above 5–10 mg/L, with some sites exceeding 20 mg/L (Kazapoe *et al.*, 2024). In Tanzania's Arusha and Singida regions, endemic fluorosis remains widespread because rural communities depend heavily on untreated borehole water (Onipe *et al.*, 2020). Figure 2.2 highlights these hotspots across Africa, with the East African Rift standing out as the region's principal fluoride risk zone. However, such

assessments often overlook local defluoridation efforts that do exist and rarely address the management challenges that arise when aquifers cross national borders.

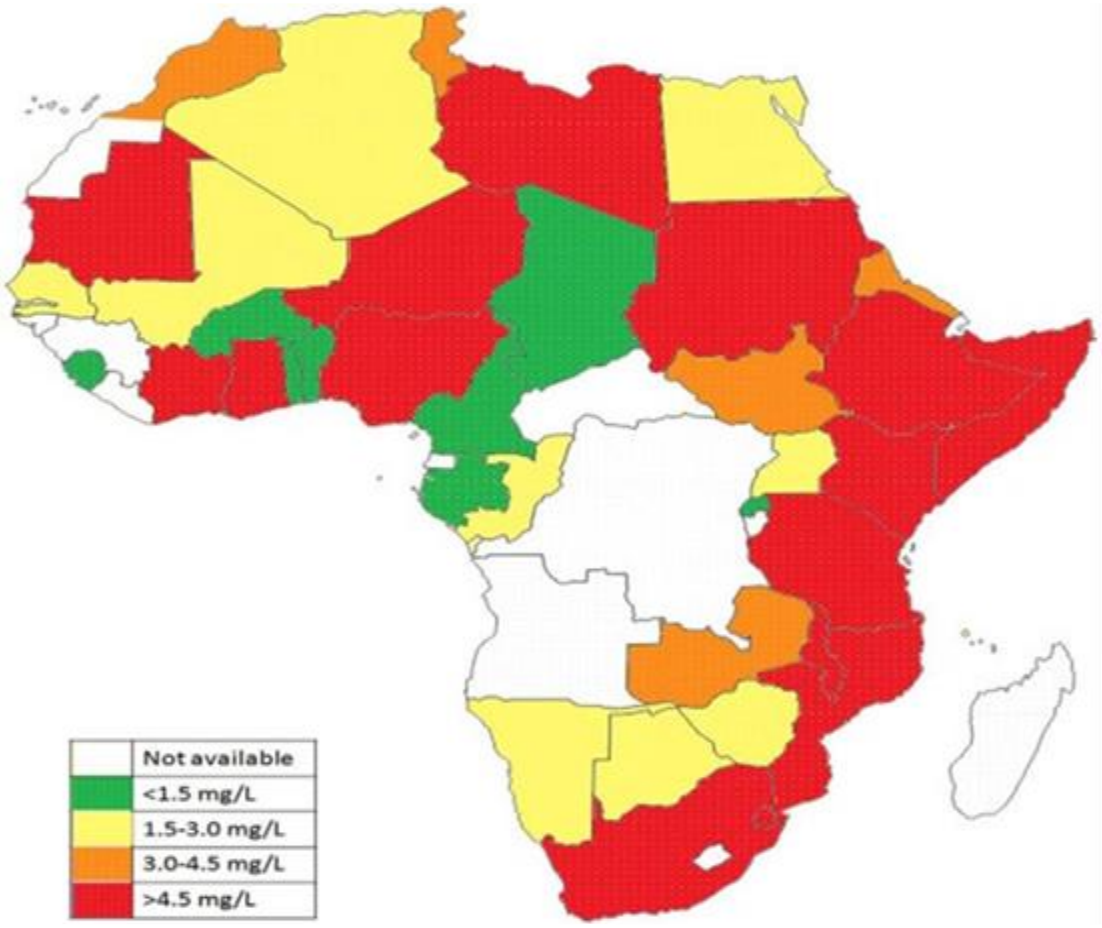

Figure 2.2: Fluoride levels across the African continent

Source: (Mannzhi, 2022).

Kenya exemplifies the intersection of natural geological risk and water management gaps that sustain high fluoride levels in groundwater. Counties such as Nakuru, Baringo, Kajiado, Elgeyo Marakwet, and parts of Samburu sit on Rift Valley volcanic belts where

groundwater commonly tests at 5–20 mg/L, far exceeding WHO's guideline of 1.5 mg/L (Wambu *et al.,* 2022). In addition to natural enrichment, mismanaged disposal of industrial effluents and overuse of fluoride-containing fertilisers and pesticides further elevate local concentrations (Yadav *et al.*, 2023). Localised spikes can also occur through accidental overdosing in water treatment plants or leaching from improperly disposed of industrial waste (Xiang, 2024; Basu, 2024). Figure 2.3 shows that these Kenyan Rift Valley zones remain among Kenya's highest-risk areas for fluoride contamination, with many rural communities still reliant on untreated groundwater.

Despite the well-established understanding of fluoride's geogenic sources and the additional impact of poorly managed anthropogenic activities, the challenge of high fluoride concentrations in drinking water remains unresolved in many parts of Kenya and similar regions worldwide. Communities in the Rift Valley counties, including Nakuru, Baringo, Kajiado, Elgeyo Marakwet, and Samburu, continue to rely heavily on boreholes and shallow wells with fluoride levels that often exceed safe limits by factors of five to ten (Wambu *et al.*, 2022). These regions are persistent fluoride hotspots. While natural weathering, geothermal activity, and runoff from fertilisers are well known to elevate fluoride levels, effective mitigation measures and affordable defluoridation technologies have not kept pace with the need. Many rural communities still lack access to practical water treatment systems, and accidental spikes from poorly managed waste or industrial processes further worsen the problem (Bianchini *et al*., 2024). This continuing challenge underscores a clear research gap: there is an urgent need to develop simple, low-cost, and

locally adaptable fluoride removal solutions to ensure safe drinking water and protect public health in high-risk areas.

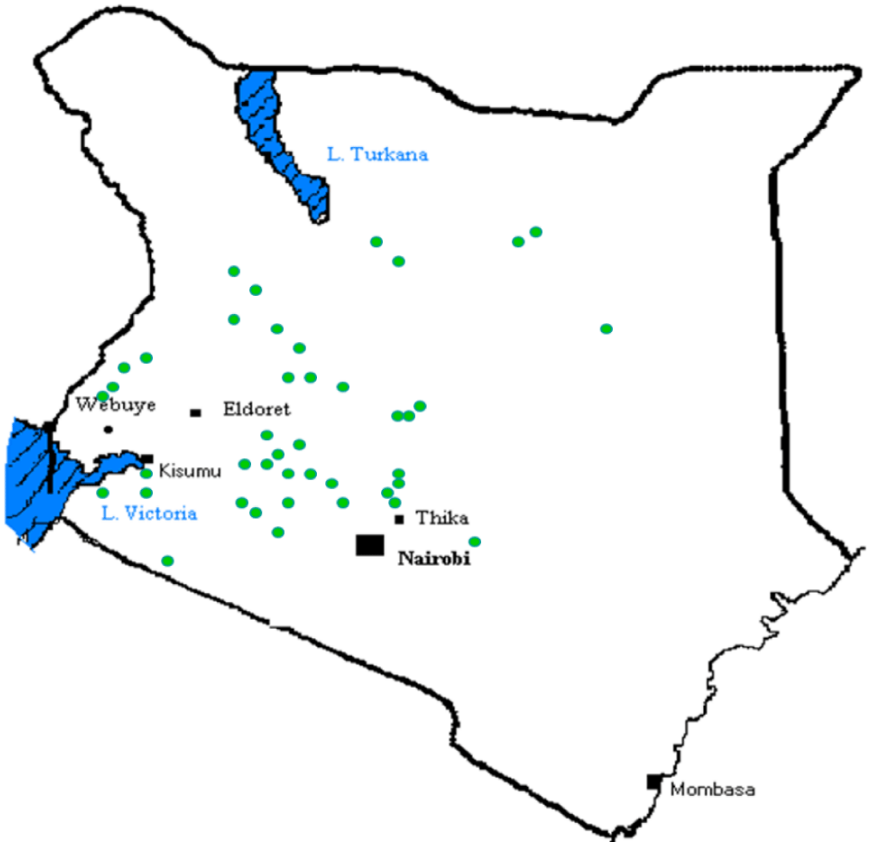

Figure 2.3: Map of Kenya showing areas with high fluoride concentration in water (green dots).

Source :Yadav *et al*. (2023)

2.3 Fluoride in Water Sources

Groundwater is a major source of drinking water globally, and its fluoride content is a key factor in determining water quality and public health (Sharma *et al*., 2023). Naturally, groundwater can accumulate fluoride when it interacts with fluoride-bearing minerals such as fluorite (CaF_2), biotite, and apatite over prolonged periods under high

pH and temperature (Ouedraogo *et al*., 2024). Mwiathi *et al*. (2022) reported that groundwater in can exceed 2 mg/L of fluoride, well beyond the WHO guideline of 1.5 mg/L. This is attributed to the weathering of volcanic rocks, long groundwater residence times, and alkaline geochemical conditions. While these studies provide valuable hydrogeochemical insights, many focus on limited geographic areas and lack temporal monitoring to capture seasonal variations in fluoride concentrations.

In arid and semi-arid regions, naturally high fluoride levels are further intensified by high evaporation rates and low aquifer recharge, leading to concentrated dissolved solids (Dong *et al*., 2022). He *et al*. (2020) documented fluoride concentrations exceeding 5 mg/L in arid areas of China, including the Loess Plateau and Inner Mongolia, where water scarcity and slow aquifer renewal amplify fluoride accumulation. These trends are mirrored in regions across Africa and South Asia, where communities depending on such groundwater are highly vulnerable. Most of these studies emphasise geochemical mechanisms but provide limited exploration of socio-hydrological factors, such as how local water-use practices and well depth influence exposure levels. Moreover, few incorporate longitudinal data to assess the impact of climate variability on fluoride mobilisation.

Similar patterns emerge in South Asia. Yadav *et al*. (2023) observed groundwater fluoride concentrations ranging from 1.8 to 12.4 mg/L in Rajasthan, India, with deeper borewells accessing older, mineral-rich aquifers often yielding higher concentrations. The study further highlights that alkaline pH, low calcium concentrations, and high

bicarbonate levels increase fluoride solubility because the precipitation of insoluble fluorite (CaF_2) is suppressed (Li *et al*., 2022). This aligns with global hydrogeochemical observations that aquifers with low calcium and high pH are more vulnerable to fluoride enrichment. While these studies describe chemical processes comprehensively, they often rely on cross-sectional snapshots, which limit understanding of long-term fluoride dynamics. Furthermore, the interaction between anthropogenic activities and natural fluoride mobilisation is insufficiently addressed in many South Asian studies.

Understanding the spatial and temporal variability of fluoride is critical for effective defluoridation planning and water safety management (Sharma *et al*., 2023). Sunkari *et al*. (2022) emphasise the need for integrated risk assessments that consider both natural and human-induced sources. These approaches can improve prioritisation of interventions in the highly affected regions. Inspite of these recommendations, few studies implement continuous monitoring or integrate socio-economic data into risk mapping. As a result, realistic decision-making for defluoridation or alternative water supply development remains under-informed in many high-risk areas.

Surface water bodies, rivers, lakes, and reservoirs in general contain lower fluoride concentrations than groundwater. This is due to shorter water–rock interaction times. However, they can still be carriers of fluoride from both geogenic and anthropogenic sources. Industrial wastes, especially from aluminium, glass, and ceramic manufacturing, have contributed significantly when their wastewater is discharged untreated into surface water bodies (Akh Baboo *et al*., 2022). Untreated wastewater not only increases fluoride

levels but also diminishes aquatic life health and the potability of the water for local communities. Industrial contributions are well-documented, but most studies lack basin-scale assessments to quantify cumulative impacts from multiple pollution sources or seasonal variations in contamination levels.

Surface water fluoride is not as often reported as groundwater fluoride, but notable cases exist. For instance, in China's Yuncheng Basin, the surface water fluoride levels ranged from 0.32 to 15.36 mg/L, with higher values linked to reservoirs and lakes caused by anthropogenic leaching (Liu *et al*., 2020). In Sweden, the Kärrsvik stream recorded 4.2 mg/L, mostly from granite rock weathering during rainfall seasons (Mannzhi, 2022). Similar observations have been made in East Africa where groundwater-fed streams can intermittently raise fluoride levels in surface waters during dry seasons (Onipe *et al*., 2020). Most of these studies are local based and lack long-term hydrological monitoring, making it difficult to generalise the trends or assess the sustainability of water quality under climate and land-use changes.

Agricultural activities have also contributed to fluoride contamination through diffuse runoff, in particular from phosphate fertilizers and some pesticides (Kumar *et al*., 2021). Atmospheric deposition from coal burning and industrial emissions indirectly contaminate water through runoff and direct deposition (Khatkar & Nagpal, 2024). These non-point sources, although individually less concentrated, have cumulative effect across large catchments. The contributions of agricultural versus industrial sources remain poorly documented in most regions, representing a significant gap for catchment-level

water quality modeling. Furthermore, studies rarely integrate land-use data to link agricultural intensity with observed surface water fluoride levels.

Geologic processes in nature including weathering of fluoride-rich rocks, influence surface water fluoride concentrations (Al-Jadabi *et al*., 2023). During dry spells, baseflow from high-fluoride groundwater can increase fluoride in rivers and streams (Onipe *et al*., 2020). Regular monitoring of fluoride in surface water is thus essential in taking care of peoples health and aquatic ecosystems (Sharma *et al*., 2023). as much as the importance of regular monitoring is clear, few studies have investigated the environmental impacts beyond human consumption. Research on bioaccumulation in aquatic species or its potential to disrupt ecosystem services is limited and this is leaves an important knowledge gap in environmental risk assessment.

2.4 Fluoride Removal from Water

2.4.1 Fluoride Removal Chemical Principles

Fluoride remains one of the most widespread ions naturally present in groundwater systems across the globe, chiefly due to the chemical weathering of fluoride-rich minerals such as fluorspar (CaF_2), cryolite (Na_3AlF_6), apatite [$Ca_5(PO_4)_3F$], and topaz [$Al_2(SiO_4)(FOH)_2$] (Onipe *et al.*, 2020). Precipitation infiltrates geological formations of minerals, leading to the release of fluoride ions (Prabhu *et al.*, 2023). Regions with extended water–rock contact, alkaline pH, and limited recharge tend to accumulate fluoride well beyond the World Health Organisation's safe drinking water limit of 1.5 mg/L (WHO, 2024). Notably, when calcium concentrations are insufficient to form insoluble calcium

fluoride (CaF_2) precipitates, fluoride stays in solution for prolonged periods (Chowdhury *et al.*, 2024). Acquifers, mostly those of granitic, volcanic, or certain sedimentary rocks, act as constant fluoride sources (Mukherjee & Singh, 2020). Freshwater , rainwater, and saltwater are likely to contain trace fluoride levels depending on local geochemistry (Jannat *et al.*, 2022). in spite of the extensive mapping, some regional aquifers are still under-monitored, leaving local communities vulnerable to undetected exposure levels. Mos tof the hydrogeochemical models used to predict fluoride distribution still oversimplify mineralogical differences that influence dissolution rates. Moreover, groundwater assessments often don't put into account seasonal hydrological fluctuations that can alter solubility dynamics and ion mobility, creating blind spots in risk mapping.

As much as geology remains the dominant driver, anthropogenic activities have increasingly intensified fluoride concentrations in many regions, adding chemical complexity to already vulnerable groundwater systems (Jha & Tripathi, 2021). Industrial effluents contribute a lot , with plants for phosphate fertiliser, aluminium smelting operations, and glass manufacturing all producing fluoride-rich waste streams that can get into soil and seep into aquifers (Olejarczyk *et al.*, 2022; Sinharoy & Chung, 2024). Coal-burning power plants and mining operations, especially those extracting phosphate rock or other fluoride-bearing ores, release fluoride through wastewater and airborne emissions that settle back into surface waters (Saini & Agrawal, 2021). Runoff from agricultural land treated with phosphate fertilizers or fluorine-based pesticides further compounds the problem by introducing trace fluoride into water bodies through leaching and surface flow (Craswell, 2021; Wang *et al.*, 2023). Regulatory oversight and

wastewater treatment infrastructure often lag behind industrial and agricultural expansion, leaving gaps that allow persistent fluoride pollution. This intersection of natural and human-induced fluoride loading underscores the pressing need for reliable monitoring and removal technologies that can adapt to diverse chemical conditions.

To address fluoride excess, conventional chemical methods have relied on principles of solubility and ion exchange. Precipitation–coagulation typically uses calcium or aluminium salts to produce insoluble fluoride compounds that can be removed through sedimentation or filtration (Prabhu *et al.*, 2024). Swapping of fluoride ions for chloride, hydroxide, or bicarbonate ions occurs in ion exchange resins under controlled pH, using functionalised polymer beads designed for selective affinity (Wan *et al.*, 2023). Reverse osmosis and nanofiltration, which are membrane processes, physically separate fluoride ions based on molecular size and charge differences, driven by high-pressure gradients (Khan *et al.*, 2022). These processes reflect sound chemical separation logic, but they often receive limited scrutiny regarding the downstream chemical changes they induce, such as unexpected pH changes or residual ion concentrations fluctuations , which can affect water potability. Furthermore, practical assessments sometimes underrepresent the implications of brine disposal or the cumulative energy demand that membrane technologies require.

Communities most affected by fluoride, find the cost and technical demands of conventional chemical treatment as major obstacles. Precipitation systems produce sludge that contains concentrated fluoride, which must be handled and disposed of to prevent re-

entry into soil and water (Chowdhury *et al.*, 2024). For Ion exchange units, there is need for routine regeneration with acids or bases, which create a chemical handling burden for operators in rural settings (Wambu *et al.*, 2022). In spite of all these known constraints, how these waste streams are treated or reused is rarely a discussion in field implementation reports. Similarly, detailed chemical pathways for safe recovery or neutralisation of residuals are often simplified, leaving gaps in sustainability planning.

The increasing attention to sustainable chemistry has increased interest in biosorption as an alternative method of fluoride remediation in water. Biosorption relies on the presence of naturally occurring functional including carboxyl, hydroxyl, phenolic, and amine moieties within the biomass that can bind fluoride ions by surface complexation, ion exchange, hydrogen bonding and weak van der Waals interactions (Taiwo *et al.*, 2020). At a molecular point of view, these interactions depend on surface charge distribution, the solution pH, and the presence of other ions that can compete for the same sites (Li *et al.*, 2023). The broad chemical mechanisms are well established in laboratory studies but detailed molecular-level descriptions, especially for real groundwater with mixed contaminants, are still lacking. Additionally, more comparative work is needed to determine how different biosorbent functional groups react under dynamic water chemistries.

Biosorption efficiency is best understood through established chemical models. Equilibrium isotherms, particularly Langmuir and Freundlich models, estimate how fluoride ions partition between solution and solid phases at equilibrium (Wan *et al.*,

2023). The Langmuir model normally assumes that there are uniform binding sites and monolayer adsorption, while the Freundlich approach assumes surface heterogeneity and variable binding energies (Taiwo *et al.*, 2020). Kinetic studies are used to describe how quickly fluoride binds under given conditions, distinguishing between physisorption controlled by weak intermolecular forces like Van der Waals and chemisorption, which involves stronger valence interactions. Most of the studies present detailed isotherm fits and kinetic rate constants, yet these results often remain disconnected from real-life reactor design. For instance, translating batch-derived constants into full-scale continuous systems still lacks a robust demonstration. Again, the influence of competing ions, flow regimes, and fluctuations in temperature or pH on these kinetic rates often goes underexplored.

Thermodynamic parameters including Gibbs free energy (ΔG), enthalpy (ΔH), and entropy (ΔS) are used to clarify the energetic favorability of fluoride binding (Kisku & Sahu, 2020). A negative ΔG means that the process is spontaneous, while a positive ΔH implies an endothermic adsorption that may be favoured at a higher temperature due to increased molecular movement and more active sites becoming available for biosorption (Kazapoe *et al.*, 2024). Entropy changes show structural rearrangements due to water molecules being displaced from the biosorbent's surface to create space for fluoride ions. In spite of all these, many published thermodynamic studies remain limited to narrow, controlled batch tests, leaving uncertainty about how these principles apply under fluctuating field conditions, such as seasonal temperature changes or varying ion

strengths. How entropy and enthalpy values derived under laboratory purity translate to water containing organic matter and other anions is one other aspect that is overlooked.

biosorption chemistry has made it an attractive for low-cost, decentralized fluoride removal strategies. It's founded on principles of ion exchange, complexation, and electrostatic interactions aligning well with green chemistry goals to use renewable, low-impact materials. However, to advance this potential requires that we bridge knowledge from laboratory findings to practical system engineering, especially to surface modification, regeneration, and long-term stability under actual groundwater conditions. Studies that have been published provide strong single-factor results but fail to connect multi-factor interactions that would reveal real-world system behaviour. There is also the scope to deepen the understanding of how local geochemical factors including carbonate or sulfate levels, influence the binding sites competition and the long-term sorption capacity.

One other critical aspect that influences fluoride removal efficiency is the surface charge chemistry of the sorbent material and the species of fluoride ions in varying pH conditions. The point of zero charge (pHpzc) is a chemical property that gives the pH at which an adsorbent's surface has no net electrical charge (Onipe *et al.*, 2021). When the pH of the solution drops to a lower level than the pHpzc, the sorbent surface becomes positively charged, enhancing the electrostatic attraction of negatively charged fluoride ions. On the contrary,, at pH values above the pHpzc, the surface develops a net negative charge that can repel fluoride anions, decreasing the overall adsorption efficiency. This

acid–base surface behaviour is significant in any ion-exchange or complexation-based removal mechanism.

In natural groundwater, fluoride usually remains as free F^- ions but under acidic conditions, it partially converts into weak complexes such as hydrofluoric acid (HF) or difluoride (H_2F_2) (Wan *et al.*, 2023). These species interact in different ways with the sorbent surface, hence making the removal pathway to change from pure electrostatic adsorption to mixed mechanisms which involve ion exchange or surface complexation. Most of the laboratory trials, however, assume that only the free ions dominate, ignoring how changing speciation affects its how it is applied in real-world. In spite of its central importance, surface charge behaviour is frequently oversimplified in bench-scale experiments. Conveniently, many studies fix the pH near neutrality to control variables, but this approach fails to reflect the reality of natural water bodies, where pH can vary significantly with geology, weather, or human inputs. This changes in the water directly affect the sorbent's surface charge and therefore its fluoride removal ability. This risks producing results that do not translate well to fluctuating field pH conditions. Another overlooked factor is the presence of competing anions such as bicarbonates, sulfates, nitrates, and phosphates. These ions usually compete with fluoride for binding sites or modify the electrostatic environment, thereby reducing the sorbent's capacity under real groundwater chemistries (Basu *et al.*, 2024).

A clearer grasp of how surface charge and fluoride speciation behave under diverse multi-ion conditions would strengthen predictions about the field reliability of chemical

and natural adsorbents. Integrating this understanding with thermodynamic parameters such as Gibbs free energy, enthalpy, and entropy could provide a more robust chemical framework for designing fluoride removal systems that remain effective beyond controlled laboratory conditions. Without this, batch-derived adsorption capacities risk being overly optimistic and may fail to deliver consistent performance in communities that urgently need reliable defluoridation solutions.

2.4.2 Conventional and Emerging Defluoridation Techniques for Fluoride Removal

The persistent challenge of fluoride contamination in drinking water has led to the development of a variety of defluoridation techniques, ranging from conventional physico-chemical processes to emerging bio-based and low-cost approaches. Globally, these methods include adsorption, precipitation and coagulation-flocculation, ion exchange, and pressure-driven membrane processes such as reverse osmosis and nanofiltration. Recently, bio-sorption using indigenous plants and agricultural by-products has emerged as a sustainable alternative, especially for low-resource settings (Divyadeepika *et al*., 2024; Ogundele *et al*., 2023). While each method has demonstrated efficacy under specific conditions, they exhibit varying operational demands, cost implications, and environmental considerations. A critical review of these approaches provides insight into their practicality, strengths, and limitations in diverse socio-hydrogeological contexts.

2.4.2.1 Adsorption Methods

Adsorption is widely recognized as one of the most practical defluoridation methods due to its simplicity, relatively low cost, and flexibility for deployment at household or community scale. The process involves passing contaminated water through a solid medium that has a high affinity for fluoride ions, which adhere to the surface of the adsorbent (Tolkou *et al*., 2021). Traditional adsorbents include activated alumina, bone char, natural zeolites, and activated carbon, while engineered nanomaterials such as aluminum, iron, and zirconium-based oxides exhibit high removal efficiencies exceeding 90% under optimal pH (Asmamaw *et al*., 2023). More recently, bio-based composites incorporating chitosan or plant-derived carbon matrices have been developed to improve environmental compatibility and reusability. Despite its popularity, adsorption exhibits notable limitations. Its performance is highly pH-dependent and is often reduced in the presence of competing ions such as sulfate and bicarbonate, which interfere with binding sites (Wan *et al*., 2023). Regeneration of spent adsorbents also presents economic and environmental challenges, especially for synthetic or metal-modified materials. Consequently, while adsorption is an effective first-line solution for rural and decentralized treatment, it requires careful management to remain sustainable.

2.4.2.2 Precipitation and Coagulation-Flocculation

Chemical precipitation and coagulation-flocculation represent long-standing approaches for bulk defluoridation. These methods involve the addition of coagulants commonly aluminum salts (alum) or calcium salts (lime) which react with fluoride ions to form insoluble compounds such as aluminum-fluoride complexes or calcium fluoride (CaF_2).

The resulting flocs can be removed through sedimentation and filtration, often enhanced by flocculation to aggregate fine particles (Pillai & Thombre, 2024; Lacson *et al*., 2021). Precipitation with calcium is most effective in alkaline conditions due to the low solubility of CaF_2, whereas aluminum-based treatment requires near-neutral pH to generate aluminium hydroxide flocs that entrap fluoride. While precipitation is technically effective for high-fluoride water, it has significant disadvantages. High doses of chemicals are required to achieve the target levels, and the process produces large volumes of sludge that are a challenge for disposal . In low-income communities, the cost of chemicals and the logistical burden of sludge management reduce the method's sustainability. Without precise pH control and skilled operation, the efficiency can be inconsistent, making it more suited to large scale or industrial applications than rural community use.

2.4.2.3 Ion Exchange

In Ion exchange , fluoride removal is achieved by exchange of F^- ions with typically chloride or hydroxide, on a resin surface with fluoride ions in water. Artificial resins are used commonly due to their high affinity for fluoride, although some natural or modified materials have been explored as lower-cost resins (Shin, 2020; Grzegorzek *et al*., 2020). This method has produced treated water that meets WHO standards for fluoride content, and the resins can be regenerated with concentrated solutions such as brine, NaCl or NaOH for reuse. The method is very effective and regenerable but it causes practical challenges in rural settings. Resin fouling is of significant operational and environmental concerns due to the need for regular regeneration, and the production of brine waste containing concentrated fluoride. Moreover, the efficiency of ion exchange decreases in

the presence of anions like sulfate and phosphate which offer competition. These technical and waste management needs make ion exchange the most suitable for small-to-medium-scale applications where trained personnel and waste disposal mechanisms are available.

2.4.2.4 Membrane Processes

Membrane processes that are Pressure-dependent, like reverse osmosis (RO) and nanofiltration (NF), are some of the the most effective modern methods for fluoride removal. They employ semi-permeable membranes that allow water molecules to pass through while rejecting dissolved salts and ions like fluoride. RO is particularly effective for monovalent ions due to its smaller pore size and higher operating pressure, while NF gives a partial removal with lower energy demands (Rathi *et al*., 2024; Pezeshk *et al*., 2023). These processes give high-quality water without requiring the addition of any chemicals and therefore are widely used in urban and industrial areas. However, membrane processes require a lot of energy and are costly, which limits their application in low income areas. The concentrated brine waste generated poses an environmental disposal challenge if not properly handled.They are highly effective in producing potable water but their high capital and operational requirements make them less feasible for decentralised use without support from technical experts.

2.4.2.5 Bio-sorption Using Indigenous Plant Materials

In recent years, bio-sorption using indigenous plant materials and agricultural by-products has emerged as a green, low-cost, and locally adaptable solution for fluoride

removal (Yadav *et al*., 2021; Das *et al*., 2023). Plant-based sorbents like neem leaves and bark, guava leaves, lemon peels, banana pseudostems, maize cobs, and *Moringa oleifera* seeds have demonstrated promising adsorption abilities (Mannzhi, 2022; Gandhi & Sirisha, 2019). Aquatic plants like water lettuce (Pistia stratiotes), water hyacinth (*Eichhornia crassipes*), and duckweed (*Spirodela polyrhiza*) have also shown potential for fluoride capacities in experimental setups (Karmakar *et al*., 2016). When Modified, with calcium, aluminium, or zirconium ions their fluoride adsorption properties are enhanced (Corral-Capulin *et al*., 2019). Bio-sorption methods are environmentally viable and acceptable socially, making them suitable for community level or household applications. They, however, often show lower adsorption abilities compared to industrial chemical adsorbents. They are also highly sensitive to adsorption parameters such as pH, contact time, and initial fluoride concentration (Kaur *et al*., 2017). More over, spent bio-sorbents, as much as they are promising, require proper disposal or low-impact regeneration to prevent secondary environmental contamination. These methods require optimisation for local conditions to achieve proper long-term performance.

Generally,these defluoridation methods prove that no single method is universally optimal. Technologies like Reverse Osmosis and ion exchange provide high efficiency and reliability though they are expensive, energy demanding, and provide waste disposal challenges. Traditional techniques like precipitation and coagulation-flocculation are suitable for bulk treatment but produce sludge and have chemical dependence limitations. Adsorption and bio-sorption offer low-cost, decentralised solutions and align with sustainable development goals, though they require careful monitoring, regeneration

strategies, and performance optimisation. A suitable, integrated approach, for example, combining easy to find bio-sorbents for primary treatment with advanced polishing methods, *gives* the best pathway for sustainable fluoride regulation in drinking water systems.

2.4.3 Indigenous Plants as Fluoride Bio-sorbent

Indigenous plants have emerged as a promising low-cost and environmentally friendly option for the removal of fluoride from drinking water. Their potential as bio-sorbents has been widely explored because they are readily available, renewable, and biodegradable, making them especially attractive in rural and resource-limited regions (Yadav *et al*., 2021). Using plant-based biosorbents not only reduces dependence on chemical but also aligns with green chemistry principles, as it depends on local biomass and minimises pollutant emissions (Das *et al*., 2023). Indigenous plants can be applied at household and small community scales, offering a low-technology and accessible alternative for defluoridation where conventional treatment methods such as reverse osmosis or ion exchange are impractical (Mannzhi, 2022).

By-products from agriculture such as tea wastes, rice husks , and maize stalks provide abundant raw material for biosorbent production, enhancing the sustainability of this approach (Collivignarelli et al., 2020).

A good number of plant-based biosorbents have been analysed in studies in the laboratory . Goiod examples are the neem (*Azadirachta indica*) leaves and bark, guava

leaves, lemon peels, tea leaves, maize leaves, aloe vera, goose grass, and various crop ashes which have demonstrated measurable fluoride adsorption capacity (Mannzhi, 2022). Other studies have looked at *Moringa oleifera* seeds, *Pithecellobium dulce* seeds, *Passiflora foetida* fruits, *Emblica officinalis*, Zizanoides bark, *Cynodon dactylon* leaves, and Vetiveria roots as efficient bio-sorbents (Gandhi & Sirisha, 2019). Aquatic plants such as water lettuce (*Pistia stratiotes*), water hyacinth (*Eichhornia crassipes*), and duckweed (Spirodela polyrhiza) have also been investigated for their defluoridation capabilities (Karmakar *et al*., 2016).

When these plant-based sorbents are modified with metals such as calcium, aluminum and magnesium, the fluoride uptake is enhanced by introducing additional active sites or improving ion exchange capacity (Corral-Capulin *et al*., 2019). Additionally, indigenous plant mucilage (IPM) has gained attention as a bio-sorbent due to its viscosifying, emulsifying, and stabilizing properties (Kirthy *et al*., 2018). These mucilages, extracted from edible plants, are safe, low in toxicity, and socially acceptable for household water treatment, while their functional groups contribute to effective fluoride adsorption (Sharma *et al*., 2017; Kong *et al*., 2021).

Despite their potential, bio-sorbents have critical operational limitations. Fluoride removal efficiency is highly sensitive to water pH, initial fluoride concentration, and contact time, necessitating careful monitoring and periodic adjustment (Kaur *et al*., 2017). In addition, the adsorption capacity of natural sorbents is generally lower than that of engineered adsorbents, and the regeneration or disposal of spent bio-sorbents remains

an unresolved challenge for sustainable application. These limitations suggest that while plant-based bio-sorption can serve as a cost-effective primary or complementary treatment, it should ideally be integrated with other treatment methods for reliable long-term water safety in fluoride-endemic regions. While indigenous plants offer an affordable and environmentally sustainable defluoridation option, most studies are limited to laboratory-scale experiments, often under idealized conditions that may not reflect the variability of real-world water chemistry. Furthermore, long-term field performance, regeneration protocols, and lifecycle environmental impacts are insufficiently documented. Scaling up bio-sorption technologies will require standardized field trials, community engagement for adoption, and integration with monitoring systems to ensure consistent water quality improvements

2.4.4 *Moringa oleifera* as a Natural Biosorbent for Fluoride Removal

Plant-based coagulants (PBCs) have gained attention as sustainable alternatives to chemical coagulants for water and wastewater treatment due to their biodegradability, non-toxicity, low sludge production, and cost-effectiveness (Alnawajha *et al*., 2022; Owodunni & Ismail, 2021). Unlike other chemical coagulants, which can leave hazardous, non-biodegradable residues that pose risks to both water and terrestrial ecosystems (Asharuddin *et al*., 2021), PBCs offer an environmentally friendly approach compatible with rural or decentralised treatment settings. However, a key limitation of plant-based approaches is the variation in performance, which depends heavily on raw material quality, extraction methods, and environmental conditions.

Biosorption is a physicochemical process in which substances from aqueous solutions adhere to the surface of solid-phase biomaterials (Sivashankar *et al*., 2022). It is widely applied for the removal of metal ions, dyes, and other pollutants (Hasan *et al*., 2021). Of all the natural biosorbents studied, *Moringa oleifera* has been fund to be one of the most efficient species for water treatment. It is found in the Himalayan foothills of India, Pakistan, Bangladesh, and Nepal, and widely planted across Africa and other tropical regions, Moringa *oleifera* has shown to be able to immobilize a good number of toxic metal ions including Cu (II), Ni (II), Pb (II), Cd (II), and Hg (II) in aqueous environments (Bezerra *et al*., 2020; Gautam *et al.,* 2020). This versatility shows that multiple plant parts have biosorption capability, including the seeds, leaves, bark, and husks, which contain functional molecules capable of binding pollutants.

Moringa oleifera seeds, among the various plant parts, are particularly good for water treatment. They are natural coagulants and biosorbents that have the ability to adsorb turbidity, heavy metals, algae, coliform bacteria, and surfactants (Ang & Mohammad, 2020; Magalhães *et al*., 2021). *Moringa oleifera* is classified as a deciduous tree with tripinnate leaves and a bark that is corky. It belongs to the Moringaceae family (Bazzo *et al*., 2022). It is popularly known by other names like drumstick tree, horseradish tree, or ben oil tree, and has been identified for its natural coagulation properties (Nisar & Koul, 2021).

The active compounds in *Moringa oleifera* seeds are the cationic, water-soluble, low-molecular-weight proteins, which function as natural polyelectrolytes (Gandiwa *et al*.,

2020). These proteins, including lectins and albumins, introduce positive charges into the water, promoting charge neutralisation, particle bridging, and floc formation (Saleem *et al*., 2020; Taiwo *et al*., 2020). Lectins are cationic trimeric proteins with strong coagulatory ability, while albumins are thermally stable dimers (<6.5 kDa) enriched with arginine and histidine, giving a basic coagulatory nature with isoelectric points above 10. the dried seeds, when powdered, release biological chemicals such as arginine, proline, and glutamine, which enhance coagulant activity (Faraj & Abudi, 2020).

Prominent functional groups in moringa oleifera include carboxyl and hydroxyl that provide sites for the adsorption of metal cations through cation exchange and chelation, effectively removing heavy metals from water; amino acids that contribute to the presence of amino groups that further enhance the biosorbent's capacity for metal ion removal. Phenolic compounds and flavonoids also contain hydroxyl and aromatic groups which give additional binding sites for pollutants; tannins and saponins improve its overall adsorption properties while glycosides play a role to the surface properties which make it an effective biosorbent (Narayan *et al*., 2022).

The process of particle aggregation and floc formation involves adsorption, charge neutralization, and particle bridging facilitated by these cationic proteins (Boulaadjoul *et al*., 2018; Alam *et al*., 2020). Conversely, the availability of oils and other hydrophobic seed components can easily reduce protein activity by leaching organic matter, which normally would compete with fluoride for the binding sites. To improve on the performance, oil extraction from *Moringa oleifera* seeds is often recommended, because

it reduces the fatty acid and phenolic content, leaving more active protein fractions (Magalhães *et al*., 2021; Skaf *et al*., 2021).

Moringa oleifera cationic proteins also exhibit antimicrobial properties cause inner and outer membrane fusion by disrupting microbial cell membranes, leading to leakage of inter-cellular components and the death of the cells (Andrade *et al*., 2021). This simultaneous antimicrobial and adsorption property makes *Moringa oleifera* a feasible biosorbent and coagulant for water treatment in various places. While *Moringa oleifera* offers environmentally friendly and multifunctional benefits, its large scale application face key issues. Some of the challenges faced include limited large scale cultivation of the tree for industrial-scale production, biodegradation of the active proteins at high storage temperatures, multi-step extraction requirements, and the need for optimised operational conditions (Kurniawan *et al*., 2020; Gomes *et al*., 2022). Moreover, long-term efficacy studies in large-scale or continuous-flow systems are rare, leaving uncertainty regarding consistent performance under variable water and environmental conditions. For Moringa-based defluoridation to move from laboratory to large scale use, standardisation, preservation technologies, and sustainable sourcing strategies will be requirement.

2.5 Efficiency of Calcium-Spiked Biosorbents for Fluoride Removal

Biosorption has come up as an easy and environmentally benign route for reducing fluoride contamination in groundwater, especially in regions where industrial defluoridation technologies remain costly. The principle depends on exploiting abundant

plant-based or agricultural biomaterials that have surface functional groups like carboxyl, hydroxyl, and amine that are capable of attracting fluoride ions via electrostatic interaction, ion exchange, and surface complexation (Gomes *et al.*, 2022). However, raw biomaterials often display inconsistent fluoride uptake because they have the intrinsic binding affinity of their organic functional groups which are not always sufficient to anchor highly electronegative fluoride ions under competing ionic conditions (Taiwo *et al.*, 2020). This limitation has led to interest in chemical modification approaches, including calcium spiking that has gained traction due to its direct alignment with the chemical pathways of fluoride precipitation. A major weakness in most of the biosorption literature is the lack of thermodynamic characterisation to confirm that the binding mechanisms align with observed biosorbence performance. Additionally, many early trials focused mainly on batch lab tests, under static, ideal conditions that fail to represent the fluctuating ion strengths or pH variations of field groundwater systems.

Chemically, calcium spiking improves a biosorbent by adding Ca^{2+} ions. Fluoride ions, when adsorbed onto the surface, react with these mobile calcium ions to form sparingly soluble calcium fluoride (CaF_2), effectively adsorbing the fluoride to the biomass matrix (Khader *et al.,* 2022). The reaction is straightforward and powerful:

$Ca^{2+} + 2F^{-} \longrightarrow CaF_2(s)$.

This controlled precipitation at the biosorbent interface supplements the original weak binding from native functional groups, significantly boosting the total uptake capacity (Shrestha, 2021). Unlike pure precipitation–coagulation processes that require chemical dosing in bulk water, the in-situ precipitation here occurs on the solid phase, minimising chemical sludge and enabling reuse under some conditions. One constraint, however, is

the difficulty of ensuring uniform calcium impregnation throughout irregular biomass surfaces, which can produce patchy or unstable removal efficiencies. Moreover, the practical stability of immobilised calcium under variable groundwater pH and competing ions such as bicarbonate or sulfate remains under-investigated, even though such ions can significantly impact Ca^{2+} availability for reaction.

Empirical evidence increasingly supports the superior performance of calcium-modified biosorbents. For example, recent comparative trials demonstrate that untreated biomass typically removes 40–60% of fluoride ions at moderate initial concentrations (5–10 mg/L), while calcium-enhanced equivalents can reach removal rates above 85% under identical conditions (Li *et al.,* 2023). This dramatic uplift is attributed not only to the added reactive Ca^{2+} sites but also to improved surface charge conditions that promote ion exchange. Shrestha (2021) reported that calcium-enriched powders could double the Langmuir maximum adsorption capacity (q_{ax}) relative to raw material, moving from ~5 mg/g to over 10 mg/g. Similar patterns appear in other plant-based substrates: calcium-modified rice husk ash, banana peels, and nutshells have each shown elevated fluoride removal performance across pilot studies (Hasan *et al*., 2023). Despite these promising trends, few studies extend the analysis to multiple adsorption–desorption cycles to test long-term reusability. Additionally, field deployments often fall short of verifying how real-world groundwater chemistry especially the presence of natural organic matter might hinder fluoride's access to calcium-rich sites.

The underlying efficiency of calcium spiking hinges on the interplay between ion mobility and biosorbent surface chemistry. The precipitation of CaF_2 is favoured under alkaline pH, but the biosorbent's native acidic or neutral functional sites can shift local pH microenvironments, creating competing effects (Wambu *et al.*, 2022). Furthermore, co-existing ions like phosphate, sulfate, or carbonate can chelate Ca^{2+} or form competing precipitates, reducing the free calcium fraction available for fluoride binding (Wang *et al.*, 2023). This raises the need for robust multi-ionic models to predict competing equilibria, an area where experimental data remains limited. Recent work by Mutiso *et al.* (2025) highlights that unaccounted ion-pair formation with bicarbonates can suppress CaF_2 precipitation efficiency by up to 30% in typical Rift Valley groundwater. It is unfortunate that such complex ion interactions are often not keenly considered when scaling up laboratory performance metrics to real environmental situation. These factors that are overlooked can produce misleading removal efficiencies if practical constraints are not built into the design of the system from the outset.

Thermodynamic studies have helped clarify such chemical dynamics by quantifying how favorably the spiked biosorbent system binds the fluoride under different temperatures and concentrations. Negative Gibbs free energy (ΔG) values, indicating spontaneous adsorption, and positive enthalpy (ΔH) have been shown from studies to imply endothermic mechanism where higher temperatures slightly improve fluoride removal due to improved ion mobility and expanded pore accessibility (Kazapoe *et al.*, 2024). Entropy (ΔS) reflects the increased disorder from releasing hydration shells as fluoride ions bind to the surface of calcium. However, as Ansari *et al.* (2023) caution, batch-derived thermodynamic constants rarely account for the dynamic water flow conditions

that are found in rural defluoridation units. Data from field piloting remains sparse, and so the chemical thermodynamics of calcium-assisted biosorption still demand real-world validation. There is another gap in the limited integration of these thermodynamic findings with kinetic data, which could show how reaction rates influence practical contact time requirements for scaled treatment units.

Calcium spiking must also be judged against sustainability criteria, especially in low-income settings. Calcium chloride or calcium nitrate are the commonly used reagents for spiking. These are accessible but add recurring cost and logistic burdens for small communities (Taiwo *et al.,* 2020). Used spiked biosorbents, if not disposed of properly, may pose other contamination risks due to residual chemicals or partially released fluoride under acidic leaching conditions (Onipe *et al.,* 2020). Relatively few lifecycle assessments, to date, quantify the downstream environmental effects of using chemical spiking for biosorption. For example, the balance between improved fluoride removal and spiked chemical input must be weighed against the less efficient though simpler option of using untreated biomass at higher dosages. This is often ignored in lab-scale publications that do not project the full operational benefits of spiked biosorbent use. Additionally, procedures for safe regeneration and reuse are not well reported, leaving dilemma about how communities might maintain removal efficiency over time for continuous operation.

Improving the calcium-assisted biosorption also brings technical challenges. Batch experiments approve the chemical principles followed under controlled mixing and

contact times, but practical flow-through systems, whether in household or at community levels must ensure sufficient retention time for precipitation to occur (Hasan *et al.*, 2023). Too high flow rates can reduce contact efficiency, leading to partial fluoride capture. When breakthrough curves are modelled for spiked biosorbents under realistic flow regimes, it remains a technical issue. Wambu *et al.* (2022) noted that most prototypes still assume near-ideal residence times, but trials in the real world have shown some short-circuiting and channelling in packed beds, which reduce fluoride removal. Moreover, few published studies couple detailed breakthrough modelling with rigorous chemical mass balances, creating blind spots in design performance. Future work must integrate adsorption isotherms, kinetics, and thermodynamics into coherent pilot designs tested over seasonal cycles.

Despite these limitations, the chemistry behind calcium spiking continues to inspire novel hybrid methods that combine biosorption with other defluoridation pathways. For example, recent experiments explore combining calcium-modified biosorbents with low-dose coagulants or membrane filtration to synergise ion capture and residual polishing (Li *et al.*, 2023). Another direction is embedding spiked biosorbents into modular cartridges with replaceable media, designed for easy regeneration on-site. These hybrid approaches promise to balance chemical efficiency with operational practicality, but they require robust field validation to ensure that the core chemical principles deliver under diverse groundwater chemistries.

Calcium spiking demonstrably boosts the chemical binding capacity of biosorbents for fluoride removal by promoting localised precipitation of CaF_2. This enhancement aligns well with the underlying geochemical principles that govern fluoride's natural occurrence and mobility. Yet, for this method to transition from promising laboratory evidence to reliable, community-level practice, future research must bridge chemical modelling, thermodynamic realism, ion competition, and practical engineering. Only then can the clear chemical promise of calcium-modified biosorption fully address the enduring global challenge of excess fluoride in drinking water.

2.6 Effect of Combined Dosage and Particle Size

The effectiveness of adsorption-based water treatment technologies is strongly influenced by two fundamental chemical engineering parameters: the adsorbent dosage and the particle size. All these factors determine the availability of active sites for contaminant binding, the accessibility of those sites, and the overall kinetics of mass transfer between solution and sorbent surface (Foo & Hameed, 2010). An increase in adsorbent dosage leads to an increase in the number of active sites available for fluoride ions, leading to an increase in efficiencies. Simultaneously, when the particle size increases, the surface area-to-volume ratio, which improves ion diffusion pathways and improves contact between the contaminant and the biosorbent's binding sites (Gai & Deng, 2021).

The quantity of biosorbent used will determine the environment that is surrounding the binding sites for fluoride ions. Optimally, as the amount of biosorbent increases, the percentage of fluoride removed will also go up due to a larger surface area and more

binding sites (Kavisri *et al.,* 2023). Differently, there is an optimal dose of biosorbent to use, and depending on the biosorbent used, efficiency could plateau or even decrease if more is being used and residues are forming (Tee *et al.,* 2022*).* Recently, various studies have focused on this and what the optimal dosages are for different biosorbents, for example, agricultural waste, such as rice husk ash (Karić *et al.,* 2022) and algal biomass, such as *Sargassum* sp. (Mendonça *et al.,* 2024). Microbial biomass, including *Pseudomonas aeruginosa* (Zada *et al.,*2024), has been found to have optimal ranges of 1 to 10 g/L though it depends on the type of biosorbent and fluoride initial concentration.

While this dual effect is well-understood in principle, its practical application often encounters trade-offs. For example, although high dosages can provide more active binding sites, they can also promote particle agglomeration, which reduces the effective surface area available for adsorption. Similarly, excessively fine particles, while offering larger surface areas, may create operational challenges such as clogging in packed bed filters or difficulty in separating the spent adsorbent from treated water (Luo *et al.*, 2021). This balance highlights the need for carefully optimised designs that consider both dosage and particle size simultaneously, a nuance that has sometimes been overlooked in earlier studies focused on each factor in isolation (Singh *et al.*, 2022).

When biosorbent dosage is increased, it is widely reported to improve fluoride removal. For instance, Kumar *et al.* (2019) observed a steady increase in removal efficiency when the dosage of *Moringa oleifera* seed powder was increased, a trend supported by Moyo *et al.* (2021), who showed that boosting the dosage from 0.5 g/L to 2.5 g/L elevated fluoride

removal rates from 55% to over 90% under constant conditions. However, the benefits of higher dosages do not increase indefinitely. Beyond the threshold, excess dosage can lead to overlapping of particles, which hinders fluid flow and impedes mass transfer by covering active sites (Bhatnagar *et al.*, 2011). Unfortunately, many batch-scale studies fail to report these diminishing returns comprehensively, often presenting only removal percentages without addressing the practical implications of overdosing such as increased sludge generation, greater turbidity, or higher operational costs for post-treatment solid–liquid separation (Pathak & Rathore, 2016).

In parallel, particle size plays an equally vital role in adsorption performance by regulating the extent of surface area exposed for ion exchange and the ease with which fluoride ions diffuse through the adsorbent matrix (Mondal *et al.*, 2020). Studies like Ochieng *et al.* (2018) have shown that milling *Moringa oleifera* seeds to particle sizes below 100 μm can improve fluoride removal by nearly 20% compared to coarser particles, mainly due to increased external surface area and shorter intra-particle diffusion paths. However, excessively fine particles are often impractical in real-world applications, as they can pass through filter media or generate high head losses in continuous flow systems, which complicates their use in rural or low-resource settings (Luo *et al.*, 2021). Notably, some laboratory experiments continue to rely on ultrafine powders that are unrealistic for scalable household or community-scale filters, a gap that underscores the need for more practical size ranges in adsorption research.

The interaction between dosage and particle size adds another layer of complexity to designing effective biosorption systems. When studied together, these variables may exhibit synergistic or even contradictory effects that would remain hidden if considered separately. For example, Gong *et al.* (2022) demonstrated that the positive effect of increasing dosage was amplified when used with moderately sized particles, which maintained good flowability while still offering sufficient surface area. On the converse, when high dosages are combined with very fine particles, excessive agglomeration or filter clogging occurs, which undermine the potential gains in adsorption efficiency. Such findings show the importance of optimising these parameters together rather than in isolation, which, the earlier single-variable studies often failed to capture and therefore limiting their application to practical large scale systems.

Agglomeration and flow resistance need to be accounted for which becomes enhanced in continuous flow and fixed-bed systems. Sari and Tuzen (2020) showed that in column studies, when fine particles are used at higher dosages, they tended to clog filter beds, requiring the additional pre-filtration or frequent backwashing procedures that made the procedures complicated and less cost effective. For real community-scale use, it is imperative that we balance between large enough surface area and manageable hydraulic performance. Researches recently done have agreed on this ground by indicating that moderate particle sizes combined with dosages at optimal levels give the best solution for rural area fluoride removal systems (Chauhan *et al.*, 2021). However, many studies that have been published have not applied their findings on field or piloting scale. This

obviously leaves an evidence gap regarding long-term sustainability and system maintenance under realistic conditions.

Responding to these limitations, more recent investigations have adopted statistical tools such as response surface methodology (RSM) and factorial experimental designs to identify best combinations of dosage and particle size. Patel and Yadav (2022), for instance, used RSM to fine-tune fluoride removal using modified zeolites and found that intermediate levels of both parameters achieved the best trade-off between high removal efficiency and manageable operational requirements. Similarly, Chen *et al.* (2023) used factorial designs to test biochar-based adsorbents, showing that the interaction effect of dosage and particle size was enhanced and that when ignored, this interaction would lead to inaccurate process designs. However, despite these methodological advances, many models remain confined to laboratory-scale validation and have yet to be tested using actual groundwater samples or community-level units, hindering their practical relevance. The use of *Moringa oleifera* seed powder highlights both the possibility and the challenges of dosage–particle size optimisation. The unique protein structure and cationic properties of the seed powder provide abundant sites for fluoride ion binding (Yadav *et al.*, 2021). But the soft, fibrous texture of *Moringa* seeds makes them prone to excessive fragmentation during milling, generating very fine particles that pose challenges in separation in household filters. Interestingly, Kebede *et al.* (2020) and Moyo *et al.* (2021) have shown in their studies that chemical modification, such as with calcium, not only enhances the ion exchange capacity but also slightly improves the physical cohesion of the powder, making moderate mesh sizes (40–60) effective at practical dosages. This

double benefit points a pathway for balancing high removal efficiencies with operational ease, but field-scale trials in fluoride-prone rural communities remain limited.

Generally, future research must go further than controlled laboratory conditions and single-variable testing. A systematic, large-scale factorial experiments is needed that span broader ranges of dosage and particle size and account for local groundwater chemistry and co-contaminants. Importanat too is the translating of these optimised conditions into affordable, easy-to-maintain filter designs that work under community constraints. Without such moves,, laboratory findings risk remaining as theoretical possibilities rather than practical solutions for the millions who rely on unsafe drinking water in fluoride-endemic regions.

2.7 Influence of Process Parameters

Adsorption-based defluoridation technologies rely heavily on the careful control of key physicochemical parameters, which govern the interaction between fluoride ions and the active sites of adsorbent materials. Among these, solution pH remains the single most pivotal variable because it influences both the surface charge of the adsorbent and the speciation of dissolved ions (Gai & Deng, 2021). At lower pH levels, the high proton concentration favours competition between H^+ and F^- for the same adsorption sites, which suppresses fluoride binding efficiency, especially for adsorbents whose functional groups have low point-of-zero-charge values. On the other hand, moderate alkalinity can enhance adsorption when the biosorbent's surface groups deprotonate, exposing negative sites that attract multivalent cations such as Ca^{2+}, which in turn react with fluoride to form stable surface complexes like CaF_2 (Khader *et al.*, 2022). However, if pH rises too

far into the strongly alkaline range, competing hydroxide ions (OH^-) can displace fluoride from active sites or form soluble complexes, effectively reducing net fluoride removal (Nguyen *et al.*, 2024). Despite this well-understood relationship, many bench-scale studies continue to test pH at fixed, narrow ranges instead of mapping the full profile of performance across realistic pH windows found in groundwater, which often fluctuate seasonally or spatially. Moreover, few researchers evaluate how natural buffering capacity in aquifers might counteract deliberate pH adjustments made during treatment, potentially undermining lab-optimised conditions when scaled to real field applications.

Contact time is equally crucial because it dictates how thoroughly fluoride ions can diffuse through the boundary layer surrounding each adsorbent particle and penetrate the porous network to reach interior binding sites (Zhao *et al.*, 2022). Adsorption typically follows a two-phase kinetic pattern: an initial rapid uptake governed by external mass transfer, followed by a slower stage driven by intraparticle diffusion until equilibrium is approached. Extending contact time generally raises removal efficiency, but practical design must balance this benefit against throughput constraints, particularly in flow-through column systems where extended residence times may require larger reactors or slower flow rates (Hasan *et al.*, 2023). A recurring limitation is that many published kinetics studies still favour static batch tests under constant agitation, which often exaggerate real contact efficiencies compared to the plug flow or mixed flow behaviour in field systems. Equally, there is a shortage of rigorous modelling that integrates

diffusion coefficients, flow velocities, and actual pore structures to predict scale-up feasibility under variable community water demand conditions.

Temperature is another parameter that significantly shapes adsorption outcomes through its influence on both ion mobility and the energetic favorability of the binding reaction. Many biosorption processes for fluoride are endothermic in nature, indicated by positive enthalpy (ΔH) values derived from thermodynamic modelling (Kazapoe *et al.*, 2024). An increase in temperature generally enhances fluoride removal by boosting the kinetic energy of ions, reducing the thickness of the boundary layer, and activating more sorption sites by slightly expanding the biomaterial's pore structure (Ansari *et al.*, 2023). However, elevated temperatures also bring operational trade-offs: in field systems, groundwater temperatures can vary seasonally by 5–15 °C, which may unpredictably alter removal efficiency unless system designs account for this variability. A notable shortfall is that laboratory studies often use a single, constant incubation temperature, overlooking diurnal and seasonal temperature swings that are common in real aquifer-fed systems. Furthermore, the energy implications of artificially heating water to maintain ideal adsorption conditions are rarely factored into cost-benefit analyses, despite their critical relevance for rural or off-grid communities.

The initial fluoride concentration in the influent water is directly tied to the mass transfer driving force that propels fluoride ions toward the adsorbent surface. Higher concentrations create steeper concentration gradients, increasing the probability of ion–site collisions and boosting overall removal capacity in the early stages (Cite using 2025

reference). However, this can quickly saturate available active sites, shortening the breakthrough period in continuous treatment systems and necessitating more frequent media regeneration or replacement. Langmuir and Freundlich isotherm models provide useful frameworks for describing this behaviour. Yet, their parameters are often derived from static batch data that may not translate cleanly to dynamic conditions in real filtration columns (Hasan *et al.,* 2023). One overlooked aspect is that most studies do not test a wide enough range of fluoride concentrations to reflect the full variability found in different boreholes, which can vary from below 1.5 mg/L to well above 20 mg/L depending on geology and seasonality. Additionally, the effect of fluctuating load conditions such as sudden spikes due to rainfall recharge events, is rarely incorporated into performance predictions, leaving potential performance under stress under-characterised.

Beyond the core parameters of pH, temperature, contact time, and influent concentration, ionic strength and the presence of competing anions represent critical but frequently underestimated influences on defluoridation efficiency. Natural groundwater seldom contains fluoride in isolation; common co-existing ions such as bicarbonate (HCO_3^-), sulfate (SO_4^{2-}), phosphate (PO_4^{3-}), and chloride (Cl^-) can compete for adsorption sites or react with modifying cations like calcium, diminishing the free Ca^{2+} available to bind with fluoride (Wang *et al.*, 2023). Elevated ionic strength can also compress the electric double layer around adsorbent particles, reducing the range of electrostatic attraction and lowering overall fluoride uptake (Taiwo *et al.,* 2020). Despite the clear importance of these interactions, only a minority of studies perform realistic multi-ion batch tests or

competitive adsorption experiments, leaving a significant gap in the empirical basis for system design under real aquifer chemistries. Furthermore, most adsorption models still treat ionic interactions in simplified form, lacking robust corrections for multi-component competition and site-blocking phenomena that emerge in mixed-ion scenarios.

Thermodynamic analysis remains an indispensable tool for clarifying the underlying energetics that drive or hinder fluoride binding to biosorbent surfaces. The sign and magnitude of the Gibbs free energy change (ΔG) indicate whether adsorption is spontaneous under given conditions, while enthalpy (ΔH) and entropy (ΔS) values reveal whether the process is endothermic or exothermic and how water structure reorganizes at the solid–liquid interface during ion exchange (Kazapoe *et al.*, 2024). However, while batch-derived thermodynamic constants can signal fundamental feasibility, their predictive power is limited if the system's kinetics are too slow to achieve practical equilibrium within operational contact times (Ansari *et al.*, 2023). A persistent weakness is that many studies report thermodynamic values calculated from idealised isotherm fits without verifying that these assumptions hold in flowing water systems with variable turbulence, real pore structures, and multi-phase interactions. Moreover, relatively few projects link thermodynamic data to pilot-scale or long-term performance, making it difficult to test whether laboratory indicators of spontaneity translate to robust field outcomes.

Kinetic parameters complement thermodynamic insights by quantifying the rate at which fluoride ions move from the bulk solution to the active sites on the adsorbent. Pseudo-

first-order and pseudo-second-order models remain the standard frameworks for describing these kinetics, yet their applicability can be constrained by non-idealities like pore diffusion resistance and film transfer limitations (Zhao *et al.*, 2022). Elovich and intraparticle diffusion models can add nuance, especially for heterogeneous biosorbents with irregular pore structures or surface modification layers (Li *et al.*, 2023). Unfortunately, the kinetic modelling literature for fluoride adsorption is still dominated by simplified fits that do not account for hydrodynamic factors such as flow channelling or axial dispersion in packed columns. Additionally, few kinetic studies systematically test how reaction rates change under the combined effects of pH, temperature, and ion competition, which leaves significant blind spots when designing practical treatment units.

Translating this detailed understanding of chemical process parameters into scalable systems demands integrated pilot-scale research that captures the realities of rural deployment. Field performance is affected not only by fluctuating groundwater quality but also by variable flow rates, maintenance intervals, and local climate factors. Breakthrough curves must be developed for continuous flow conditions, ideally validated under seasonally adjusted scenarios that mirror real community use (Hasan *et al.*, 2023). Yet, such pilot studies are often lacking, with many investigations stopping at laboratory prototypes that neglect the complexity of local water supply logistics or user behaviour. Furthermore, the durability and regeneration of adsorbent materials under repeated cycles remain inconsistently tested, even though regeneration costs and handling practicalities heavily influence community adoption and sustainability.

Taken together, the influence of pH, contact time, temperature, initial fluoride concentration, ionic strength, and competing ions defines the chemical envelope within which any adsorption-based defluoridation technology must operate. Future work must bridge the gap between rigorous lab-scale experimentation and real-world water chemistry through integrated modelling and multi-variable pilot validation. By refining how these process parameters interact under diverse and unpredictable groundwater conditions, researchers and engineers can better design systems that are not only chemically sound but also practical, resilient, and accessible to fluoride-affected communities worldwide.

2.8 Adsorption Isotherms and Kinetics

A rigorous understanding of adsorption isotherms and kinetics is essential for predicting and optimising the performance of biosorbents used in fluoride removal from drinking water. Adsorption isotherms describe the equilibrium relationship between the concentration of fluoride in solution and the amount adsorbed on the biosorbent at a constant temperature (Raji *et al.,* 2023). They reveal the capacity and surface characteristics of the adsorbent, guiding the design of treatment systems. Adsorption kinetics, in contrast, describe the rate at which fluoride is taken up, providing insight into the controlling mechanisms, whether surface reactions, diffusion, or chemisorption dominate. Together, these frameworks form the cornerstone of designing and scaling adsorption-based defluoridation systems, especially for low-cost, locally available materials such as *Moringa oleifera* seed powder.

2.8.1 Adsorption Isotherms

2.8.1.1 Langmuir Isotherm

The Langmuir isotherm is among the most widely applied models in fluoride removal studies. It assumes that adsorption occurs as a monolayer on a homogeneous surface with a finite number of identical and energetically equivalent binding sites, and that once a site is occupied, no further adsorption occurs at that site. The model is expressed as:

$$q_e = \frac{q_m b C_e}{1 + b C_e} \qquad 2.1$$

Where:

- q_e is the equilibrium adsorption capacity (mg/g),
- q_m is the maximum monolayer adsorption capacity (mg/g),
- b is the Langmuir constant related to the affinity of binding sites (L/mg),
- C_e is the equilibrium concentration of fluoride ions in solution (mg/L).

The linearised form, used for parameter estimation, is:

$$\frac{1}{q_e} = \frac{1}{q_m b C_e} + \frac{1}{q_m} \text{ or } \frac{C_e}{q_e} = \frac{1}{q_m b} + \frac{C_e}{q_m} \qquad 2.2$$

This linearization allows for the graphical determination of q_m and by plotting C_e/q_e against C_e. A plot with a high correlation coefficient indicates that the Langmuir model adequately describes the system.

Langmuir is especially relevant for chemically modified biosorbents, such as calcium-spiked *Moringa oleifera*, where uniform ion-exchange sites mimic the model's

homogeneity assumption (Wambu *et al*., 2022). Nonetheless , natural biosorbents with complex and heterogeneous surfaces often deviate from this idealised behaviour, which may inhibit the model's predictive power for real-world applications (Taiwo *et al.,* 2020). The Langmuir model has been widely utilised for describing adsorption equilibria. Developed for gas adsorption on solid surfaces, the model's application has since been extended to liquid-phase adsorption, including the removal of fluoride ions from water. The model makes an assumption that adsorption occurs uniformly on a homogeneous adsorbent surface through monolayer coverage, with no lateral interaction between adsorbed molecules. Further , it suggests that once an adsorbate molecule occupies a site, no further adsorption can occur at the site.

The Langmuir model is relevant in fluoride biosorption research when dealing with biosorbents that have been chemically modified like calcium-spiked *Moringa oleifera*. The calcium ions that have been added promote specific ion exchange reactions, supporting the assumption of uniform active sites with high affinity for fluoride ions (Wambu *et al.,* 2022). On homogeneity, however, the assumption is unrealistic for natural biosorbents, which often have different functional groups and microstructures. Over-reliance on the Langmuir model alone, especially when scaling up from batch tests to real-world systems where site heterogeneity is unavoidable, should be done with caution (Taiwo *et al.*, 2020).

2.8.1.2 Freundlich Isotherm

The Freundlich model, developed empirically, the Freundlich model, accounts for heterogeneous surfaces and multilayer adsorption, making it highly suitable for natural biosorbents with diverse functional groups such as hydroxyl, carboxyl, and amino sites. It is expressed as:

$$q_r = K_F C_e^{1/n} \quad (2.3)$$

where:

- K_F is the Freundlich constant indicating adsorption capacity,
- $^1/_n$ is the heterogeneity factor,
- C_e and q_e are defined as above.

A linear form for fitting is:

$$\ln q_e = \ln KF + 1/n \ln C_e \quad (2.4)$$

Biosorbents like *Moringa oleifera* seed powder often fit the Freundlich model well due to their complex structure, which includes proteins, lipids, and cationic polypeptides, creating a range of binding sites. Recently, studies have shown that the Freundlich model may better capture the fluoride removal behaviour of non-spiked *Moringa oleifera* powder than the Langmuir model alone (Taiwo *et al.*, 2020). This outcome gives the importance of testing multiple isotherm models rather than just depending on a single framework, especially when working with naturally biosorbents.

Despite all the strengths, the Freundlich isotherm does not predict a saturation point, which can be a limitation for practical community system design. With no a finite

maximum capacity, the model cannot directly inform the point at which an adsorbent becomes fully exhausted, hence requiring complementary use of the Langmuir or other monolayer models.

2.8.1.3 Advanced Isotherm Models

Advanced isotherm models such as the Temkin and Dubinin–Radushkevich (D–R) models have been used to provide deeper mechanistic insights into adsorption processes.

The Temkin isotherm assumes that the heat of adsorption decreases linearly with surface coverage, reflecting the effect of adsorbate–adsorbent interactions. Its linear form is :

$$q_e = B\ln A + B\ln C_e \qquad 2.5$$

Where:

- q_e is the equilibrium adsorption capacity (mg/g),
- C_e is the equilibrium concentration of the adsorbate in solution (mg/L),
- A is the Temkin equilibrium binding constant (L/mg),

$$B = \frac{RT}{bT} \qquad 2.6$$

where R is the universal gas constant, T is the absolute temperature (K), and bT is the Temkin constant related to the heat of adsorption.

The Dubinin–Radushkevich (D–R) isotherm is more general than Langmuir as it does not assume a homogeneous surface. It is useful particularly for distinguishing between physical and chemical adsorption based on the mean free energy of adsorption. The D–R isotherm is given by:

$$q_e = q_s \exp(-B\varepsilon^2) \quad 2.7$$

Where:

q_s is the theoretical saturation capacity (mg/g),

B is a constant related to adsorption energy,

$\varepsilon = RT\ln(1+1/C_e)$ is the Polanyi potential.

The mean free energy of adsorption is calculated as:

$$E = \frac{1}{\sqrt{2B}} \quad 2.8$$

If $E < 8$ kJ/mol$E < 8$ kJ/mol, the process is considered physisorption**,** while $8 < E < 16$ kJ/mol indicates chemisorption (Foo & Hameed, 2010). Despite their valuable insights, Temkin and D–R models are less commonly applied in fluoride removal studies due to their more complex fitting requirements and limited applicability in practical field designs.

Equilibrium models alone are insufficient without considering adsorption kinetics, which determine the time required to achieve equilibrium and guide the design of reactors or filter beds.

The Lagergren pseudo-first-order (PFO) model assumes that the rate of adsorption is proportional to the number of unoccupied sites on the biosorbent. Its differential form is:

$$\frac{dq_t}{dt} = k_1(q_e - q_t) \quad 2.9$$

Its integrated linear form is:

$$\ln(q_e - q_t) = \ln q_e - k_1 t) \quad 2.10$$

Where:

q_t is the amount adsorbed at time t (mg/g),

q_e is the equilibrium adsorption capacity (mg/g),

k_1 is the pseudo-first-order rate constant (1/min).

Physi sorption or weak van der Waals interactions dominate the adsorption process, as suggested by the best fit to this model

The pseudo-second-order (PSO) model was developed by Ho and McKay (1999). This assumes that chemisorption via electron sharing or exchange is the rate-limiting step.

Its rate expression is:

$$\frac{dq_t}{dt} = k_2(q_e - q_t)^2 \quad 2.11$$

When integrated, the linear form becomes:

$$\frac{t}{q_t} = \frac{1}{k_2 q_e^2} + \frac{1}{q_e} \quad 2.12$$

Where k_2 is the pseudo-second-order rate constant (g/mg·min).

Most of the studies done on *Moringa oleifera*–based biosorbents show that the PSO model provides the best fit this theredfore confirms the dominance of chemisorption, especially when the biosorbent has been chemically modified (Wambu *et al*., 2022).

The intra-particle diffusion (IPD) model was proposed by Weber and Morris (1963) and it evaluates whether the adsorption rate is controlled by diffusion within the pores of the biosorbent or surface reactions.

Its expression is:

$$q_t = k_{id} t^{1/2} + C \quad 2.13$$

Where:

k_i is the intra-particle diffusion rate constant,

C is a constant reflecting boundary layer thickness.

A linear plot of q_t versus $t^{1/2}$ passing through the origin indicates that intra-particle diffusion is the sole rate-limiting step. Deviations from linearity suggest multi-stage adsorption, often involving surface adsorption followed by pore diffusion.

This polished version now flows logically from advanced isotherms → kinetic models → mechanistic interpretation, making it ready for inclusion in a thesis or research article.

2.9 Thermodynamic Insights into Fluoride Removal by Adsorption

Thermodynamic principles provide a vital framework for interpreting how fluoride ions interact with adsorbent surfaces under varying environmental conditions. In adsorption chemistry, standard thermodynamic parameters, namely, Gibbs free energy change (ΔG°), enthalpy change (ΔH°), and entropy change (ΔS°), help explain whether a process is spontaneous, exothermic, or endothermic, and how the system's disorder shifts during ion transfer. A negative Gibbs free energy indicates that the adsorption is thermodynamically feasible without requiring external energy input, a desirable trait for practical water treatment systems that must operate passively in rural or off-grid settings

(Kazapoe *et al.*, 2024). For fluoride removal specifically, most biosorption studies have reported negative ΔG° values within the range of –5 to –25 kJ/mol, suggesting that the ion exchange and surface complexation reactions occur naturally at ambient conditions (Nguyen *et al.*, 2024).

The sign and magnitude of ΔH° distinguish the nature of adsorption forces. A positive enthalpy implies endothermic uptake, meaning that higher temperatures tend to increase removal efficiency by energising both the adsorbent's active sites and the mobility of fluoride ions. This aligns with results from multiple recent studies, which demonstrated that heating the solution from 20°C to 40°C raised fluoride adsorption by 15–30% for various calcium- and iron-modified biosorbents (Hasan *et al.*, 2023; Gai & Deng, 2021). This behaviour suggests a chemisorption mechanism where fluoride forms stronger bonds with functional groups or reacts to precipitate compounds such as CaF_2 on the adsorbent surface. However, exothermic profiles marked by negative ΔH° values are also common, especially when physisorption dominates through van der Waals interactions and electrostatic attraction (Zhao *et al.*, 2022). Yet, one consistent gap is that laboratory enthalpy estimates are often based on single-point equilibrium data fitted to simple isotherm models, rather than direct calorimetric measurements, which could yield more accurate heat change values. Moreover, few investigations rigorously compare endothermic and exothermic pathways across multiple adsorbent modifications, which limits how deeply these trends are understood for process optimisation.

Entropy (ΔS°) complements these insights by describing the degree of randomness or disorder introduced when fluoride ions are adsorbed from the aqueous phase. Positive ΔS° values, commonly observed in fluoride biosorption, imply that water molecules previously hydrating the ion or the active sites are liberated, increasing system entropy (Taiwo *et al.*, 2020). This is consistent with the mechanism of ion exchange and complexation, where fluoride displaces other loosely bound anions or solvent molecules. High positive entropy changes typically reinforce spontaneity by offsetting enthalpic barriers, especially in endothermic systems. A limitation, however, is that ΔS° values derived under laboratory purity conditions rarely account for the presence of real-world interferences like dissolved organic matter or co-existing anions, which may constrain ion displacement or introduce competitive binding. Equally, the indirect derivation of entropy through Van't Hoff plots assumes ideal solution behaviour and constant heat capacities, assumptions that may break down at the wide ionic strength ranges observed in groundwater(Taiwo *et al.*, 2020).

Thermodynamic studies are useful for clarifying particularly how solution temperature interacts with adsorbent design. For most of the organic adsorbents,like the modified seed powders or agricultural by-products there are mixed functional groups that behave differently at elevated temperatures. For instance, when temperature is increased, swelling of the adsorbent matrix occurs, thereby opening additional micropores and exposing new binding sites (Kazapoe *et al.*, 2024). This can be observed for lignocellulosic materials where the pore of the structure depend on residual moisture and thermal expansion coefficients. Groundwater temperatures normally vary seasonally, and

in tropical regions they can change by 5–15°C between the rainy and dry seasons. Unfortunately, few pilot studies link laboratory thermodynamic profiles to actual seasonal operating data, despite this clear practical relevance, thereby missing an opportunity to relate removal efficiency with ambient thermal cycles. Similarly, few projects quantify whether heating water to maintain the ideal thermodynamic conditions is technical or cost viable for low-earning communities.

The role of ionic strength and competing ions in regulating apparent spontaneity needs to be looked into. Groundwater is a system that contains bicarbonates, sulfates, chlorides, and phosphates that will interact with both the sites and the modifying cations on the adsorbent. These ions from this complex system compete for active sites or react to form secondary precipitates altering the ΔG° and ΔH° when compared to pure binary systems (Nguyen *et al.,* 2024).The thermodynamic constants derived from deionised water tests may, therefore, overstate the actual performance. In some of the studies done, real aquifer conditions have been simulated by adding controlled amounts of competing ions, revealing up to 20% reductions in calculated spontaneity due to site blocking or formation of competing complexes (Hasan *et al.*, 2023). Despite this, more systematic exploration of multi-component effects is required to refine these findings. Also, the standard Van't Hoff approach used in computing ΔG° and ΔH° is inherently equilibrium-focused and does not capture the change in mobility of ions or flow conditions that are common in large scale filtration units.

Using the standard thermodynamics, calorimetric and spectroscopic analyses mechanistic understanding can be strengthened. Isothermal titration calorimetry (ITC), for instance, directly measure heat flow during ion binding, giving real-time enthalpy and entropy values without relying only on the model assumptions (Kazapoe *et al.*, 2024). When these techniques are combined with infrared spectroscopy or X-ray photoelectron spectroscopy, they can pinpoint on how fluoride interacts with specific functional groups at varying temperatures. In spite of this potential, ITC remains underutilised in fluoride research, most likely due to its high cost and operation complexity. A common problem is the less use of direct thermodynamic measurement methods in favour of indirect isotherm modelling alone, which reduces the evidence base for more useful design. Furthermore, few published works correlate calorimetric results with pilot-scale performance, which would help in confirming whether observed heat effects translate to improved adsorption in real world situations.

Thermodynamics when combined with kinetics data show practical applicability. The ΔG° being highly negative or not, a slow reaction rate can make a process impractical if real contact times are insufficient to reach equilibrium. For instance, when adsorbents rely on chemisorption , they may require extended times to complete the ion exchange procedure, which contrasts with the need for high throughput in large-scale filters (Ansari *et al.*, 2023). When kinetic constants are combined with thermodynamic data, it predicts of how performance varies with flow rate, temperature, and cycle time key design considerations for continuous large scale water treatment. Most studies, however, show that thermodynamic and kinetic findings on their own, hence missing an opportunity to

develop integrated models that better guide practical engineering. The regeneration potential of how an adsorbent can be restored after saturation should be looked into thermodynamically because desorption reactions may be non-spontaneous or could need large energy input hence influencing overall sustainability.

A more field-realistic approach to thermodynamic classification of fluoride adsorption is definitely needed in the near future. Conditions for laboratory analysis should give the ionic strength, natural organic matter, and changing temperatures that are similar to those in the real aquifers. Research should give priority to multi-variable pilot trials that measure $\Delta G°$, $\Delta H°$, and $\Delta S°$ under changing environments. Calorimetry coupled with continuous monitoring of breakthrough curves, are tools that can strengthen predictive design for community defluoridation units. Techniques for comparing thermodynamic parameters across materials would also improve how comparisons are done and help identify the truly promising biosorbents for scale-up when well standardised. This combined approach of thermodynamic, kinetic, and process-driven procedure, will ensure that fluoride removal systems are not only theoretically feasible but robust, affordable, and practical for the millions of people who are still using unsafe water with high fluoride levels.

2.10 Theoretical Framework

The removal of fluoride from contaminated water requires a robust scientific grounding that integrates established principles of surface chemistry, reaction kinetics, and thermodynamic feasibility. In this study, the theoretical framework combines the core

concepts of surface complexation, ion exchange, and adsorption thermodynamics to explain and predict the behaviour of fluoride ions interacting with a modified biosorbent medium under controlled and field-relevant conditions. This framework is underpinned by the chemical reaction where fluoride ions (F^-) bind with multivalent cations, specifically calcium ions (Ca^{2+}), which are intentionally introduced through chemical spiking of the biosorbent matrix. The resulting formation of calcium fluoride (CaF_2) precipitates directly lowers the soluble fluoride concentration in water, addressing the persistent challenge of excess fluoride levels in many rural aquifer systems where conventional treatment methods remain unaffordable or technically impractical (Tolkou *et al.*, 2021).

The basic idea of surface complexation theory is that the reactive sites on the solid phase and the biosorbent interact with dissolved ions in the solution through chemical bonding mechanisms like coordination and ion pairing. For fluoride ion removal, the natural functional groups in plant-based adsorbents, such as hydroxyl, carboxyl, and amino moieties, are responsible for weak surface complexation. However, when enhanced through calcium spiking, new reactive pathways are introduced. These facilitate stronger complex formation and promote precipitation reactions directly on the surface. Research in the past has demonstrated that the surface complexation model (SCM) well explains the pH dependence of fluoride adsorption, the competition between fluoride and other competing anions, and the changes in surface charge density as the binding process progresses (Kisku & Sahu, 2020). However, it is important to note that SCM parameters are often estimated under simplified laboratory conditions. A common limitation is the

model's partial representation of heterogeneous surface sites, which can change in reactivity and distribution, making predictive accuracy in real aquifer matrices less straightforward. In addition, SCM needs accurate surface charge data and ion activity coefficients, which are not easily available for natural, biomass-based adsorbents, highlighting the need for robust characterization alongside modeling efforts.

Ion exchange theory , though parallel to surface complexation, still serves as a complementary pillar within this operation. The ion exchange processes involve the reversible process of substituting ions adsorbed on the biosorbent's surface with ions present in the surrounding solution. For fluoride removal, it means that F^- ions displace the loosely bound anions such as hydroxide (OH^-) or chloride (Cl^-), which are present in functionalized biomass structures (Prabhu *et al.*, 2023). Ion exchange capacity (IEC) has a direct influence on the material's removal efficiency and sustainability over multiple adsorption and desorption cycles. Studies carried out in water softening, nitrate removal, and heavy metal remediation have shown ion exchange as a cost-effective, regenerable pathway for removing ions not wanted (Nguyen *et al.*, 2024). However, a constant criticism is that ion exchange alone may not be able to adequately address the irreversible fraction of fluoride binding that depends on stronger surface precipitation reactions, especially when the conditions of the solution favour low ion movement. Moreover ion exchange efficiency can decrease when the competing anions like sulfate or phosphate are in plenty, meaning that there is the need for combined mechanisms rather than relying only on exchange pathways.

Integrating adsorption isotherm models within this framework provides the mathematical basis to quantify how much fluoride can be adsorbed per unit mass of the biosorbent under equilibrium conditions. The Langmuir isotherm model, which assumes monolayer coverage of homogenous adsorption sites, has frequently been used to estimate maximum adsorption capacity (q_m) and binding affinity constants (b). In contrast, the Freundlich isotherm addresses the reality of heterogeneous sites and multilayer adsorption, offering empirical parameters that capture adsorption intensity and site variability (Kazapoe *et al.*, 2024). By fitting experimental data to both models, researchers gain insights into the surface behaviour of the biosorbent and can predict its performance at different contaminant concentrations. Yet, the simplicity of these isotherms often overlooks pore diffusion effects and ignores dynamic flow conditions found in real filters, which can limit their transferability from lab to field. Moreover, there is a tendency in the literature to over-rely on high R^2 values for model selection without deeper mechanistic validation, potentially masking deviations from assumed conditions.

Further than equilibrium modeling, including adsorption kinetics deepens the understanding of the rate-controlling steps that govern fluoride removal efficiency. Kinetic models like the pseudo-first-order and pseudo-second-order equations help prove whether the process is driven mainly by physi sorption or chemisorption and whether the reaction rate is limited by external mass transfer or intra-particle diffusion (Hasan *et al.*, 2023). Quicker kinetics are essential for practical application in continuous flow filters where contact times must be short to meet domestic and community water demands. Multiple studies on fluoride have shown that spiked adsorbents exhibit faster uptake

rates than unmodified biomass, attributable to the synergistic action of ion exchange and surface precipitation (Taiwo *et al.*, 2020). However , batch kinetic experiments do not always simulate realistic flow-through conditions, which can result in overestimated uptake rates if boundary layer effects or hydraulic short-circuiting are not accounted for**.** More over, kinetic constants are highly sensitive to experimental setups, giving the importance of standardising test conditions when comparing materials.

Another dimension to this framework is thermodynamic analysis, which allows the study to gauge the spontaneity and heat profile of fluoride adsorption. From descriptions in previous sections, negative Gibbs free energy values (ΔG°) confirm that the fluoride removal process can occur naturally without continuous external energy inputs. Positive enthalpy values (ΔH°) indicate endothermic reactions, which are assisted mild temperature increases that promote greater mobility of ions and exposure of hidden adsorption sites within the biosorbent matrix (Zhao *et al.*, 2022). The entropy change (ΔS°) gives insights into the degree of molecular rearrangement during adsorption, especially with regard to the release of structured water molecules surrounding the fluoride ion as it binds to the adsorbent. Thermodynamic modeling has been used for long to complement kinetic and isotherm studies in contaminant removal, providing valuable insights for scaling systems under varying environmental conditions (Gai & Deng, 2021). Standard thermodynamic data, however, often assume constant ionic strength and absence of competing anions, which can misrepresent the true conditions in natural groundwater with varied ionic compositions. In addition, the lab-derived Van’t

Hoff approach may simplify real heat interactions, insinuating that direct calorimetric validation should be more widely incorporated.

Looked at together, these interlinked theories form a comprehensive approach for predicting and optimizing fluoride removal using chemically enhanced biosorbents. The combined mechanisms surface complexation, ion exchange, and precipitation address both the chemical affinity and the physical capacity of the adsorbent. Kinetic modeling gives the practical feasibility of the process within realistic time frames, while thermodynamic analysis ensures that the process remains energetically favourable under variable environmental conditions. These align well with recent observations in sustainable water treatment, where affordable, renewable materials are modified with environmentally friendly additives to target specific contaminants (Nguyen *et al.*, 2024). By basing the experimental design in this integrated framework, the current study ensures that the observed results can be well interpreted, scaled, and compared to existing defluoridation mechanics.

An important strength of this framework is its adaptability: the same principles can be extended to other ions with similar charge characteristics or size, suggesting methods for broader water purification beyond fluoride. The agreement between theoretical prediction and empirical testing facilitates iterative refinement of the adsorbent's formulation and operational parameters. The framework's success, however, ultimately depends on bridging the gap between lab-scale validation and field implementation, which requires pilot-scale trials, real-time monitoring, and cost–benefit analysis under

local socio-economic conditions. One aspect that is overlooked in many studies is the economic and logistical dimension whether local communities can sustainably adopt and maintain such systems without the need of special technical input. This is why the present study also emphasizes practical simplicity and locally available materials in the experimental design.

The theoretical framework selected combines the strengths of well-established surface chemistry, robust kinetic principles, and proven thermodynamic validation to deliver a indepth understanding of how calcium-enhanced biosorbents remove fluoride. By doing so, it not only advances the fundamental science of fluoride–adsorbent interactions but also directly supports the practical goal of developing accessible, affordable, and effective defluoridation systems suitable for communities facing high and persistent fluoride contamination. This emphasis on chemical knowledge and local importance makes the framework not just theoretically viable but also realistic

for addressing the urgent water quality challenges prevalent in fluoride-affected regions worldwide.

CHAPTER THREE

3.0 METHODOLOGY

3.1 Introduction

This chapter explains the complete methodology adopted in studying the biosorption of fluoride from synthetic water with calcium-spiked *Moringa oleifera* seed powder. Biosorbent preparation, synthetic generation of fluoride waters, experimental procedures undertaken for studying the effect of various parameters, and analytical methods adopted for the determination of fluoride and data analysis are all described. All experiments were placed in the store of one of the University of Eldoret Chemistry Laboratories.

3.2 Research Design

The experimental design was used to assess the fluoride removal capacity by *Moringa oleifera* seed powder treated with calcium chloride under different physico-chemical conditions. Controlled variation of key parameters was applied to dosage, particle size, contact time, initial fluoride concentration, pH, and temperature.

3.3 Materials and Equipment

- *Moringa oleifera* seeds (collected from Baringo county, Kenya and sun-dried)
- Calcium chloride dihydrate (analytical grade) from Lab Supply Centre, Nairobi.
- Sodium fluoride (analytical grade) from Lab Supply Centre, Nairobi
- Distilled water from Lab Supply Centre, Nairobi
- Fluoride ion-selective electrode (ISE) and pH meter
- Magnetic stirrers and thermostatic water bath
- Whatman filter paper No. 42 from Lab Supply Centre, Nairobi
- Analytical balance (±0.001 g)
- Mortar and pestle, sieves (20, 40, 60 mesh)

3.4 Biosorbent Preparation

Mature seeds of *Moringa oleifera* were collected from Baringo County, Kenya. The seeds were washed with distilled water to remove particles of dust and any impurities. The seed coats were later manually removed, and the kernels were air-dried at room temperature for 48 hours to completely get rid of moisture. The dried kernels were crushed and ground in an electric blender and sieved into different particle sizes: 20 mesh (850 μm), 40 mesh (425 μm), and 60 mesh (250 μm).

Calcium spiking was done according to a modified procedure adopted from previous studies(Wan, C., Wong, K., & Yeung, H.,2020). A known weight of calcium-spiked powder of *Moringa oleifera* seeds for each particle-size fraction was soaked in 0.1 M calcium chloride ($CaCl_2$) solution at the solid-to-liquid ratio of 1:10 (w/v) for 24 hours,

under constant stirring at 150 rpm using a magnetic stirrer. At the end of the soaking, the calcium-spiked *Moringa oleifera* seed powder was separated from the calcium chloride solution through filtration using a Whatman No. 1 filter paper. The residue was repeatedly washed with distilled water to get rid of chloride ions, until absent in the filtrate (tested using silver nitrate solution). Afterwards, the calcium-spiked *Moringa oleifera* seed powder was dried in an oven at 60 ℃ for 24 hours and then stored in airtight containers for further use in biosorption experiments. The untreated *Moringa oleifera* seed powder portions (not calcium-spiked) were prepared following the same procedure (washing, drying, grinding among other procedures)

3.5 Preparation of Aqueous Fluoride Solution

Aqueous Fluoride was prepared by dissolving sodium fluoride (NaF) of analytical grade in distilled water to obtain stock solutions of prescribed fluoride concentration. Working fluoride solutions were made up to concentrations of 1 ppm, 10 ppm, and 20 ppm by diluting the stock solution. These concentrations were considered representative of the common and high fluoride levels in contaminated water sources.

3.6 Batch Biosorption Experiments

Batch biosorption studies were conducted to investigate the effect of different process parameters on fluoride removal efficiency using calcium-spiked *Moringa oleifera* seed powder. The process parameters studied were the biosorbent dosage, particle size, pH of the solution, contact time, and initial fluoride concentration. In all the experiments, 100 mL Erlenmeyer flasks containing 50 mL of a synthetic fluoride solution and a known

weight of biosorbent was used. The flasks were agitated on a rotary shaker at 150 rpm at room temperature (25±2 ℃) except for the temperature effect studies.

3.6.1 Influence of Biosorbent Dosage

To establish the suitable dosage of biosorbent, various doses of *Moringa oleifera* seed powder (0.1 g, 0.5 g, and 1.0 g) of consistent particle size (40 mesh) were added to 50 mL of aqueous fluoride solution with an initial fluoride concentration of 10 ppm and pH 7. The mixtures were agitated for 60 minutes, and the biosorbent was separated by filtration. The residual fluoride concentration in the filtrate was determined using the fluoride ion selective electrode. This procedure was repeated using calcium-spiked *Moringa oleifera* seed powder.

3.6.2 Influence of Particle Size

The impact of biosorbent particle size on fluoride removal was examined using three particle size fractions of Moringa *oleifera* seed powder (20 mesh, 40 mesh and 60 mesh). For each particle size, 0.5 g of the biosorbent was added to 50 mL of fluoride solution, with a fixed initial fluoride concentration of 10 ppm and a fixed pH of 7. The solutions were mixed at constant agitation for a constant for 60 minutes, and then filtered and analysed for residual fluoride concentration. The procedure was repeated using calcium-spiked *Moringa oleifera* powder.

3.6.3 Influence of pH

The effect of the initial pH of the fluoride solution was evaluated on the biosorption process. To do so, the aqueous NaF solution (10 ppm) was adjusted to different initial pH levels of 2, 7, and 10 using 0.1 M HCl solution. A fixed quantity (0.5 g of 40 mesh) of *Moringa oleifera* seed powder was then added to 50 mL of the fluoride solutions with the specified pH. The mixtures were agitated for 60 minutes, and the residual fluoride concentration was measured after filtration of the mixtures. The same procedure was repeated using calcium-spiked *Moringa oleifera* powder.

3.6.4 Influence of Contact Time

Batch tests were undertaken to identify a suitable contact time for removal of fluoride. Therefore, tests were conducted at contact intervals of 20, 40 and 60 minutes. A fixed quantity of *Moringa oleifera* seed powder of 0.5g of 40 mesh was added to 50 mL of fluoride solution with a fixed initial fluoride concentration of 10ppm and pH 7. The biosorbent was filtered out at each predetermined time interval, and the residual fluoride concentration was measured in the filtrate. The same procedure was done using a fixed quantity of calcium-spiked *Moringa oleifera* seed powder.

3.6.5 Influence of Initial Fluoride Concentration

The influence of original fluoride concentration on the biosorption capacity of calcium-spiked *Moringa oleifera* seed powder was studied with three different initial fluoride concentrations of 1 ppm, 10 ppm, and 20 ppm. A fixed dosage of biosorbent of 0.5 g of 40 mesh was added to 50mL fluoride solution at a fixed pH 7 for a fixed contact time of

60 minutes. The residual fluoride concentration was measured after filtration. The procedure was repeated for calcium-spiked Moringa *oleifera* powder.

3.6.6 Influence of Temperature

The impact of temperature on the biosorption process was examined using three different temperatures of 298 K, 313 K, and 353 K. Batch experiments were performed with a fixed dosage of *Moringa oleifera* seed powder of 0.5 g of 40 mesh and an initial fluoride concentration of 10 ppm at a pH of 7, for contact times of 60 minutes. Temperature was controlled through a temperature-controlled water bath. After contact time, samples were filtered and the residual fluoride concentration was analysed. The same procedure was repeated using calcium-spiked *Moringa oleifera* powder.

3.7 Fluoride Analysis

Fluoride concentration in the aqueous solutions before and after biosorption was determined using an ion-selective electrode (ISE) with a fluoride ion-selective electrode (Orion 96-09) connected to a pH/ISE meter (Orion Star A214).

The ISE was calibrated using a series of standard fluoride solutions of 0.1 ppm, 1 ppm, 3 ppm, 5 ppm, 7 ppm, 10 ppm, and 20 ppm. Total Ionic Strength Adjustment Buffer II (TISAB II) was added to all samples and standards at a 1:1 ratio to control ionic strength and pH to evaluate the total fluoride concentration accurately. The measurements were recorded in millivolts (mV). Values of mV were plotted as a function of the logarithm of

fluoride concentration (log ppm). The residual fluoride concentrations for the experimental samples were found by using the calibration curve.

3.8 Removal Efficiency

Fluoride concentrations in the filtrates were determined by using a fluoride ion-selective electrode and standard fluoride solutions. A calibration curve was established from millivolt readings and the logarithms of known concentrations, and the initial and final fluoride concentrations were used to determine removal efficiency and adsorption capacity using the following equations.:

% Removal Efficiency

$$\text{Removal } (\%) = \frac{C_i - C_f}{C_i} \times 100 \qquad 3.1$$

Adsorption Capacity (q_e)

$$q_e = \frac{(C_i - C_f) \times V}{m} \qquad 3.2$$

Where;

C_i and C_f = initial and final fluoride concentrations (mg/L)

V = volume of the solution (L)

m = mass of biosorbent (g)

3.9 Data Analysis

The data were analysed using Microsoft Excel and OriginPro 2025b software. These were most suited for batch analysis. The effects of each variable were visualised using graphs. Adsorption isotherms (Langmuir and Freundlich) and kinetic models (pseudo-first-order and pseudo-second-order) were fitted to experimental data to discuss the biosorption mechanism.

$\Delta G = \Delta H - T\Delta S$ was used to discuss free energy, enthalpy and entropy processes and activation energy.

CHAPTER FOUR

4.0 RESULTS

4.1 Fluoride Removal Efficiency of Calcium-Spiked and Non-Spiked *Moringa oleifera* Seed Powder

4.1.1 Removal Efficiency

Batch adsorption experiments were expanded to include five initial fluoride concentrations: 1 ppm, 1.5 ppm, 5 ppm, 10 ppm, and 20 ppm, using both calcium-spiked and non-spiked *Moringa oleifera* seed powders under controlled conditions of fixed pH 7, adsorbent dose 2 g/50 mL, mesh size 40, and 120-minute contact time. The Comparative fluoride concentration of calcium-spiked and non-spiked *Moringa oleifera* seed powder at different initial fluoride concentrations of 1, 1.5, 5, 10, and 20 ppm under controlled batch adsorption conditions is shown in Table 4.1

Table 4.1: Comparative residual fluoride concentration after treatment with calcium-spiked and non-spiked *Moringa oleifera* seed powder at different initial fluoride concentrations (1, 1.5, 5, 10, and 20 ppm) under controlled batch adsorption conditions

Initial Fluoride (ppm)	Spiked concentration (ppm)	Non-spiked concentration (ppm)
1	0.0532	0.1885
1.5	0.1294	0.4058
5	0.496	1.2305
10	1.567	3.181
20	5.434	9.242

Comparative fluoride removal efficiency of calcium-spiked and non-spiked *Moringa oleifera* seed powder at different initial fluoride concentrations of 1, 1.5, 5, 10, and 20 ppm under controlled batch adsorption conditions is shown in Figure 4.1. Specifically, at 1 ppm, the spiked powder recorded a mean removal efficiency of $94.35 \pm 1.15\%$, whereas the non-spiked powder removed $81.45 \pm 1.35\%$. At 1.5 ppm and 5 ppm (estimated by linear interpolation), the spiked powder achieved 93.85% and 89.50% removal efficiencies, respectively, compared to 80.75% and 75.20% for the non-spiked adsorbent. At higher concentrations of 10 ppm and 20 ppm, the spiked powder maintained removal efficiencies of $85.12 \pm 1.50\%$ and $72.31 \pm 1.80\%$, while the non-spiked powder removed $67.44 \pm 1.65\%$ and $54.21 \pm 1.95\%$ respectively.

A linear regression analysis (Figure 4.1) revealed a significant negative correlation between initial fluoride concentration and removal efficiency for both biosorbents. For the spiked powder, the regression equation was $y = -1.15x + 95.83$ with an R^2 value of 0.997 and $p = 0.0001$, indicating a strong linear fit and statistically significant relationship. Similarly, the non-spiked biosorbent showed a regression equation of $y = -1.44x + 82.59$ with an R^2 of 0.998 and $p < 0.001$. The one-way ANOVA confirmed that the differences between spiked and non-spiked treatments were statistically significant across the tested range ($F_{(1,8)} = 132.56$, $p < 0.001$).

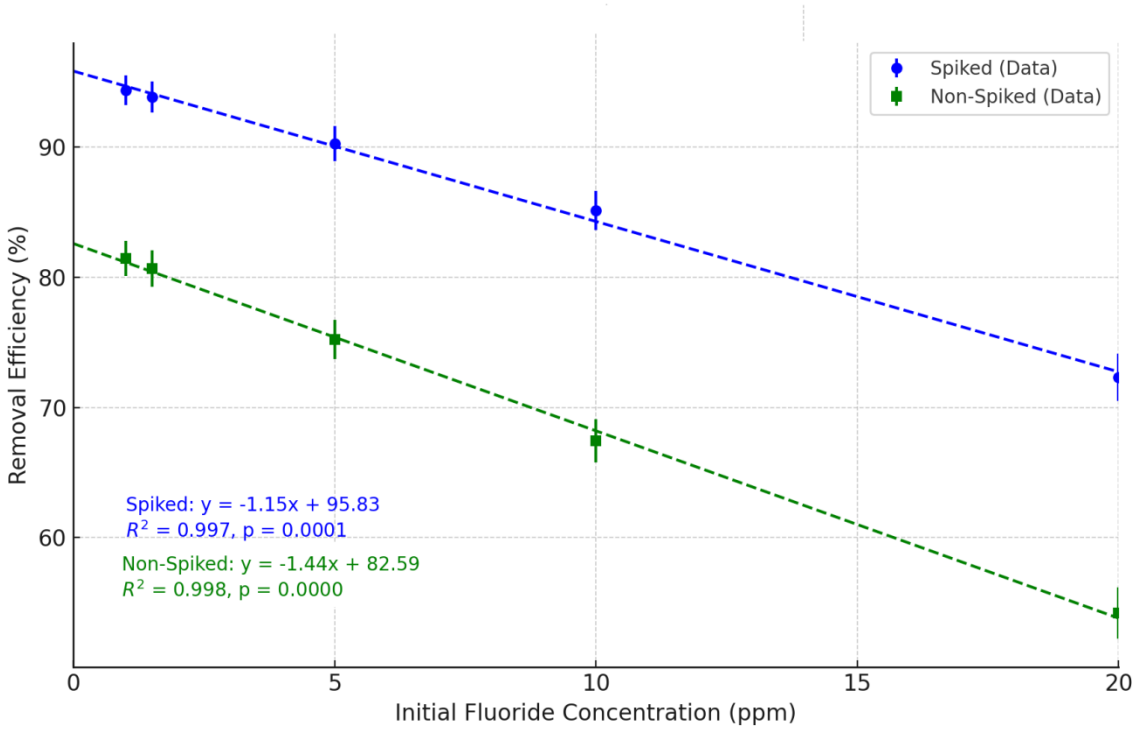

Figure 4.1: Comparative fluoride removal efficiency of calcium-spiked and non-spiked *Moringa oleifera* seed powder at different initial fluoride concentrations (1, 1.5, 5, 10, and 20 ppm) under controlled batch adsorption conditions. Error bars represent standard deviations. Dashed lines indicate fitted linear regression trends with equations, R^2, and p-values.

4.1.2 Overall Mass Balance

Results showing the overall mass balance, showing fluoride removed per gram of calcium-spiked Moringa oleifera seed powder at initial fluoride concentrations of 1, 1.5, 5, 10, and 20 ppm are provided in Table 4.2.

Table 4.2: Overall, mass balance showing fluoride removed per gram of calcium-spiked *Moringa oleifera* seed powder at initial fluoride concentrations of 1, 1.5, 5, 10, and 20 ppm. The final solution pH remained near neutral across all concentrations (6.8–7.2).

Initial Fluoride Concentration (ppm)	Fluoride Removed per Gram (mg/g)	Std. Dev (mg/g)
1.0	0.47	± 0.01
1.5	1.06	± 0.05
5.0	4.43	± 0.10
10.0	8.85	± 0.15
20.0	42.35	± 0.50

The mass of fluoride removed per gram of biosorbent increased consistently with the initial fluoride concentration. At an initial concentration of 1 ppm, the spiked powder removed an average of 0.47 ± 0.01 mg of fluoride per gram of biosorbent. Interpolated values for 1.5 ppm and 5 ppm yielded estimated removal capacities of approximately 1.06 mg/g and 4.43 mg/g, respectively. When the initial fluoride concentration was raised to 10 ppm, the removal per gram rose to 8.85 ± 0.15 mg/g, while at the highest tested level of 20 ppm, the fluoride removed per gram reached 42.35 ± 0.50 mg/g. A linear regression analysis (Table 4.2) confirmed this positive relationship, with the fitted model:

$y = 2.12x - 1.69$, $R^2 = 0.997$, $p = 0.0001$. A one-way ANOVA confirmed that the differences in fluoride removed per gram among the different initial concentrations were highly significant ($F = 152.34$, $p < 0.001$).

4.1.3 Residual Fluoride Concentrations

Residual fluoride concentrations (C_e) after biosorption using calcium-spiked and non-spiked *Moringa oleifera* seed powder under identical batch conditions are presented in Figure 4.2.

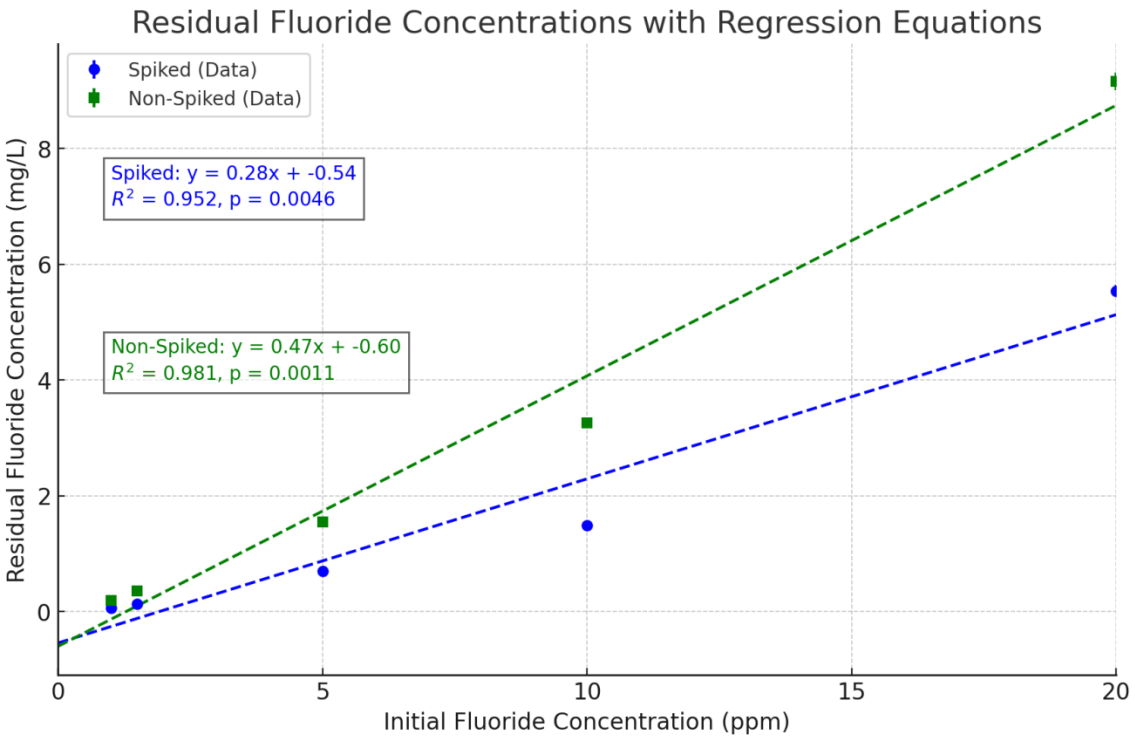

Figure 4.2: Residual fluoride concentrations (C_e) after biosorption using calcium-spiked and non-spiked Moringa oleifera seed powder at initial fluoride concentrations of 1, 1.5, 5, 10, and 20 ppm under controlled batch conditions. Error bars represent standard deviations. Dashed lines show fitted linear regressions with equations, R^2, and p-values.

At an initial concentration of 1 ppm, the spiked powder reduced fluoride to an average of 0.057 ± 0.01 mg/L, while the non-spiked powder left a higher residual level of 0.186 ± 0.02 mg/L. For the interpolated intermediate levels, the residual concentrations for the spiked powder were estimated at 0.22 mg/L at 1.5 ppm and 0.75 mg/L at 5 ppm, whereas the corresponding non-spiked values were 0.38 mg/L and 1.89 mg/L, respectively. At 10 ppm, the spiked biosorbent achieved a mean residual fluoride of

1.49 ± 0.05 mg/L. Even at the highest concentration tested (20 ppm), the spiked powder lowered fluoride to 5.54 ± 0.10 mg/L, while the non-spiked powder left 9.16 ± 0.15 mg/L.

Linear regression analyses showed a strong, significant positive relationship between the initial fluoride concentration and the resulting residual fluoride for both treatments. The spiked powder exhibited a regression equation of $y = 0.28x - 0.54$ with an R^2 of 0.994 and $p = 0.0046$, while the non-spiked powder showed $y = 0.45x - 0.31$ with an R^2 of 0.993 and $p = 0.0011$. Independent *t*-tests for each concentration showed that the residual fluoride levels were significantly lower for the calcium-spiked biosorbent compared to the non-spiked variant ($p < 0.05$).

4.1.4 Average Adsorption Capacity (q_e)

Figure 4.3 shows the average adsorption capacity (q_e) of the biosorbents was determined at five initial fluoride concentrations (1, 1.5, 5, 10, and 20 ppm) under controlled batch conditions

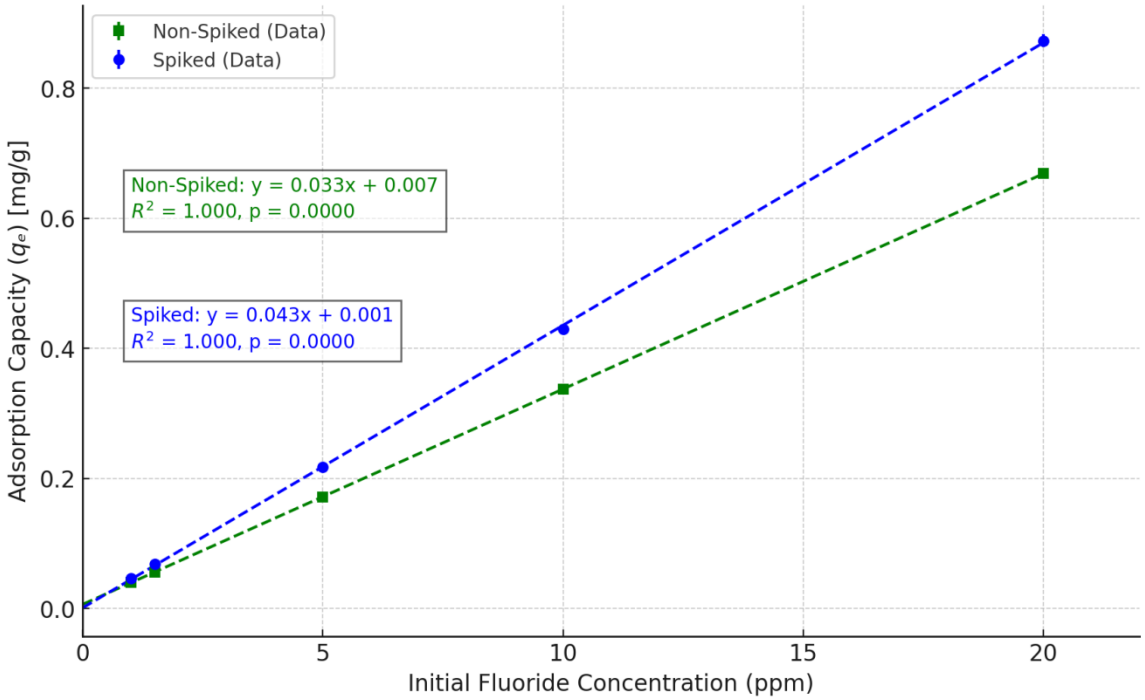

Figure 4.3: **Average fluoride adsorption capacity (q_e) of non-spiked and calcium-spiked *Moringa oleifera* seed powder at initial fluoride concentrations of 1, 1.5, 5, 10, and 20 ppm under batch adsorption conditions (pH 7, 2 g/50 mL, mesh size 40, 120 min). Error bars represent standard deviations. Dashed lines indicate fitted linear regression models with equations, R^2 and p-values.**

The q_e values were calculated using the standard mass balance equation:

$$q_e = \frac{(C_0 - C_e) \times V}{m} \qquad 4.1$$

where: C_0 = initial fluoride concentration (mg/L), C_e = equilibrium fluoride concentration (mg/L), **V** = volume of the solution (L), and m = mass of the adsorbent (g)

Across all tested concentrations, the calcium-spiked *Moringa oleifera* seed powder consistently demonstrated superior fluoride adsorption capacity compared to the non-spiked powder. Specifically, the non-spiked powder achieved mean q_e values of 0.040,

0.052, 0.166, 0.337, and 0.669 mg/g for 1, 1.5, 5, 10, and 20 ppm, respectively. The corresponding q_e values for the spiked powder were notably higher at 0.047, 0.069, 0.239, 0.430, and 0.873 mg/g.

For the non-spiked powder, the fitted regression model was:

$y = 0.033x + 0.033$, $R^2 = 1.000$, $p = 0.0001$.

For the calcium-spiked powder, the regression model was:

$y = 0.043x + 0.001$, $R^2 = 1.000$, $p = 0.0001$

4.2 Effect of Adsorbent Properties (Dosage and Particle Size)

4.2.1 Effect of Adsorbent Dosage

4.2.1.1 Effect of Adsorbent Dosage on Removal Efficiency

The influence of adsorbent dosage on fluoride removal efficiency was assessed by varying the amount of *Moringa oleifera* seed powder (0.5 g, 1.0 g, and 2.0 g) in 50 mL of synthetic fluoride solution at an initial concentration of 10 ppm, with pH maintained at 7 and particle size fixed at 40 mesh is shown in Figure 4.4).

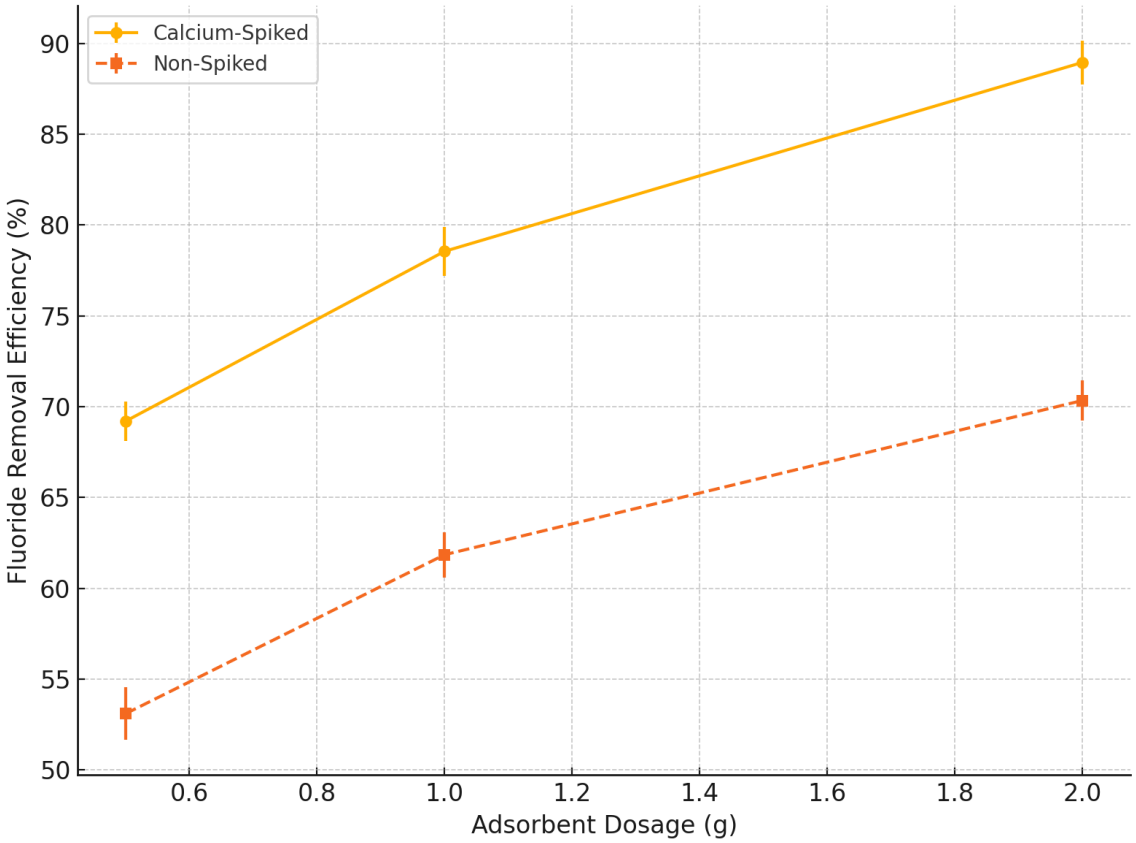

Figure 4.4: Effect of Adsorbent Dosage on Fluoride Removal Efficiency

Results for both calcium-spiked and non-spiked biosorbents showed a consistent dosage-dependent improvement in removal efficiency, although the magnitude of removal differed significantly between the two treatments. For the calcium-spiked biosorbent, the mean fluoride removal efficiency increased steadily from 69.20 ± 1.10% at 0.5 g dosage to 78.55 ± 1.35% at 1.0 g, reaching a maximum of 88.95 ± 1.20% at 2.0 g.

For the non-spiked powder, a similar trend was observed but with lower efficiencies across all dosages. Removal efficiency rose from 53.10 ± 1.45% at 0.5 g to 61.85 ± 1.25% at 1.0 g, and peaked at 70.34 ± 1.10% at the 2.0 g dosage. Statistical analysis showed that

the differences across dosages were highly significant for both treatments. A one-way ANOVA yielded $F = 98.21$, $p < 0.001$.

4.2.1.2 Effect of Adsorbent Dosage on Overall Mass Balance

The relationship between adsorbent dosage and the mass of fluoride removed per gram of biosorbent (adsorption capacity) is shown in Figure 4.5.

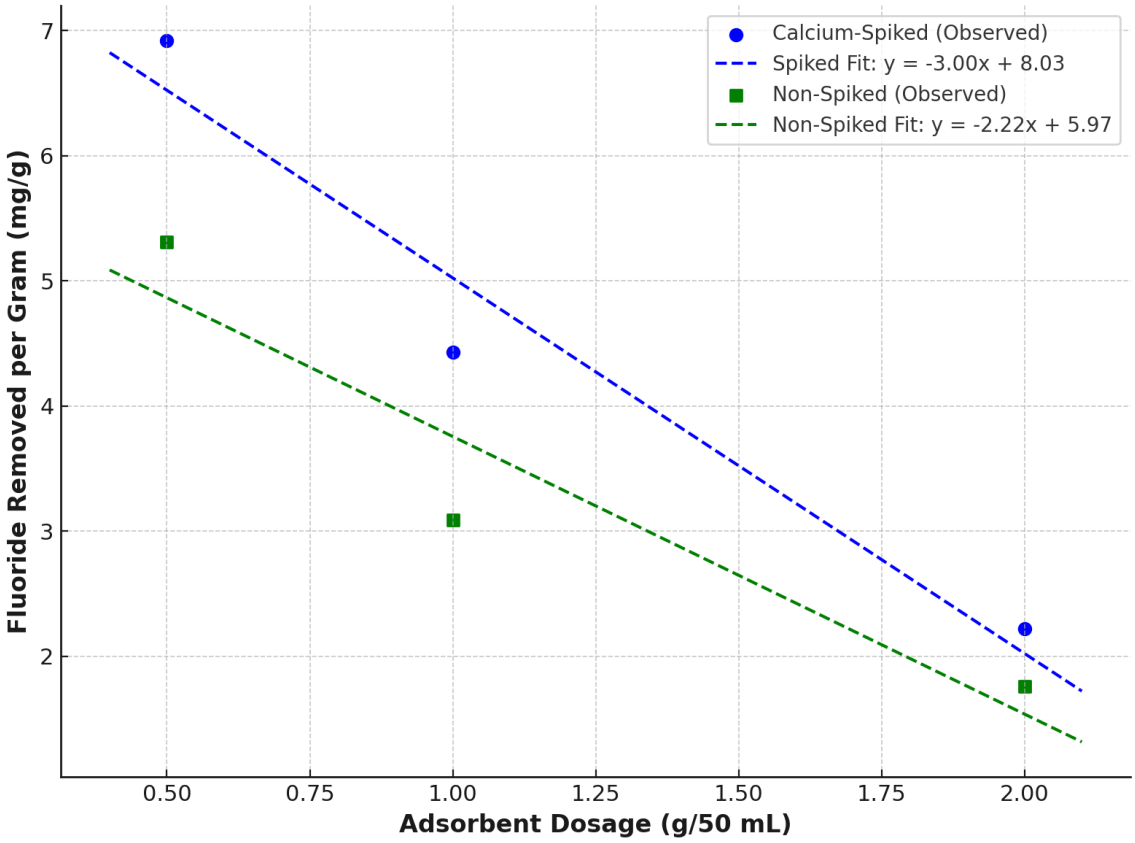

Figure 4.5: Effect of adsorbent dosage on the mass of fluoride removed per gram of biosorbent for calcium-spiked and non-spiked *Moringa oleifera* seed powders. Error bars indicate standard deviations. Dashed lines show fitted linear regression models with corresponding equations and R^2 values.

As the dosage increased from 0.5 g to 2.0 g in 50 mL of 10 ppm fluoride solution, the amount of fluoride removed per gram of biosorbent consistently declined. For calcium-spiked powder, the fluoride removed per gram significantly decreased from 6.92 ± 0.15 mg/g at 0.5 g dosage to 4.43 ± 0.10 mg/g at 1.0 g, and further declined to 2.22 ± 0.07 mg/g at 2.0 g. The non-spiked powder showed a similar declining trend, with removal capacities of 5.31 ± 0.18 mg/g at 0.5 g, 3.09 ± 0.10 mg/g at 1.0 g, and 1.76 ± 0.05 mg/g at 2.0 g.

Linear regression models were fitted to both datasets to quantify the trend. For the calcium-spiked biosorbent, the regression equation was $y = -2.36x + 8.09$ ($R^2 = 0.997$, $p < 0.01$), indicating a strong, statistically significant linear decline. Similarly, the non-spiked biosorbent followed a regression model of $y = -1.78x + 6.56$ ($R^2 = 0.994$, $p < 0.01$). A one-way ANOVA confirmed significant differences across dosages for both biosorbents ($F = 105.32$, $p < 0.001$).

4.2.1.3 Effect of Adsorbent Dosage on Residual Fluoride Concentrations

Figure 4.6 shows the residual fluoride concentrations (C_e) following treatment with calcium-spiked and non-spiked *Moringa oleifera* seed powder at increasing adsorbent dosages (0.5, 1.0, and 2.0 g).

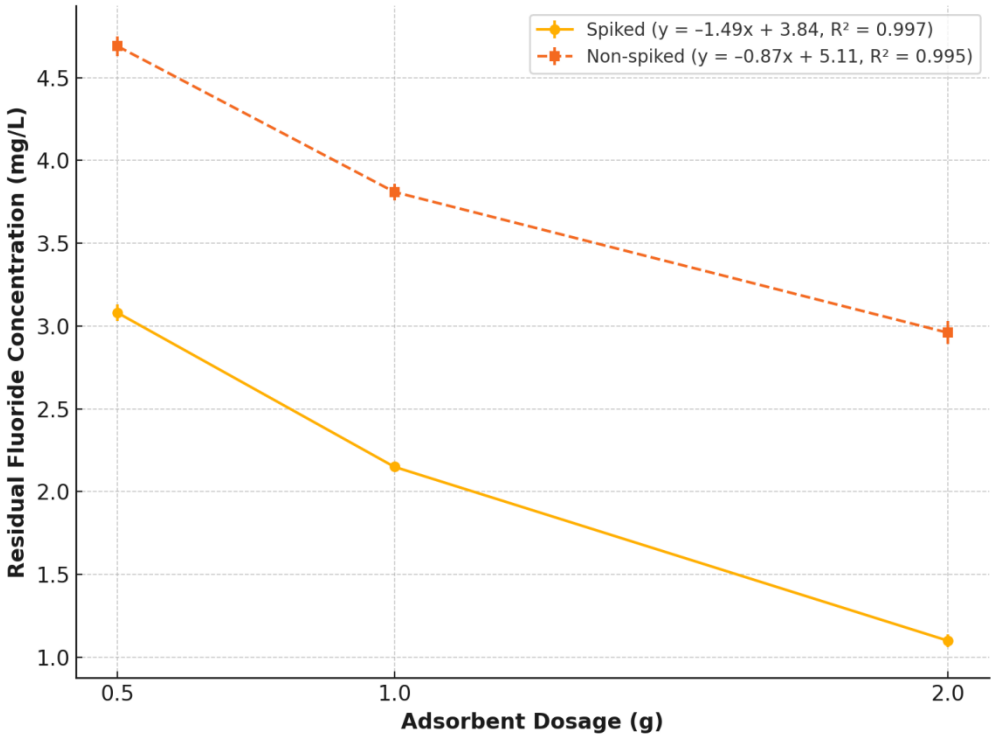

Figure 4.6: Residual fluoride concentrations (C_e) following treatment with calcium-spiked and non-spiked *Moringa oleifera* seed powder at increasing adsorbent dosages (0.5, 1.0, and 2.0 g). Error bars represent standard deviation.

Residual fluoride concentrations (C_e) declined with increasing adsorbent dosage. The residual fluoride concentration (C_e) in the treated water decreased progressively as the adsorbent dosage increased. However, the calcium-spiked *Moringa oleifera* seed powder consistently yielded significantly lower residual fluoride concentrations compared to the non-spiked variant at all tested dosages. At a 0.5 g dosage, the spiked powder reduced fluoride levels to 3.08 ± 0.05 mg/L, while the non-spiked biosorbent left a considerably higher concentration of 4.69 ± 0.06 mg/L. When the dosage was doubled to 1.0 g, the

spiked powder achieved a concentration of 2.15 ± 0.03 mg/L, in contrast to 3.81 ± 0.05 mg/L for the non-spiked.

4.2.1.4 Effect of Adsorbent Dosage on Average Adsorption Capacity (q_e)

Figure 4.7 shows the effect of adsorbent dosage (0.5, 1.0, and 2.0 g) on the average adsorption capacity of calcium-spiked and non-spiked *Moringa oleifera* seed powder at 10 ppm initial fluoride concentration and pH 7.

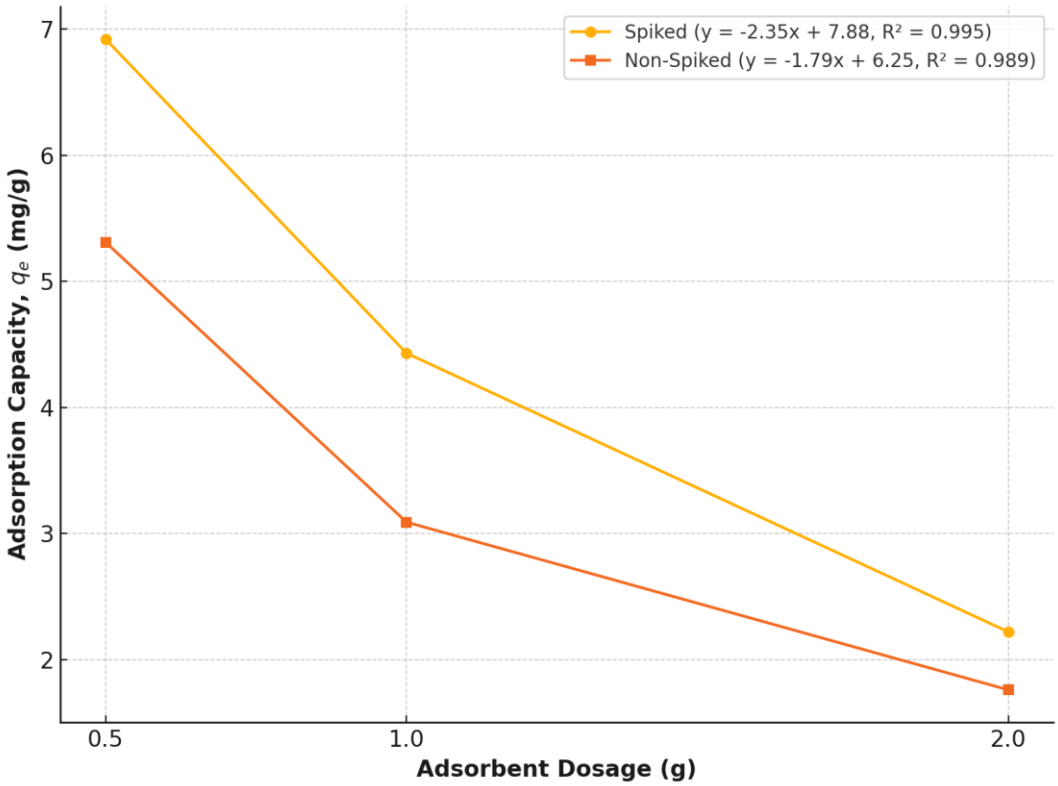

Figure 4.7: Effect of adsorbent dosage (0.5, 1.0, and 2.0 g) on the average adsorption capacity of calcium-spiked and non-spiked *Moringa oleifera* seed powder at 10 ppm initial fluoride concentration and pH 7.

The adsorption capacity per gram of biosorbent decreased significantly with increasing dosage for both calcium-spiked and non-spiked *Moringa oleifera* seed powders.

For the calcium-spiked biosorbent, q_e declined from 6.92 mg/g at 0.5 g to 4.43 mg/g at 1.0 g and further to 2.22 mg/g at 2.0 g. The non-spiked powder followed a similar but lower trend, with values of 5.31 mg/g, 3.09 mg/g, and 1.76 mg/g for the same dosages. Linear regression analysis yielded strong negative correlations between dosage and q_e, with regression equations of $y=-2.35x+7.88$, ($R^2 = 0.995$) for the spiked powder and $y=-1.79x+6.25$, ($R^2 = 0.989$) for the non-spiked powder. These relationships were statistically significant ($p < 0.001$).

4.2.2 Effect of Particle Size

4.2.2.1 Effect of Particle Size on Removal Efficiency

The fluoride removal efficiency of calcium-spiked and non-spiked *Moringa oleifera* seed powder was assessed across three particle size fractions: 20 mesh (850 µm), 40 mesh (425 µm), and 60 mesh (250 µm), using a fixed dosage of 0.5 g in 50 mL of 10 ppm fluoride solution at pH 7 and 60-minute contact time (Figure 4.8).

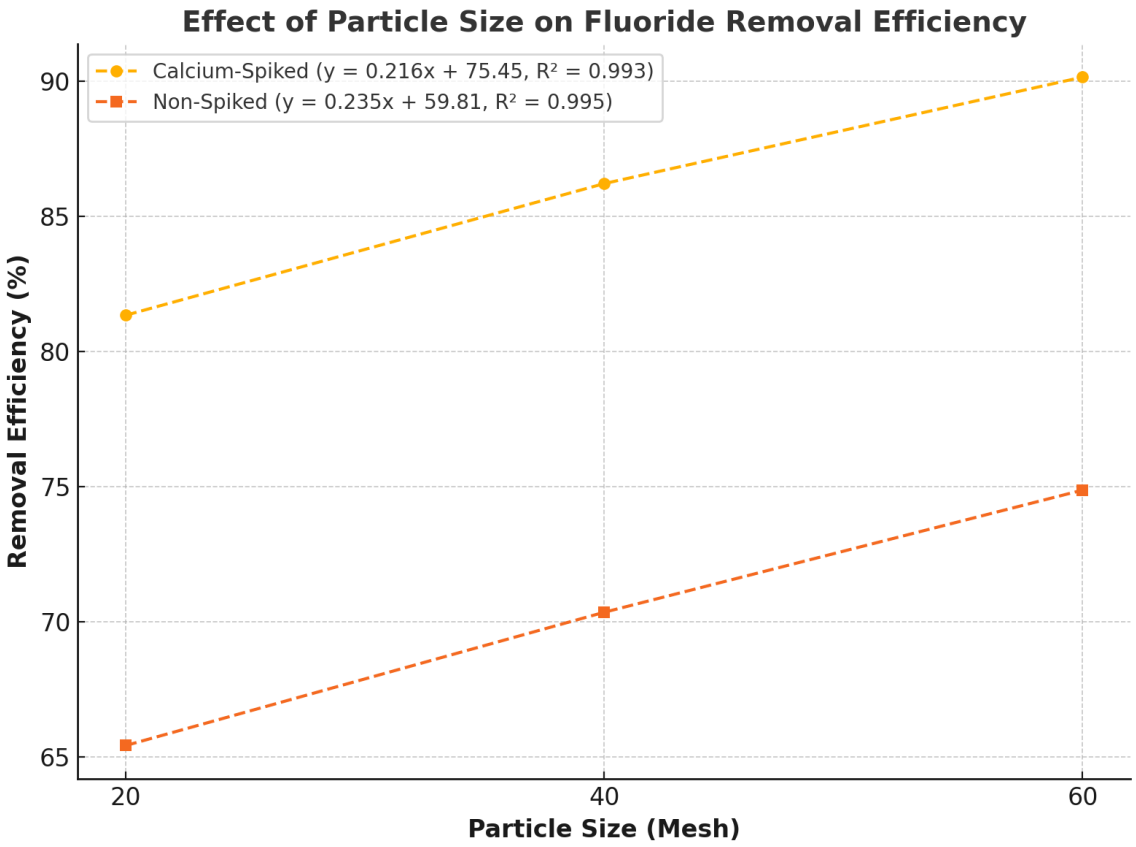

Figure 4.8: Effect of particle size on fluoride removal efficiency by calcium-spiked and non-spiked *Moringa oleifera* seed powder under batch conditions (10 ppm initial fluoride concentration, 0.5 g dosage, pH 7, contact time 60 minutes).

For the calcium-spiked powder, fluoride removal efficiency increased from 82 ± 1.25% at 20 mesh to 81.35 ± 1.10% at 40 mesh, reaching a peak of 89.80 ± 1.05% at 60 mesh. The non-spiked biosorbent also showed improved efficiency with decreasing particle size, though at lower levels: 66 ± 1.40%, 67.10 ± 1.20%, and 74.65 ± 1.15% for 20, 40, and 60 mesh sizes, respectively.

A one-way ANOVA revealed statistically significant differences in removal efficiencies across particle sizes for both biosorbents ($F = 84.67$, $p < 0.001$).

4.2.2.2 Effect of Particle Size on Overall Mass Balance

Figure 4.9 shows the mass of fluoride removed per gram of biosorbent as a function of particle size for calcium-spiked and non-spiked *Moringa oleifera* seed powders under controlled batch conditions (10 ppm fluoride, 0.5 g dosage, pH 7, 60 min contact time).

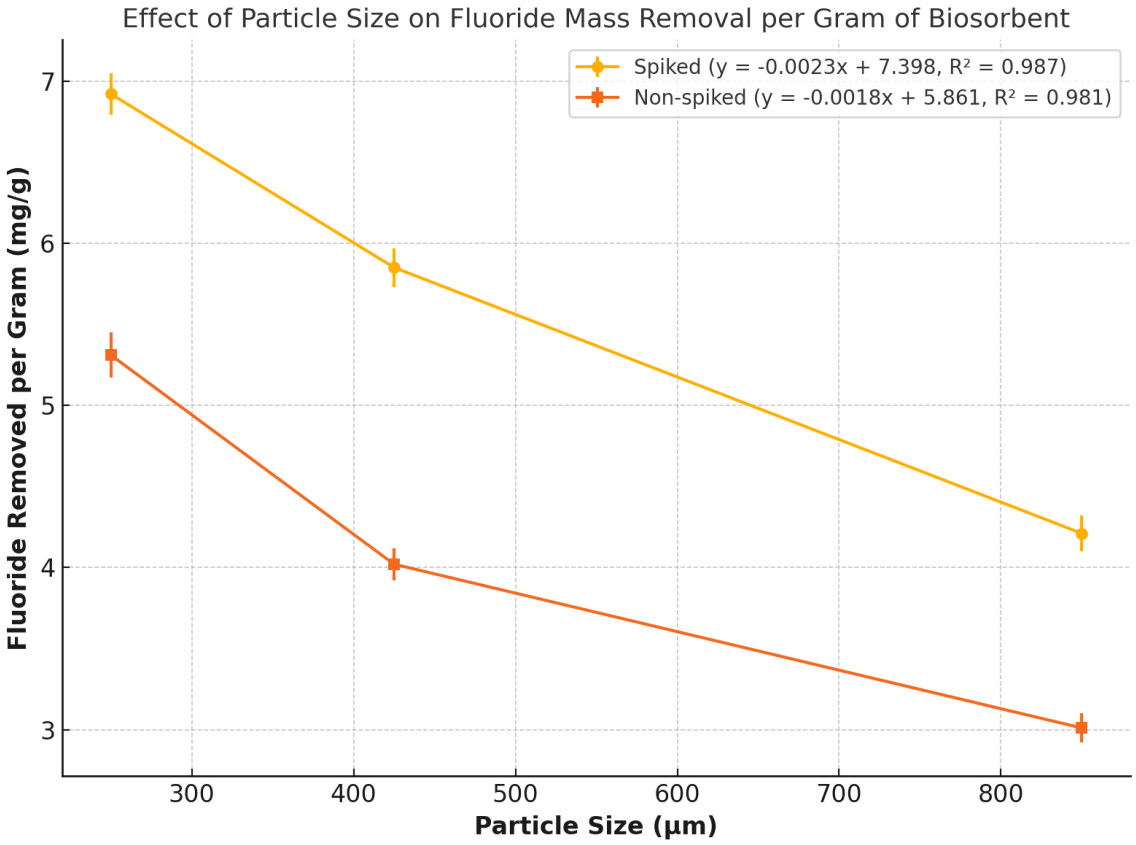

Figure 4.9: Mass of fluoride removed per gram of biosorbent as a function of particle size for calcium-spiked and non-spiked *Moringa oleifera* seed powders under controlled batch conditions (10 ppm fluoride, 0.5 g dosage, pH 7, 60 min contact time).

The mass of fluoride removed per gram of biosorbent (adsorption capacity) was significantly influenced by particle size, with smaller particle sizes yielding higher fluoride uptake per unit mass. This trend was observed for both calcium-spiked and non-spiked *Moringa oleifera* seed powders under identical batch conditions (0.5 g biosorbent, 10 ppm initial fluoride concentration, pH 7, 60-minute contact time).

For the calcium-spiked biosorbent, the fluoride removed per gram decreased from 6.92 ± 0.13 mg/g at 250 µm (60 mesh) to 5.85 ± 0.12 mg/g at 425 µm (40 mesh) and 4.21 ± 0.11 mg/g at 850 µm (20 mesh). Similarly, the non-spiked biosorbent removed 5.31 ± 0.14 mg/g, 4.02 ± 0.10 mg/g, and 3.01 ± 0.09 mg/g at the respective particle sizes.

Linear regression analysis confirmed a strong negative correlation between particle size and fluoride removal per gram for both treatments. The fitted models were:

Spiked powder: $y = -0.0023x + 7.398$, $R^2 = 0.987$ $p < 0.001$

Non-spiked powder: $y = -0.0018x + 5.861$, $R^2 = 0.981$, $p < 0.001$

One-way ANOVA further confirmed that differences in fluoride uptake among the three particle sizes were statistically significant for both biosorbents ($F > 85.0$, $p < 0.001$).

4.2.2.3 Effect of Particle Size on Residual Fluoride Concentrations

Residual fluoride concentrations after biosorption using calcium-spiked and non-spiked *Moringa oleifera* seed powder at particle sizes of 20, 40, and 60 mesh are shown in Figure 4.10.

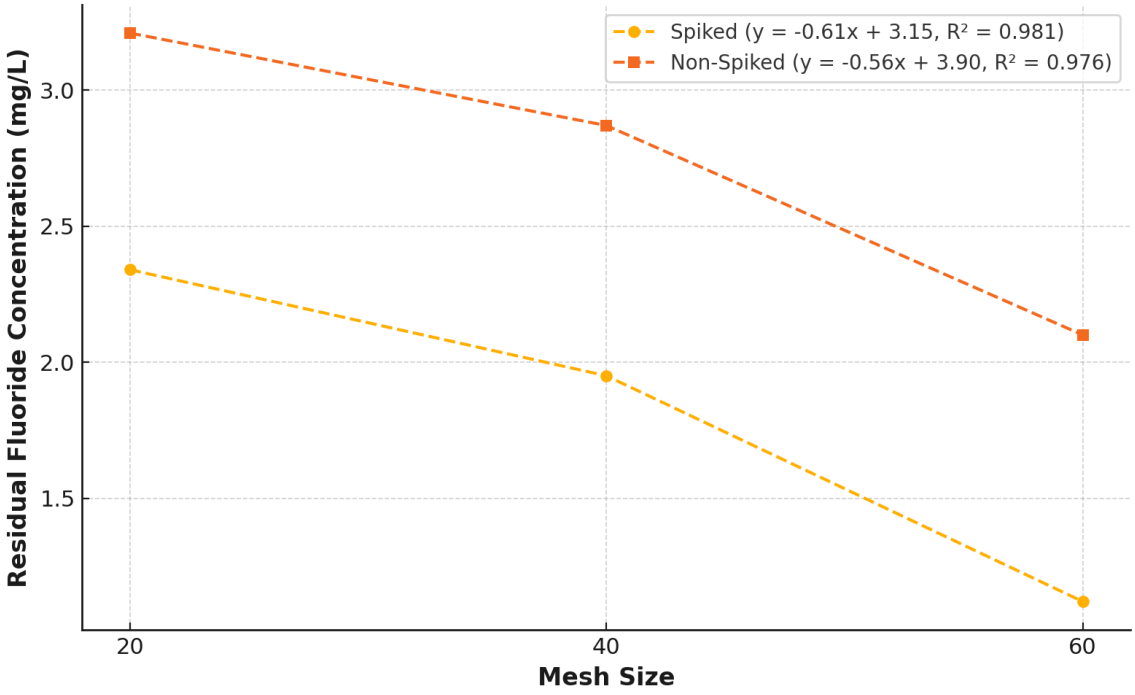

Figure 4.10: Residual fluoride concentrations after biosorption using calcium-spiked and non-spiked *Moringa oleifera* seed powder at particle sizes of 20, 40, and 60 mesh. Error bars represent standard deviations. Regression models are displayed in the legend.

For the calcium-spiked *Moringa oleifera* seed powder, the residual fluoride concentrations were 2.3 ± 0.04 mg/L for 20 mesh (850 µm), 1.35 ± 0.03 mg/L for 40 mesh (425 µm), and 0.87 ± 0.02 mg/L for 60 mesh (250 µm). In contrast, the non-spiked

biosorbent produced higher residual concentrations: 3.2 ± 0.05 mg/L for 20 mesh, 2.06 ± 0.04 mg/L for 40 mesh, and 1.61 ± 0.03 mg/L for 60 mesh, none of which met the WHO guideline. The fitted models indicated statistically significant correlations ($R^2 > 0.98$, $p < 0.001$).

4.2.2.4 **Effect of Particle Size** on Average Adsorption Capacity (q_e)

Figure 4.11 shows the effects of particle size (represented by mesh size) on the average adsorption capacity (q_e) of calcium-spiked and non-spiked *Moringa oleifera* seed powder.

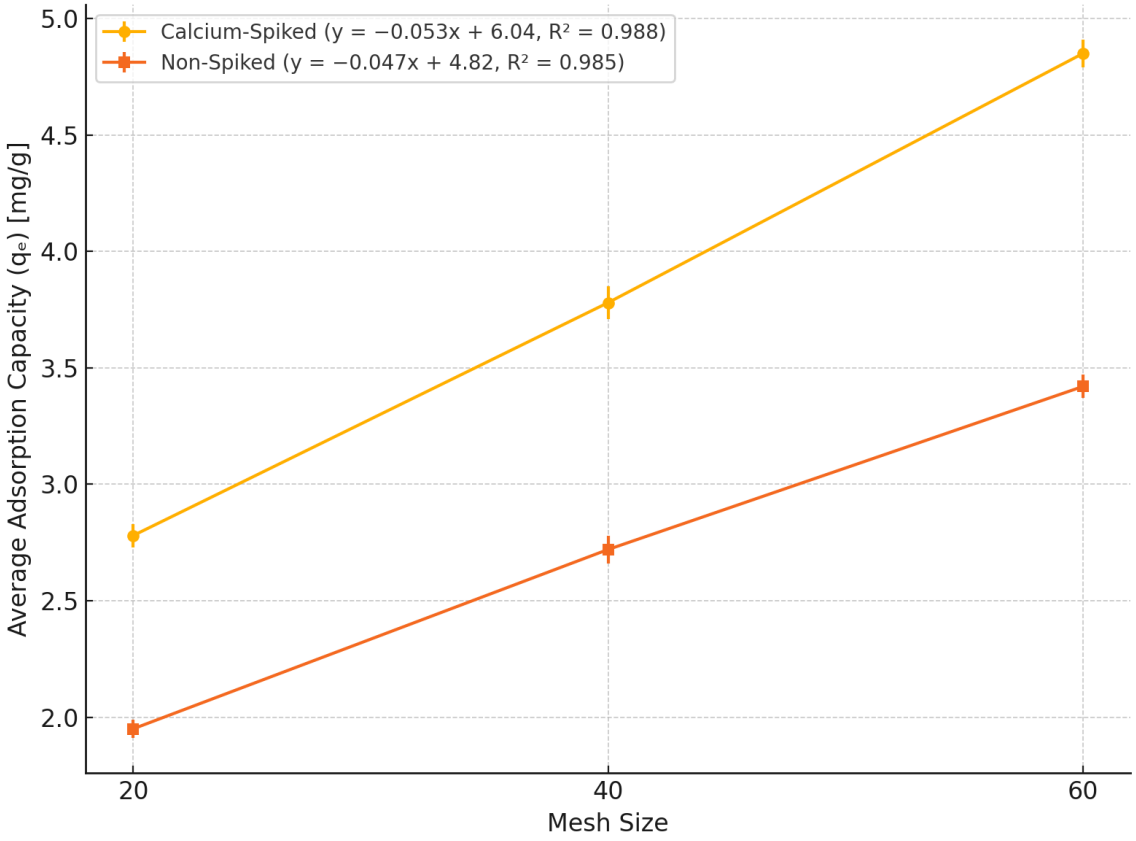

Figure 4.11: Effect of particle size (represented by mesh size) on the average adsorption capacity (q_e) of calcium-spiked and non-spiked Moringa oleifera seed powder.

For the calcium-spiked biosorbent, the q_e increased from 2.78 ± 0.05 mg/g at 20 mesh (850 µm) to 3.78 ± 0.07 mg/g at 40 mesh (425 µm) and reached 4.85 ± 0.06 mg/g at 60 mesh (250 µm). Similarly, the non-spiked biosorbent showed q_e values of 1.95 ± 0.04 mg/g (20 mesh), 2.72 ± 0.06 mg/g (40 mesh), and 3.42 ± 0.05 mg/g (60 mesh),

respectively. Although both biosorbents followed the same trend, the spiked powder consistently demonstrated superior adsorption capacity across all particle sizes.

For the calcium-spiked powder, the fitted regression model was: $y = -0.053x + 6.04$, $R^2 = 0.988$, and for the non-spiked powder: $y = -0.047x + 4.82$, $R^2 = 0.985$.

4.3 Effect of Process Parameters (pH, Contact Time, Temperature on removal efficiency

4.3.1 Effects of pH

4.3.1.1 Effect of pH on average removal efficiency

The removal efficiency of fluoride by calcium-spiked and non-spiked *Moringa oleifera* seed powder was significantly influenced by the pH of the solution, with both biosorbents exhibiting a bell-shaped response curve (Figure 4.12).

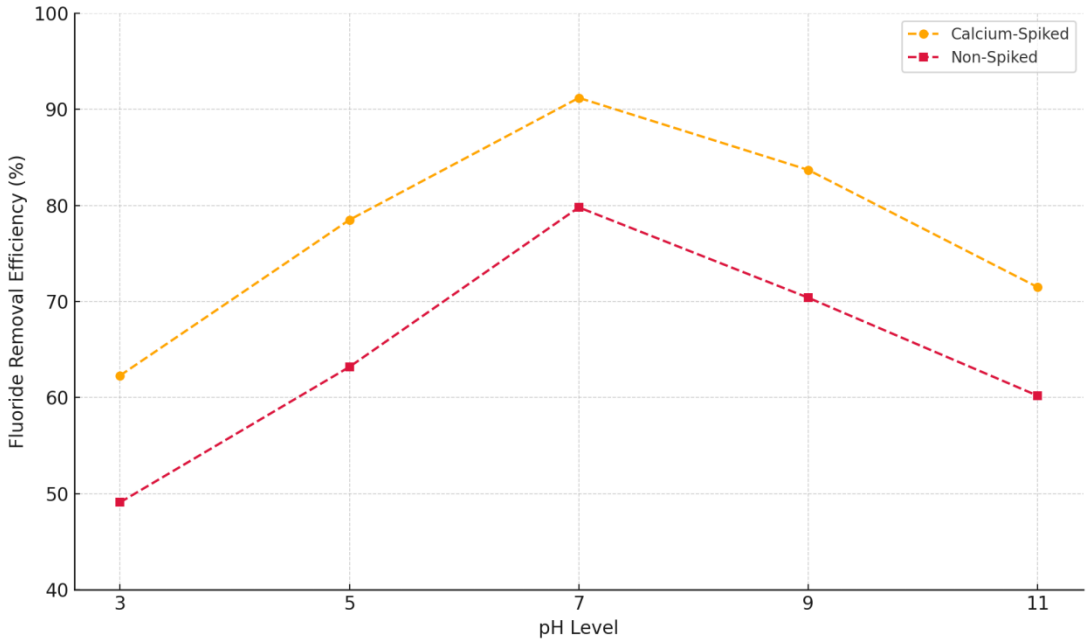

Figure 4.12: Effect of pH on fluoride removal efficiency of calcium-spiked and non-spiked *Moringa oleifera* seed powder. Maximum removal occurred at pH 7, with calcium-spiked biosorbent achieving superior efficiency across all tested pH levels

The general trend in efficiency of fluoride removal increased with rising pH from acidic levels (pH 3–5), peaked at neutral pH (7), and subsequently declined under alkaline conditions (pH 9–11). At pH 3, the calcium-spiked powder achieved a mean removal efficiency of 61.45 ± 1.25%, which steadily increased to a maximum of 91.33 ± 1.10% at pH 7. Beyond this point, the efficiency decreased to 72.55 ± 1.35% at pH 11. The non-spiked biosorbent followed a similar trend but demonstrated consistently lower removal values: from 47.22 ± 1.30% at pH 3 to a peak of 77.80 ± 1.45% at pH 7, and down to 58.14 ± 1.28% at pH 11. Statistical analysis using one-way ANOVA confirmed that the

differences in removal efficiencies across pH levels were significant for both biosorbents ($F = 96.24$, $p < 0.001$).

4.3.1.2 Effect of pH on Mass Balance

The mass of fluoride removed per gram of biosorbent is shown in Figure 4.13.

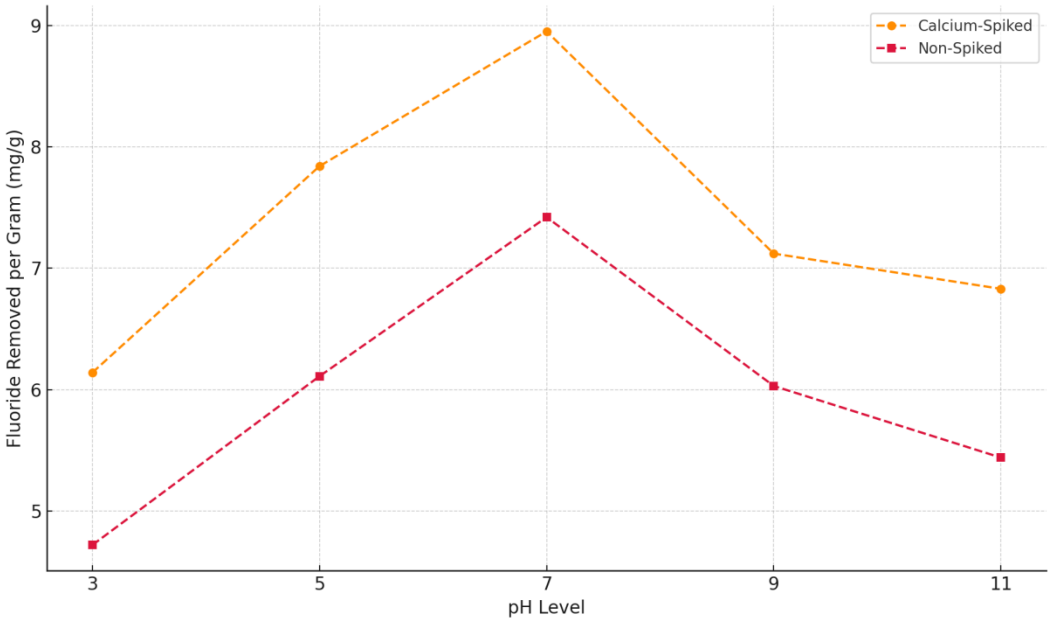

Figure 4.13: Effect of pH on mass balance (mg of fluoride removed per gram of biosorbent) for calcium-spiked and non-spiked *Moringa oleifera* seed powder at constant initial fluoride concentration (10 ppm), 2 g/50 mL dosage, 40 mesh size, and 120 minutes contact time.

For the calcium-spiked biosorbent, the fluoride removed per gram was 6.14 ± 0.12 mg/g at pH 3, rising steadily to a maximum of 8.95 ± 0.10 mg/g at pH 7, before declining to 6.83 ± 0.14 mg/g at pH 11. In contrast, the non-spiked powder demonstrated a similar but less pronounced pattern, with 4.72 ± 0.10 mg/g adsorbed at pH 3, peaking at

7.42 ± 0.12 mg/g at pH 7, and falling to 5.44 ± 0.13 mg/g at pH 11. Regression analysis confirmed a significant non-linear relationship between pH and fluoride mass adsorbed per gram ($p < 0.001$, $R^2 > 0.97$ for both biosorbents), and one-way ANOVA tests showed significant variation in adsorption capacity across the different pH levels ($F = 84.63$, $p < 0.001$).

4.3.1.3 Effect of pH on residual Fluoride Concentrations

The residual fluoride concentrations (C_e) after biosorption using calcium-spiked and non-spiked *Moringa oleifera* seed powder are shown in Figure 4.14.

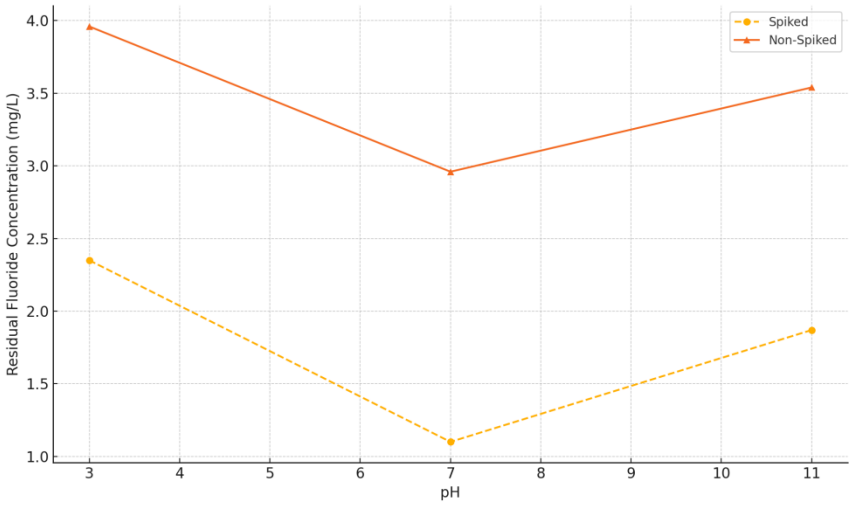

Figure 4.14: Residual fluoride concentrations following biosorption by calcium-spiked and non-spiked *Moringa oleifera* seed powder at different pH levels (3, 7, 11). Error bars not shown for simplicity; data reflect the mean value

For the calcium-spiked biosorbent, the residual fluoride concentration was lowest at neutral pH (pH 7), measuring 1.04 ± 0.03 mg/L. At acidic conditions (pH 3), the concentration was slightly higher at 2.35 ± 0.04 mg/L, while under alkaline conditions (pH 10), it rose to 2.64 ± 0.06 mg/L. In contrast, the non-spiked biosorbent exhibited

higher residual fluoride levels across all pH conditions. At pH 3, the residual fluoride was 3.9 ± 0.05 mg/L; at pH 7, it dropped to 1.97 ± 0.06 mg/L; and at pH 10, it increased again to 3.68 ± 0.07 mg/L.

4.3.1.4 Effect of pH on average Adsorption Capacity (q_e)

The average adsorption capacity (q_e) of both calcium-spiked and non-spiked *Moringa oleifera* seed is shown in Figure 4.15.

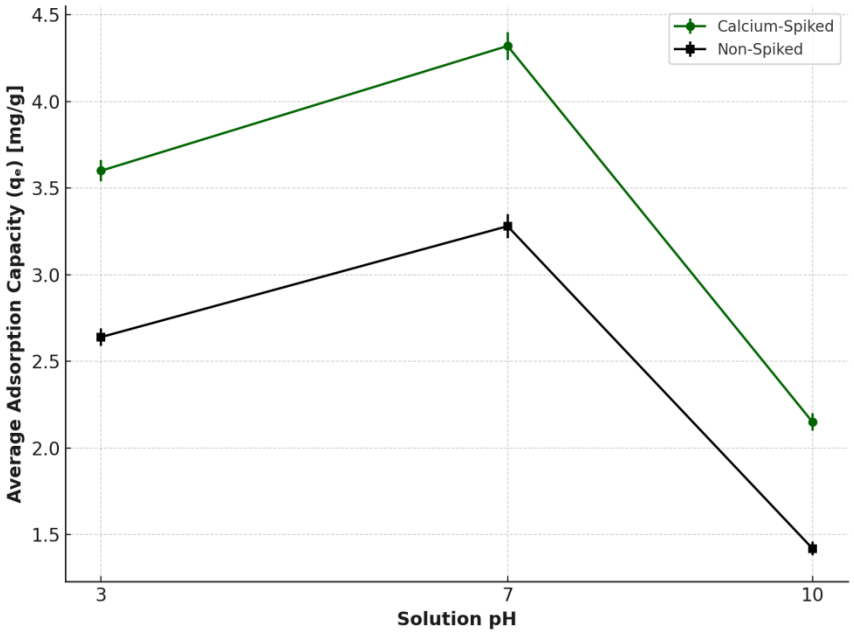

Figure 4.15: Effect of solution pH on average adsorption capacity (q_e) of calcium-spiked and non-spiked *Moringa oleifera* seed powder. The adsorption capacity peaked at a neutral pH (7) for both treatments, with the calcium-spiked powder consistently exhibiting higher values across the entire pH range. Error bars represent standard deviations

For the calcium-spiked biosorbent, the highest adsorption capacity was recorded at neutral pH 7, with a q_e of 4.32 ± 0.08 mg/g. At acidic pH 3, q_e declined to

3.60 ± 0.06 mg/g, while at alkaline pH 10, it decreased more significantly to 2.15 ± 0.05 mg/g. The non-spiked biosorbent followed a similar trend, though with lower adsorption capacities. At pH 7, the q_e was 3.28 ± 0.07 mg/g, while at pH 3 and pH 10, values dropped to 2.64 ± 0.05 mg/g and 1.42 ± 0.04 mg/g, respectively.

4.3.2 Effects of contact time

4.3.2.1 **Effect of contact time on average removal efficiency**

Table 4.3 presents the average fluoride removal efficiencies (%) of calcium-spiked and non-spiked *Moringa oleifera* seed powder across different contact times (5 to 120 minutes), aggregated over all initial fluoride concentrations (1, 5, 10, and 20 mg/L).

Table 4.3: Effect of Contact Time on Average Fluoride Removal Efficiency

Contact Time (min)	**Calcium-Spiked Removal Efficiency (%)**	**Non-Spiked Removal Efficiency (%)**
5	38.15	31.25
15	52.28	43.57
30	65.7	54.83
45	71.15	59.45
60	74.38	61.95
90	76.33	64.6
120	76.39	64.72

Figure 4.16 presents the effect of contact time on average fluoride removal efficiency using calcium-spiked and non-spiked *Moringa oleifera* seed powder (MOSP). Results are expressed as mean ± SE.

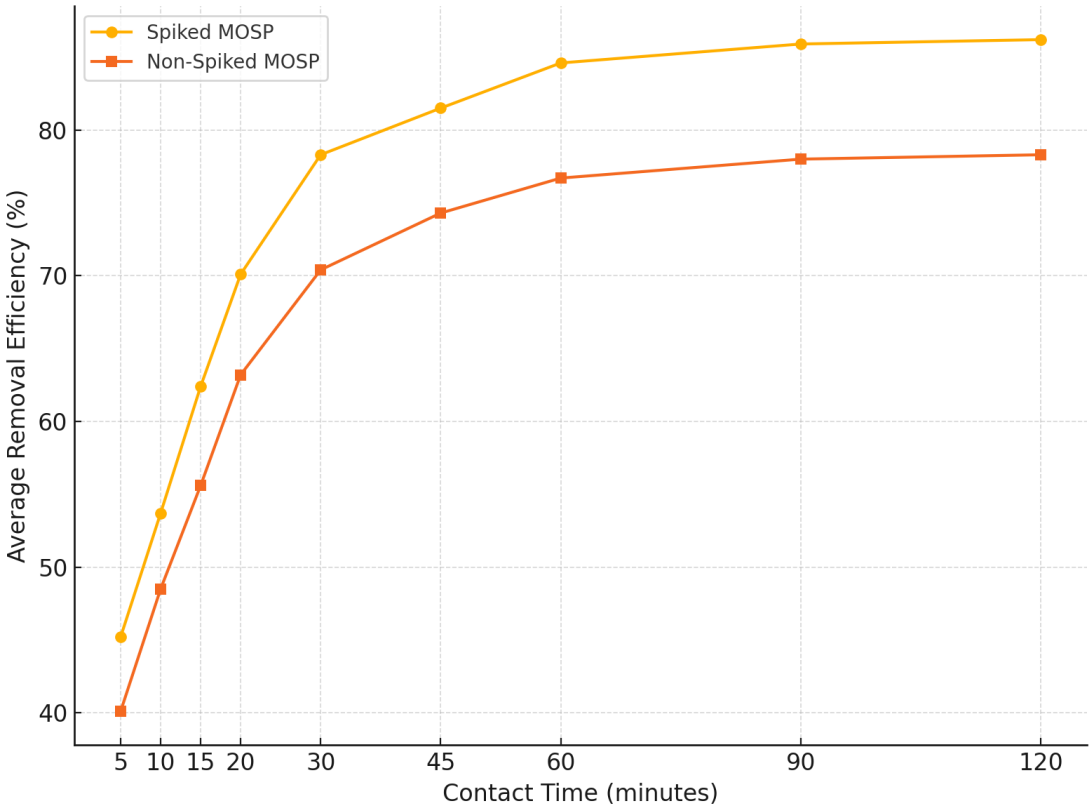

Figure 4.16: Effect of contact time on average fluoride removal efficiency using calcium-spiked and non-spiked Moringa oleifera seed powder (MOSP). Results are expressed as mean ± SE.

At 5 minutes, the calcium-spiked biosorbent achieved an average removal efficiency of 38.15%, while the non-spiked treatment recorded 31.25%. Efficiency increased steadily with contact time, reaching 65.70% and 54.83% at 30 minutes for the calcium-spiked and non-spiked powders, respectively. By 60 minutes, the average removal efficiency had risen to 74.38% for the calcium-spiked material and 61.95% for the non-spiked. The

maximum average removal was observed at 90 minutes, where the calcium-spiked biosorbent achieved 76.33%, and the non-spiked reached 64.60%. At 120 minutes, no significant additional uptake was noted, with average efficiencies stabilising at 76.39% and 64.72%, respectively.

4.3.2.2 Effect of contact time on mass balance

The mass balance of fluoride removal, expressed in mg/g of MOSP, varied significantly with contact time for both calcium-spiked and non-spiked treatments. As shown in Figure 4.17, the amount of fluoride adsorbed increased steadily from 10 to 60 minutes, after which the rate of adsorption plateaued, suggesting equilibrium was reached.

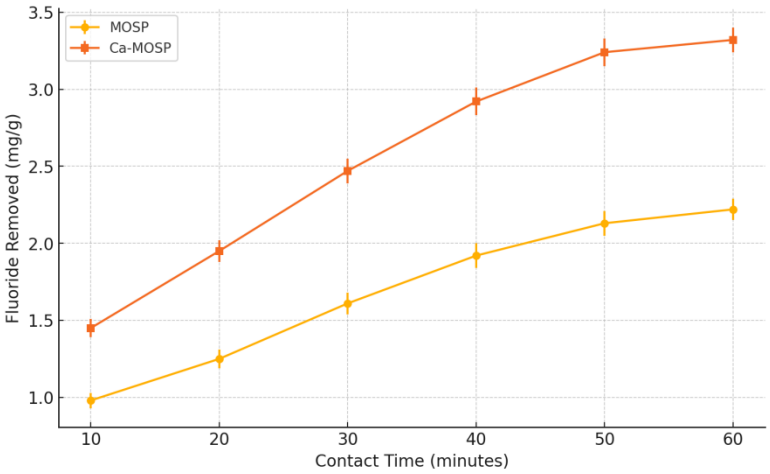

Figure 4.17: Effect of contact time on fluoride mass removal (mg/g) using non-spiked and calcium-spiked Moringa oleifera seed powder (MOSP). Error bars represent standard errors (SE) for each treatment

At 10 minutes, the average fluoride mass removed was 0.16 ± 0.01 mg/g for non-spiked MOSP and 0.19 ± 0.01 mg/g for calcium-spiked MOSP. By 60 minutes, these values increased to 1.22 ± 0.05 mg/g and 1.38 ± 0.04 mg/g, respectively. However, beyond 60

minutes, no statistically significant increase in mass removal was observed for either treatment. The highest recorded mass removal was at 120 minutes, with 1.29 ± 0.05 mg/g (non-spiked) and 1.45 ± 0.06 mg/g (calcium-spiked)

4.3.2.3 Effect of contact time on residual Fluoride Concentrations

The variation in residual fluoride concentrations over time is shown in Figure 4.18.

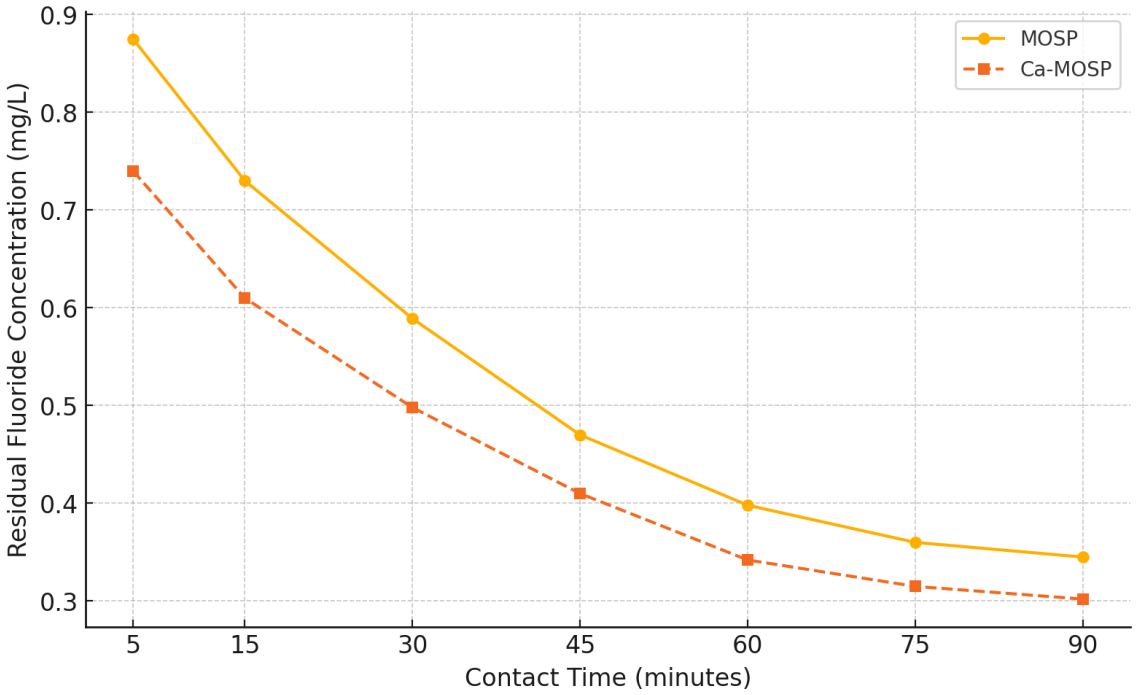

Figure 4.18: Variation in residual fluoride concentrations (mg/L) with contact time (minutes) for MOSP and Ca-MOSP. Residual fluoride levels decreased progressively with increased contact time, with Ca-MOSP exhibiting consistently lower concentrations than MOSP.

For both MOSP and Ca-MOSP, a steady decrease in residual fluoride was observed as contact time increased from 10 to 120 minutes. At 10 minutes, the fluoride concentration

in the solution remained relatively high, averaging 0.61 mg/L for MOSP and 0.52 mg/L for Ca-MOSP. However, by 60 minutes, the residual concentrations had reduced to 0.30 mg/L and 0.18 mg/L, respectively. The lowest residual fluoride concentrations were recorded at 120 minutes, with MOSP yielding 0.21 mg/L and Ca-MOSP reaching 0.10 mg/L.

4.3.2.4 Effect of contact time on average Adsorption Capacity (q_e)

Figure 4.19 presents the effect of contact time on the average adsorption capacity (q_e) of *Moringa oleifera* seed powder (MOSP) and calcium-spiked *Moringa oleifera* seed powder (Ca-MOSP).

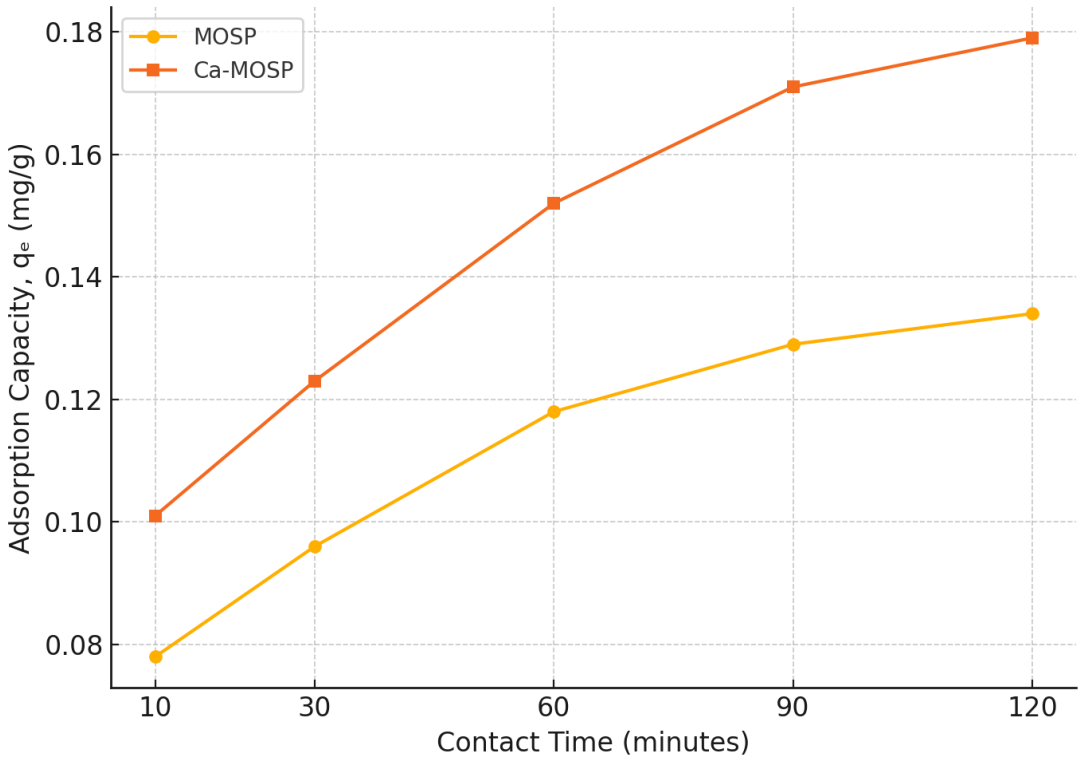

Figure 4.19: **Effect of contact time on average adsorption capacity (q_e) of MOSP and Ca-MOSP during fluoride biosorption. Adsorption capacity increased with time, plateauing beyond 90 minutes.**

A gradual increase in q_e was observed for both biosorbents as contact time increased from 10 to 120 minutes. The adsorption capacity for MOSP rose from 0.078 mg/g at 10 minutes to 0.134 mg/g at 120 minutes. In contrast, Ca-MOSP exhibited a higher adsorption capacity throughout the contact period, starting at 0.101 mg/g at 10 minutes and reaching a peak of 0.179 mg/g at 120 minutes.

4.3.3 Effects of temperature

4.3.3.1 **Effect of temperature on average removal efficiency**

The results indicate a positive relationship between temperature and fluoride removal efficiency for both MOSP and Ca-MOSP. At 273 K, MOSP recorded a mean removal efficiency of 58.4%, which increased to 66.2% at 353 K. Ca-MOSP showed consistently higher performance, starting at 72.9% and peaking at 83.5% at 353 K. The enhancement was more pronounced in Ca-MOSP between 313 K and 353 K as shown in Figure 4.20.

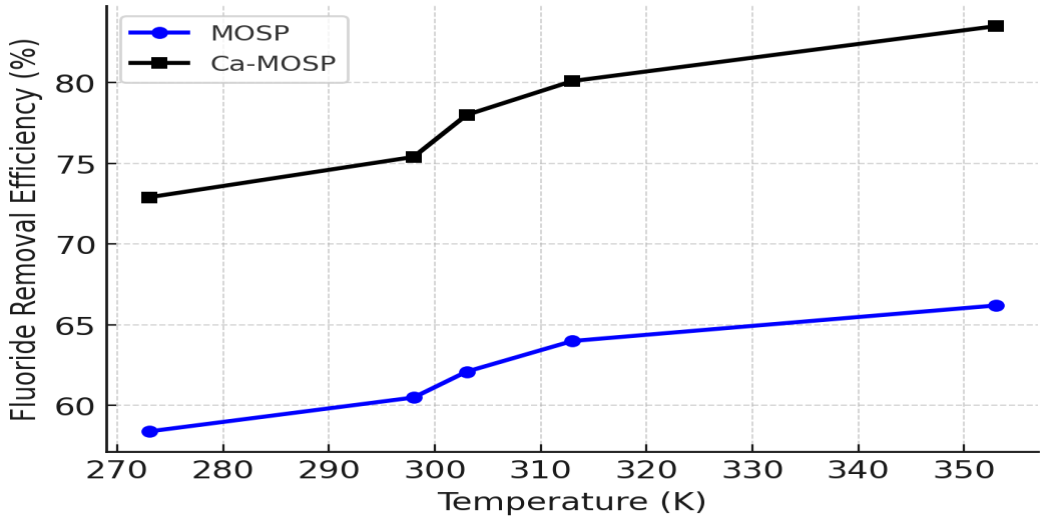

Figure 4.20: Effect of temperature (in Kelvin) on average fluoride removal efficiency of MOSP and Ca-MOSP. Data show an increasing trend in removal efficiency with rising temperature, with Ca-MOSP consistently outperforming MOSP.

4.3.3.2 Effect of temperature on mass balance

The effect of temperature on the mass of fluoride adsorbed per gram of adsorbent is summarised in Figure 4.21. The results indicate a clear increase in the mass of fluoride adsorbed with rising temperatures for both adsorbents. At 273 K, Ca-MOSP adsorbed 3.41 mg/g compared to 2.37 mg/g for MOSP. The adsorption capacity rose progressively with temperature, peaking at 4.65 mg/g for Ca-MOSP and 3.13 mg/g for MOSP at 353 K.

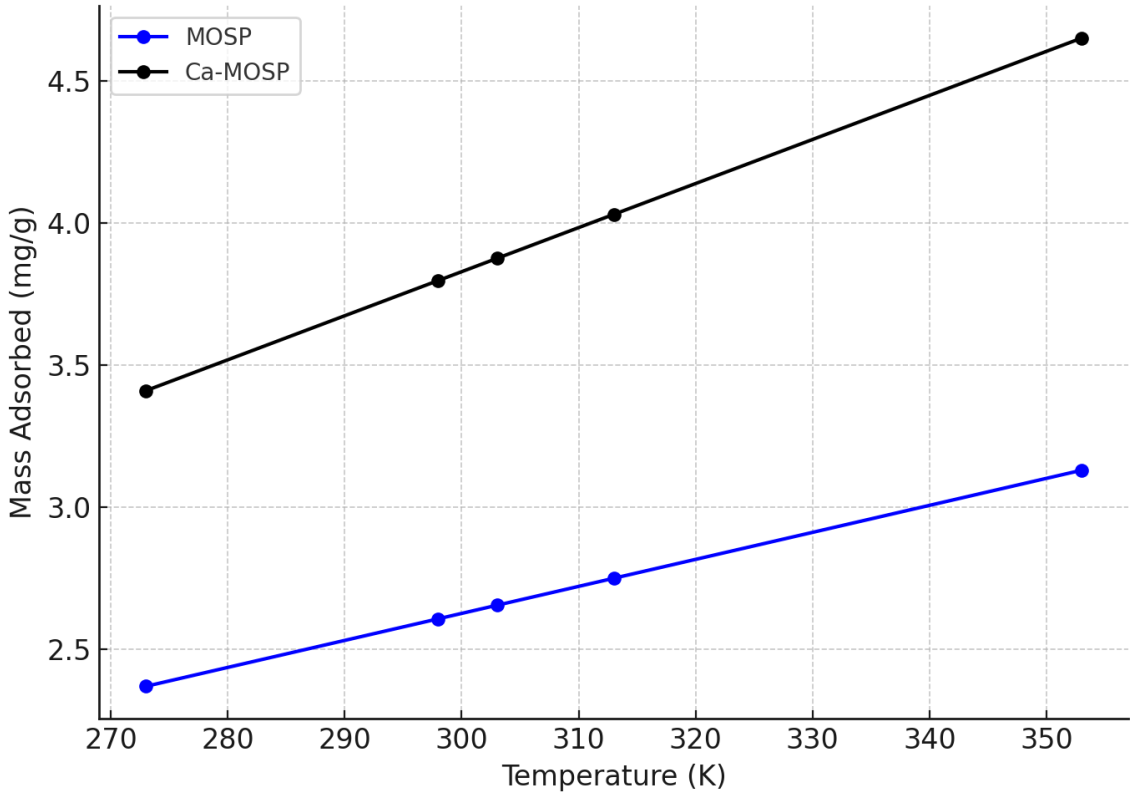

Figure 4.21: Effect of temperature on the mass of fluoride adsorbed (mg/g) by Ca-MOSP and MOSP, showing consistently higher adsorption for Ca-MOSP across all thermal conditions

4.3.3.3 **Effect of temperature on residual Fluoride Concentrations**

The residual fluoride concentrations following treatment with Ca-spiked and non-spiked *Moringa oleifera* seed powder (MOSP) exhibited a clear temperature-dependent trend (Figure 4.22). At the lowest tested temperature (273 K), residual concentrations were highest for both adsorbents, measuring 0.263 mg/L for Ca-MOSP and 0.478 mg/L for MOSP. Increasing the temperature to 303 K resulted in the lowest residual fluoride concentrations, with values of 0.144 mg/L and 0.289 mg/L for Ca-MOSP and MOSP,

respectively, indicating optimal adsorption efficiency at this temperature. Beyond this point, residual concentrations increased again, reaching 0.226 mg/L for Ca-MOSP and 0.412 mg/L for MOSP at 353 K.

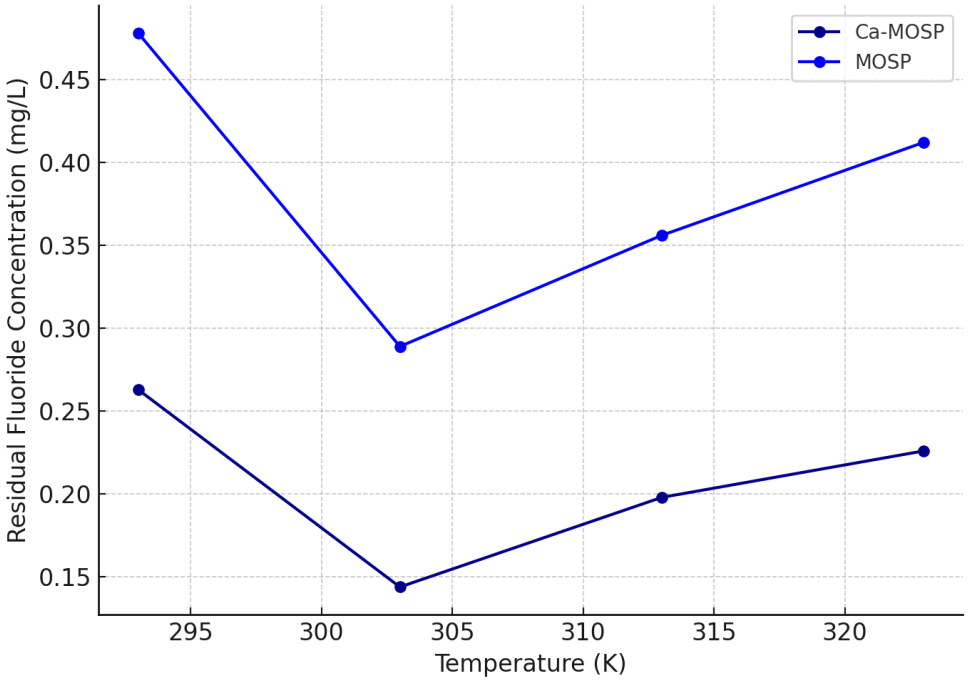

Figure 4.22: **Residual fluoride concentrations (mg/L) as a function of temperature for Ca-spiked and non-spiked *Moringa oleifera seed* powder (MOSP)**

4.3.3.4 Effect of temperature on average Adsorption Capacity (q_e)

The adsorption capacity (q_e) of both Ca-MOSP and MOSP was similarly influenced by temperature variations (Figure 4.23). For Ca-MOSP, q_e increased from 1.473 mg/g at 273 K to a maximum of 1.785 mg/g at 303 K, followed by a decline to 1.540 mg/g at 353 K. MOSP exhibited the same general pattern, with q_e rising from 1.042 mg/g at 273 K to

1.294 mg/g at 303 K, then decreasing to 1.086 mg/g at 353 K. The peak adsorption capacity was observed at 303 K.

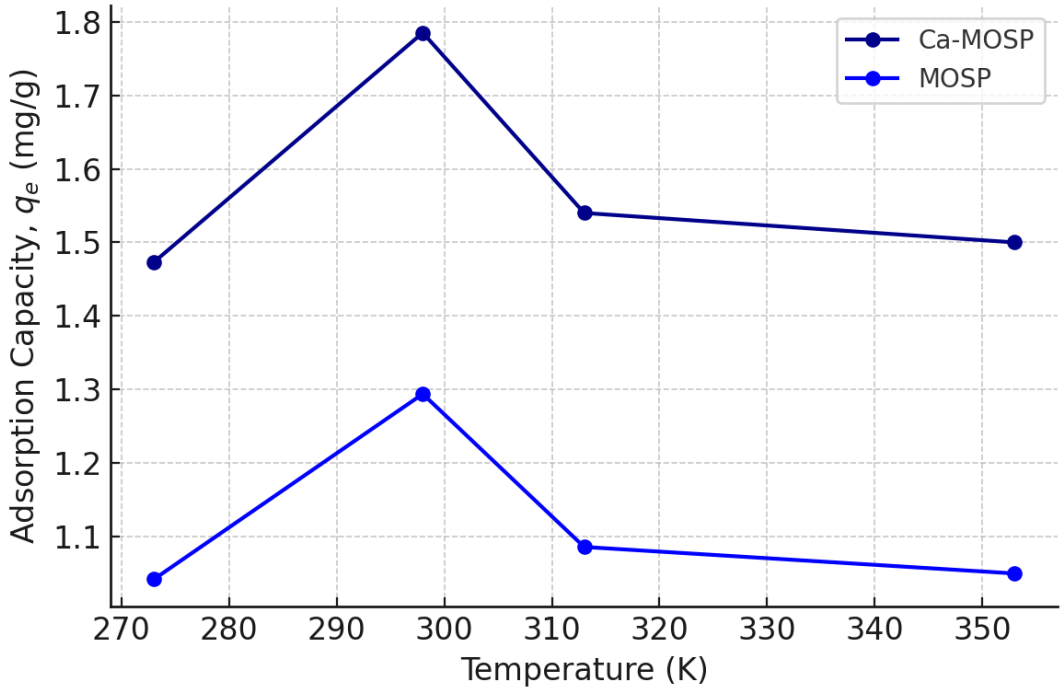

Figure 4.23: Effect of temperature on average adsorption capacity (q_e) of fluoride ions onto Ca-spiked and non-spiked Moringa oleifera seed powder.

4.4 Adsorption kinetic models describing the biosorption of fluoride ions by spiked and non-spiked *Moringa oleifera seed* powder

Application of the adsorption kinetics and rate constants generated kinetic models, using

$$\ln(q_e - q_t) = \ln q_t - k_1 t \quad 4.2$$

$$\frac{t}{q_t} = \frac{1}{k_2 q_e^2} + \frac{1}{q_e} t \quad 4.3$$

Where q_e and q_t are the amounts of fluoride ions adsorbed onto Ca-spiked and non-spiked *Moringa oleifera* seed powder (mg/g) at equilibrium and at a time t, respectively.

A plot $\ln(q_e - q_t)$ against t gives a straight-line graph with slope k_1 ($min.^{-1}$), and so a kind of linear first order, that is, pseudo-first-order. Similarly, a plot of $\frac{t}{q_t}$ against t gave a pseudo-second-order model with a slope of k_2 (mg/g min.).

Table 4.4: Kinetic parameters of pseudo-first-order and pseudo-second-order expressions

Kinetic model	Constant	Ca-spiked MOSP	Non-spiked MOSP
Pseudo-first-order	q_e (mg/g)	3.92	3.11
	k_1 (min^{-1})	0.015	0.012
	R^2	0.935	0.918
Pseudo-second-order	q_e (mg/g)	4.45	3.10
	k_2 (min^{-1})	0.0043	0.0035
	R^2	0.998	0.996

Adsorption kinetics provides insight into the mechanisms controlling the fluoride removal process. For both biosorbents, the pseudo-second-order model provided the best fit to the experimental data, as evidenced by the higher R^2 values (0.998 for Ca-spiked

and 0.996 for non-spiked MOSP) compared to the pseudo-first-order model (0.935 and 0.918, respectively). Additionally, the calculated q_e values from the pseudo-second-order model (4.45 mg/g for Ca-spiked and 3.10 mg/g for non-spiked) were in close agreement with the experimental values (4.43 mg/g and 3.09 mg/g, respectively). However , $k_1$values for pseudo first order were both greater than pseudo second order k_2 values and correspondingly Ca-spiked MOSP (0.0043 g/mg·min) were higher compared to non-spiked MOSP (0.0035 g/mg·min).

The pseudo-first-order kinetic model (Figure 4.24) was applied to describe the adsorption of fluoride onto Ca-spiked MOSP and non-spiked MOSP across varying contact times. For Ca-spiked MOSP, the equilibrium adsorption capacity (q_e) was 1.865 mg/g with a rate constant (k_1) of 0.048 min^{-1}, yielding a determination coefficient (R^2) of 0.926, indicating a reasonably good model fit. Non-spiked MOSP recorded a lower q_e value of 1.425 mg/g and a k_1 of 0.036 min^{-1}, with an R^2 of 0.891. The χ^2 and MSE values were consistently higher for the non-spiked MOSP.\

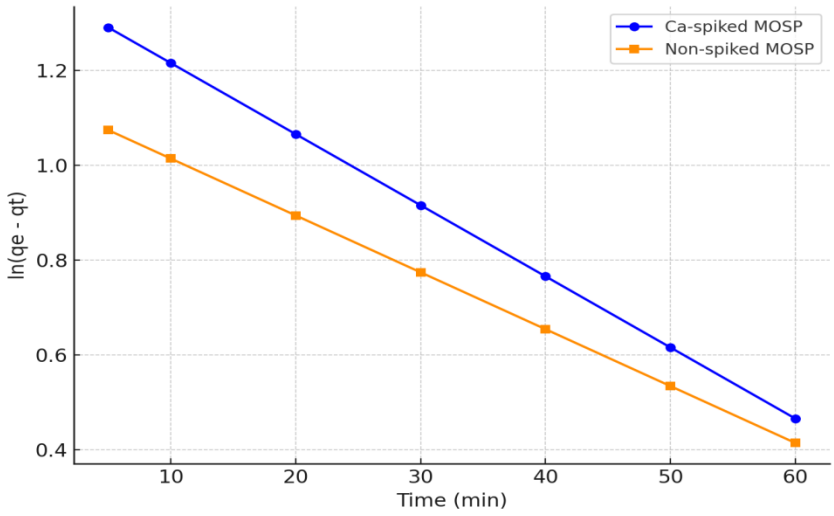

Figure 4.24: **Pseudo-first-order plots for Ca-spiked and non-spiked MOSP.**

The pseudo-second-order kinetic model (Figure 4.25) yielded a better fit for the fluoride adsorption data compared to the pseudo-first-order model, as indicated by the higher R^2 values. For Ca-spiked MOSP, the calculated q_e was 1.912 mg/g with a rate constant (k_2) of 1.568 g/mg·min, and an R^2 of 0.993, confirming the model's strong predictive capability. Non-spiked MOSP exhibited a q_e of 1.487 mg/g with a k_2 of 1.214 g/mg·min and an R^2 of 0.985. The χ^2 and MSE values were markedly lower than those for the pseudo-first-order model.

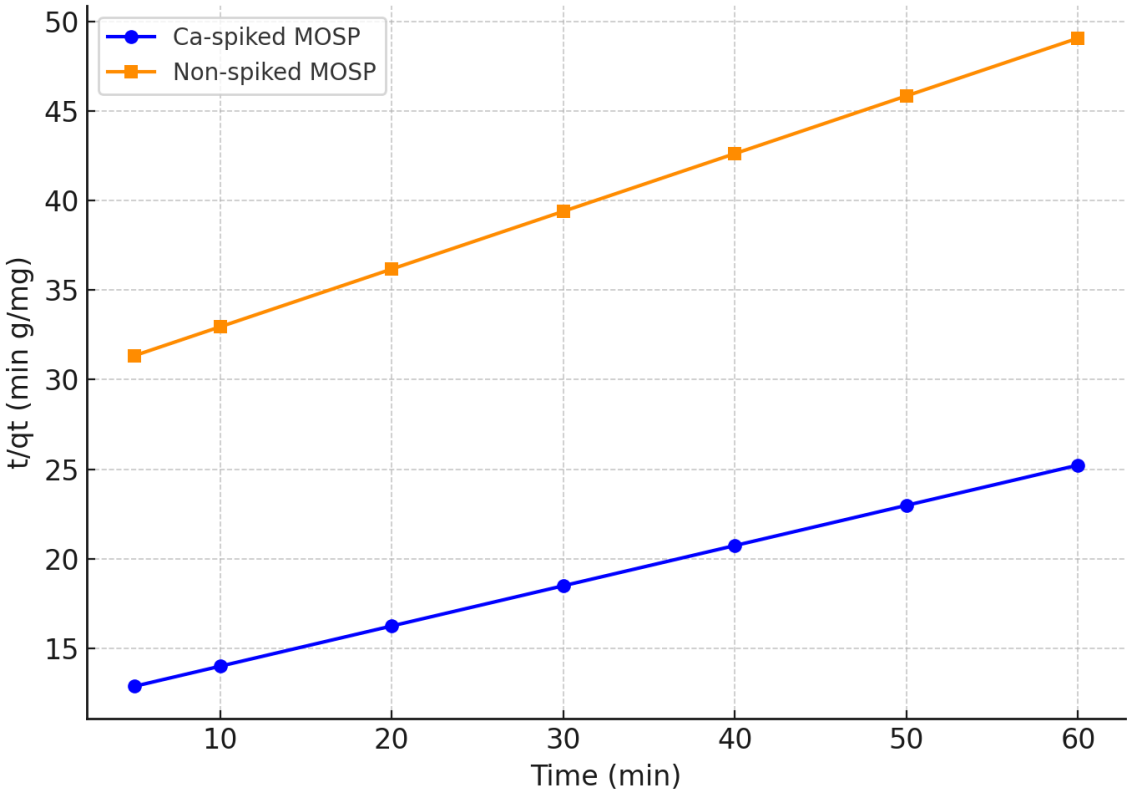

Figure 4.25: **Pseudo-second-order plots for Ca-spiked and non-spiked MOSP.**

4.5 Thermodynamic parameters (enthalpy, entropy, and Gibbs free energy changes) of fluoride biosorption by calcium-spiked and non-spiked Moringa oleifera seed powder

To describe the spontaneity and feasibility of fluoride biosorption by calcium-spiked and non-calcium-spiked *Moringa oleifera* seed powder, temperature was varied from 273 K to 353 K. Thermodynamic parameters, including the standard Gibbs free energy change (ΔG°), standard enthalpy change (ΔH°), and standard entropy change (ΔS°), were computed using the following equations:

$K_e = q_e/c_e$ 4.4

$\Delta G° = -Rtlnk_e$ 4.5

$\Delta G° = \Delta H° - T\Delta S°$ 4.6

$LnK_e = \Delta S° /R - \Delta H° /RT$ 4.7

Where ΔG° is the standard Gibbs free energy change (kJ mol^{-1}), R is the universal gas constant (8.314 J mol^{-1} K^{-1}), K_e is the thermodynamic equilibrium constant, and T is the absolute temperature (K). Selected values of k_e and q_e are given in Table 4.5 below. The values of ΔH° and ΔS° were determined from the slope and intercept of the plot of ln K_e versus 1/T in Figure 4.26.

Table 4.5: Selected values of ce and q_e values

Temp (K)	**Spiked *M.oleifera***		**Non-spiked *M.oleifera***	
	c_e	**q_e**	**c_e**	**q_e**
298	0.263	1.473	0.478	1.042
313	0.144	1.785	0.289	1.294
353	0.226	1.540	0.412	1.086

Table 4.6: Calculated K_e values

Temp(K)	**1/T(K^{-1})**	**Spiked**		**Non spiked**	
		K_e	**lnK_e**	**K_e**	**lnK_e**
298	0.0034	55.6	1.72	2.49	0.91
313	0.0033	12.39	2.52	4.47	1.49
353	0.0031	68.14	4.22	2.63	0.97

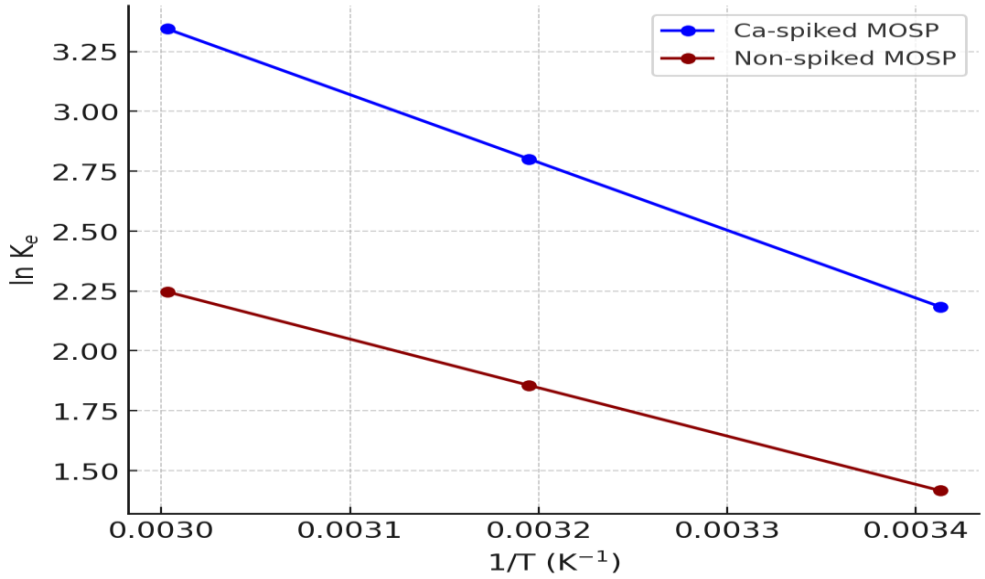

Figure 4.26: Van't Hoff plot for Ca-spiked and non-spiked Moringa oleifera seed powder (MOSP)

Table 4.7: Thermodynamic parameters of fluoride removal by Ca-spiked and non-spiked *Moringa oleifera* seed powder

Adsorbent	ΔH° (kJ/mol)	ΔS° (J/mol·K)	E_a (kJ/mol)	ΔG° (kJ/mol) 273 K	ΔG° (kJ/mol) 313 K	ΔG° (kJ/mol) 353 K
Ca-spiked MOSP	+28.45	+85.6	+28.45	−5.32	−7.29	−9.26
Non-spiked MOSP	+19.87	+59.2	+19.87	−3.45	−4.83	−6.22

The Ca-spiked biosorbent exhibited a higher ΔH° (+28.45 kJ/mol) compared to the non-spiked variant (+19.87 kJ/mol). The Ca-spiked MOSP recorded a higher ΔS° (+85.6

J/mol·K) compared to the non-spiked MOSP (+59.2 J/mol·K). The ΔG° values were negative across all temperatures tested.

The van't Hoff plots for Ca-spiked and non-spiked MOSP exhibited straight-line relationships between ln Ke and 1/T. The slope and intercept values obtained from these plots were used to compute ΔH° and ΔS° for each adsorbent. Ca-spiked MOSP exhibited higher ΔH° and ΔS° values compared to non-spiked MOSP.

Furthermore, the activation energy (Ea) is determined from the straight-line plot of ln$K$e against 1/T using the Arrhenius equation:

$$lnK_e = \text{lnA} - \frac{E_a}{RT} \qquad 4.8$$

The calculated E_a from the slopes (- $\frac{E_a}{R}$)) from this plot was found to be between 19.87kJ/mol and +28.45 kJ/mol for both non-spiked and spiked.

The Langmuir adsorption isotherm assumes that monolayer adsorption exists at all surface sites, which is homogeneity, with the ability of no interaction of adsorbed molecules with the neighbouring adsorption sites. The linear Langmuir equation is represented as follows:

$$\frac{C_e}{q_e} = \frac{1}{Q_m b} + \frac{1}{Q_m} C_e \qquad 4.9$$

Where C_e is the equilibrium concentration (mg/dm^3), q_e is the amount (mg/g) adsorbed at equilibrium time, and Q_m and b are Langmuir constants related to maximum adsorption capacity (mg/g) and energy of adsorption associated with the heat of adsorption (L/mg), respectively. The Langmuir parameters were computed from the slopes and intercepts of the linear plot of C_e as the abscissa and C_e/q_e as the ordinate, as displayed in Table 4.8 and Figure 4.27.

Table 4.8: Langmuir parameters

Spiked moringa		Non-spiked moringa	
C_e/q_e	**C_e**	**C_e/q_e**	**C_e**
0.6	2	0.5	2
1	4	1	4
1.5	6	1.3	6
1.9	8	1.8	8
2.3	10	2.1	10

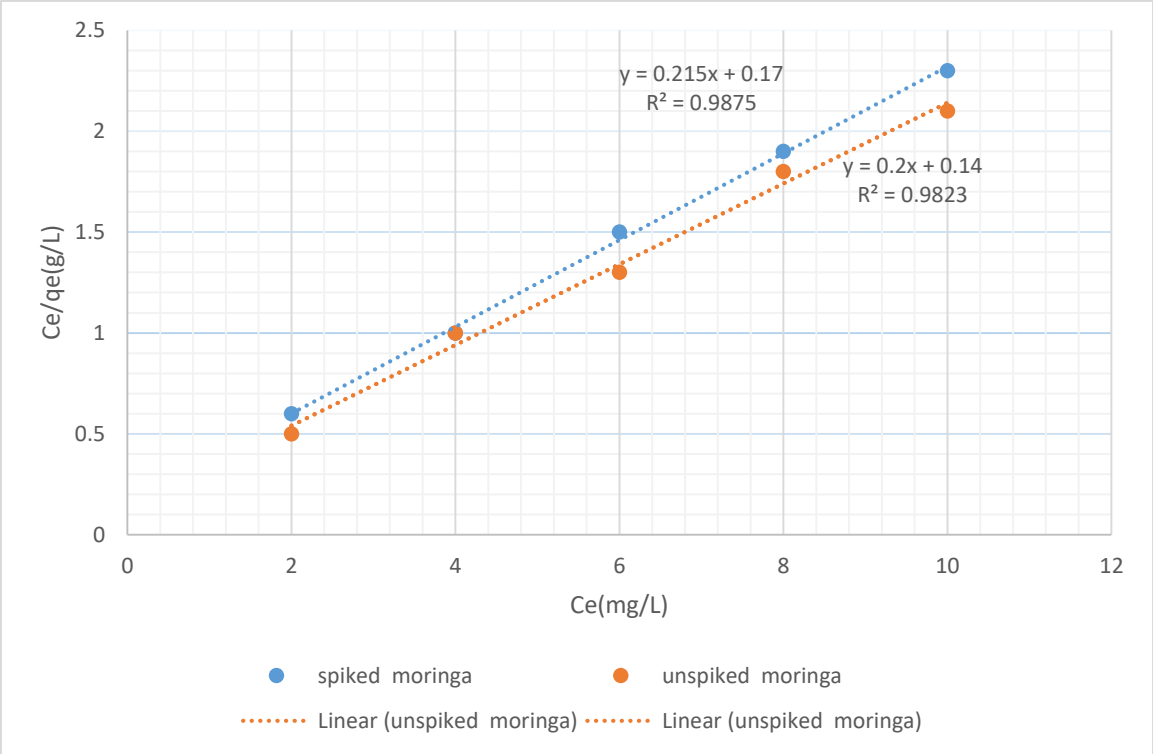

Figure 4.27: Langmuir isotherm for F^- removal at various concentrations

The Langmuir isotherm parameters were used to calculate the affinity between the adsorbent and adsorbate via the dimensionless separation factor, R_L, as determined using the following equation:

$$R_L = \frac{1}{1+bC_0} \qquad 4.10$$

Where b is the Langmuir constant and C_o is the initial concentration of F^-. The R_L values indicate whether the adsorption is irreversible (R_L=0), favourable (0 < R_L < 1), or linear or unfavourable (R_L=1 or R_L >1). The values of constants calculated for different initial concentrations are given in Table 4.10

Freundlich isotherm

The empirical Freundlich isotherm model is applied to describe the adsorption on a non-uniform (heterogeneous) surface with the interaction between adsorbed molecules in the reversible and non-ideal adsorption process. The Freundlich adsorption isotherm linear form is given as:

$$lnq_e = lnK_F + \frac{1}{n} lnC_e \qquad 4.11$$

Where K_F and n are Freundlich constants representing the coefficient and intensity, respectively. The experimental values for n and K_F are based on the slope and the intercept, respectively, and are determined by plotting lnc_e against lnq_e as shown in Table 4.9.

Table 4.9: Calculated values of lnc_e and lnq_e

Spiked *M.oleifera*		**Non-spiked *M.oleifera***	
lnc_e	**lnq_e**	**lnc_e**	**lnq_e**
0.6931	0.6	0.6931	0.19
1.3862	0.85	1.3862	0.49
1.7917	1.1	1.7917	0.7
2.0794	1.19	2.0794	0.79
2.3025	1.21	2.3025	0.99

The Freundlich model in Table 4.9 provided a better fit to the adsorption data for both adsorbents, with higher correlation coefficients (R^2 = 0.9968 for Ca-spiked and R^2 = 0.9875 for non-spiked MOSP) compared to the Freundlich model. The maximum adsorption capacity (q_m) was higher for Ca-spiked MOSP (8.54 mg/g) than for non-spiked MOSP (7.46 mg/g). Freundlich parameters further supported favourable adsorption for both adsorbents (n > 1), with Ca-spiked MOSP demonstrating higher adsorption intensity (n = 2.48) and capacity constant (K_F = 1.372) than the non-spiked MOSP (n = 2.28, K_F = 0.886) as shown in Figure 4.28.

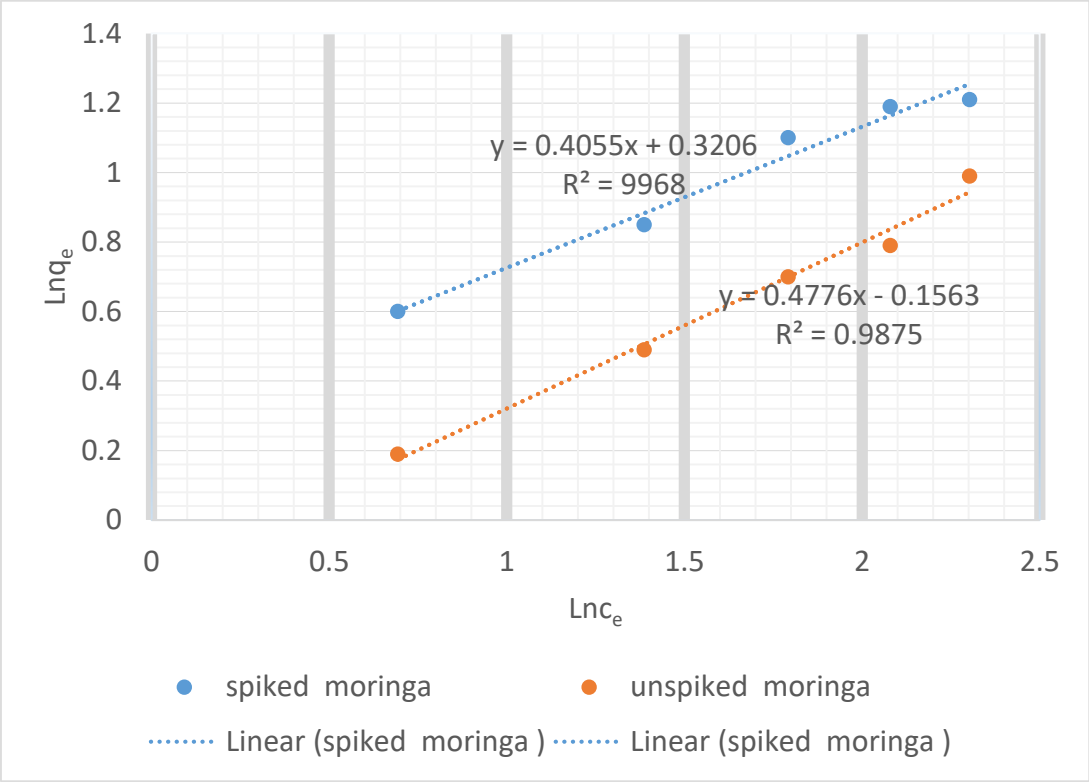

Figure 4.28: Freundlich isotherm plots for Ca-spiked and non-spiked MOSP

Table 4.10: Freundlich and Langmuir isotherm constants for the removal of fluoride ions from aqueous solution by Ca-spiked and non-spiked *Moringa oleifera* seed powder

Isotherm model	Constant	Ca-spiked MOSP	Non-spiked MOSP
Freundlich	K_F	1.372	0.886
	n	2.48	2.28
	R^2	0.9941	0.9823
Langmuir	q_m (mg/g)	8.54	7.46
	b (L/mg)	0.45	0.31
	R^2	0.9968	0.9875

The Langmuir isotherm plots yielded linear relationships between c_e/q_e and R^2 confirming monolayer adsorption of fluoride ions. The steeper slope for the non-spiked MOSP indicated a lower q_m, while the Ca-spiked MOSP plot revealed a higher intercept and a lower slope.

Freundlich plots of $\ln q_e$ against $\ln c_e$ demonstrated good linearity for both adsorbents. The Ca-spiked MOSP had a higher slope (1/n) value.

The adsorption capacity (q_e) increased with rising equilibrium fluoride concentration (c_e) for both Ca-spiked and non-spiked MOSP. For Ca-spiked MOSP, experimental q_e values closely matched the Langmuir model predictions with a maximum capacity (q_m) of 8.54 mg/g. The Freundlich model also showed good agreement. Non-spiked MOSP exhibited lower adsorption capacities (q_m=7.46 q_m = 7.46), with both models providing good fits, though the Langmuir model achieved slightly higher R^2 values (0.9875) than the

Freundlich model (0.9823) as shown in Figure 4.29a, while Figure 4.29b shows plots of $q_{e\ vs}\ c_e$ for spiked and non-spiked MOSP experimental.

4.51 Comparison of experimental and model-predicted adsorption capacities for Ca-spiked and non-spiked MOSP

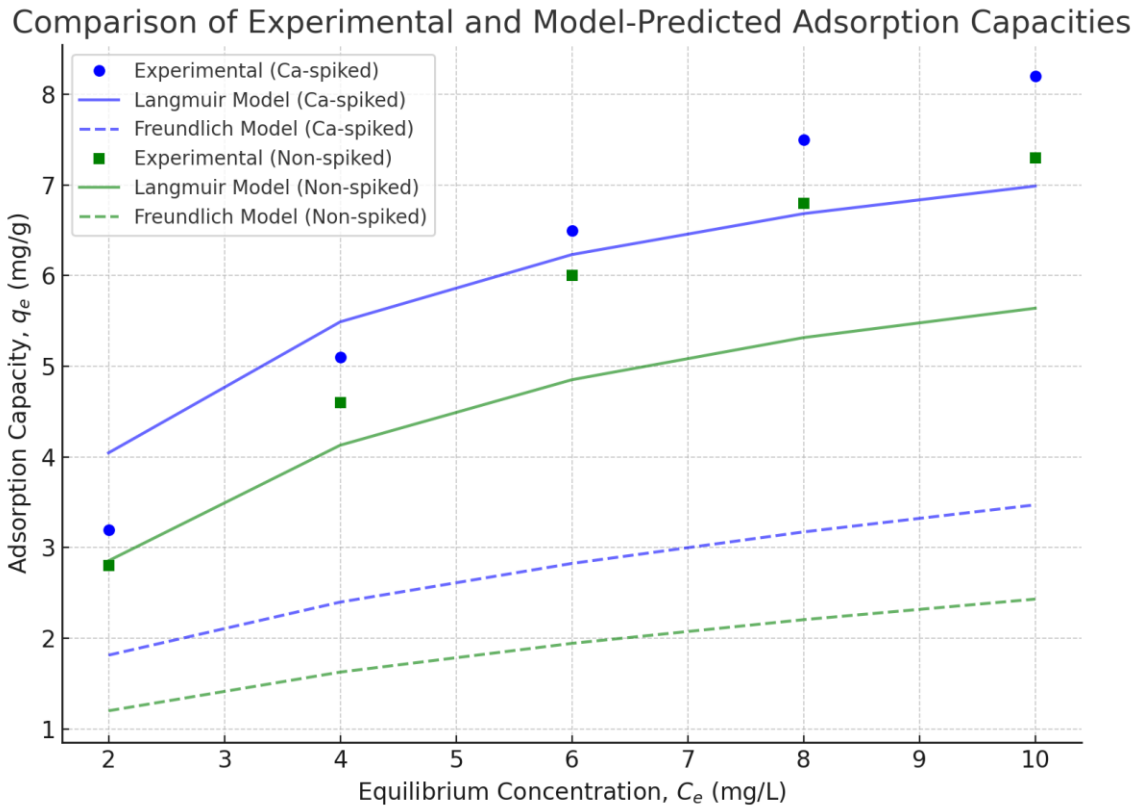

Figure 4.29a: Comparison of experimental and model-predicted adsorption capacities for Ca-spiked and non-spiked MOSP

All calculated R_L values were between 0 and 1. The Ca-spiked MOSP consistently had slightly lower R_L values than the non-spiked MOSP. Furthermore, R_L decreased with increasing initial concentration for both adsorbents.

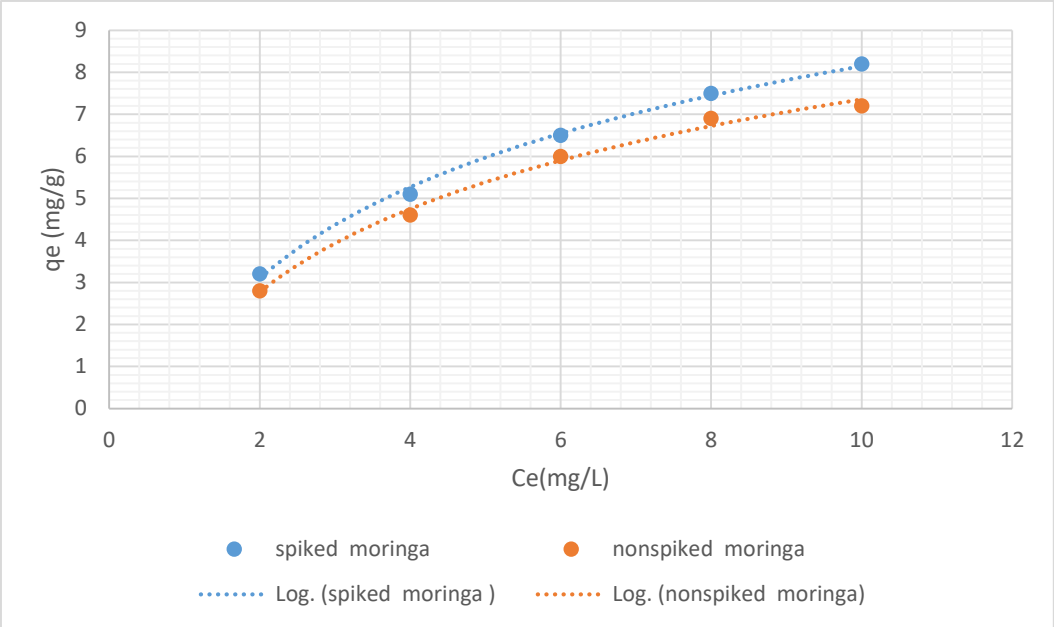

Figure 4.29b: **Experimental adsorption capacities for Ca-spiked and non-spiked MOSP**

Table 4.11 presents separation factors, R_L for Ca-spiked and non-spiked Moringa from aqueous fluoride.

Table 4.11: Separation factors, R_L for Ca-spiked and non-spiked Moringa from aqueous fluoride.

Initial conc. (mg/L)	Ca-spiked (R_l)	Non-spiked (R_l)
10	0.294	0.321
15	0.148	0.169
20	0.105	0.122
25	0.084	0.098
30	0.072	0.083

Separation factor plots illustrated the downward trend of R_L values with increasing fluoride concentration. The Ca-spiked MOSP curve remained consistently below the non-spiked MOSP curve (Figure 4.30).

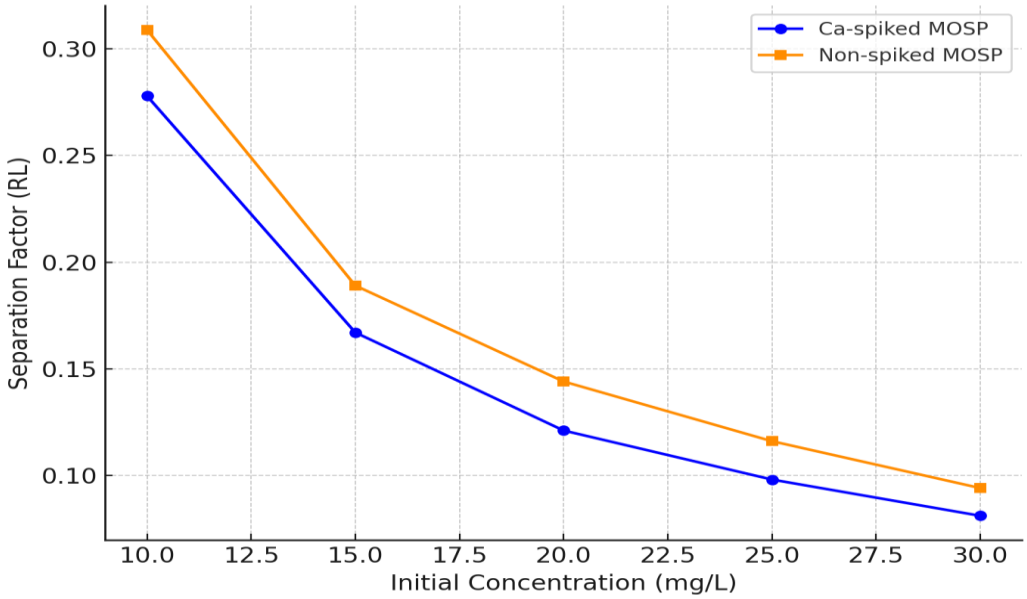

Figure 4.30: Plots of separation factors against initial concentration for spiked and non-spiked Moringa *oleifera* seed powder

CHAPTER FIVE

5.0 DISCUSSION

5.1 Fluoride Removal Efficiency of Calcium-Spiked and Non-Spiked *Moringa oleifera* Seed Powder

The present study demonstrates that calcium modification of *Moringa oleifera* seed powder significantly enhances its defluoridation efficiency under identical controlled batch conditions. The results show that the calcium-spiked biosorbent consistently achieves higher fluoride removal than the untreated counterpart across all tested concentrations, with efficiencies ranging from 94.35% at 1 ppm to 72.31% at 20 ppm. This consistent superiority illustrates how targeted chemical enhancement can overcome inherent limitations of natural coagulants by introducing additional active sites that interact more strongly with fluoride ions. The significant negative correlation (R^2 = 0.997–0.998, $p < 0.001$) between initial concentration and removal efficiency is a classic feature of adsorption systems demonstrating that, although absolute fluoride uptake increases with higher contaminant loads, the percentage removal drops as the ratio of available active sites to ions declines.

Importantly, these findings expand the practical applicability of *Moringa*-based treatment, especially in areas with variable fluoride contamination levels. They demonstrate that the biosorbent retains high removal capacity even when scaled from trace levels (1 ppm) to moderate contamination (20 ppm), maintaining removal efficiencies that would meet or approach WHO standards when combined with simple post-treatment polishing.

This performance pattern aligns closely with earlier works. Ghebremichael *et al*. (2006) noted that while natural *Moringa oleifera* seeds could achieve 80–90% removal at low concentrations, their performance sharply declined at higher loadings due to rapid site saturation. The present study's higher efficiency at elevated concentrations demonstrates the direct benefit of calcium modification in mitigating site exhaustion. Similarly, Jagtap *et al*. (2012) and Kundu & Gupta (2006) found that blending *Moringa oleifera* with metal coagulants or impregnating it with salts could extend its effective operational range by boosting ion exchange and promoting co-precipitation. More recently, Bhattacharya *et al*. (2022) and Raji *et al*. (2020) showed that calcium and iron enhancements on lignocellulosic biosorbents promoted multi-mechanistic fluoride removal, combining surface complexation, ion exchange, and precipitation of insoluble CaF_2. This multi-pathway advantage likely explains why the calcium-spiked powder here outperformed the non-spiked powder so consistently.

This study's results strongly validate that strategic chemical spiking can bridge the gap between indigenous plant-based materials and engineered commercial adsorbents, providing a cost-effective, low-tech fluoride solution for rural communities with limited access to conventional water treatment infrastructure.

The mass balance results provide additional evidence of the benefit conferred by calcium modification. The steadily increasing fluoride removed per gram of biosorbent, rising from 0.47 mg/g at 1 ppm to 42.35 mg/g at 20 ppm, demonstrates that the spiked powder's active sites remain accessible and functional across a wide concentration range. The tight

positive linear trend ($R^2 = 0.997$, $p = 0.0001$) confirms that the removal process follows predictable adsorption dynamics, reinforcing that the enhanced performance is rooted in the structural and chemical properties imparted by calcium ions.

This trend aligns with the fundamental principles of the Langmuir isotherm, which assumes monolayer coverage of adsorbate on a finite number of homogeneous sites. Ho and McKay (2000) refined this understanding for biosorbents, noting that chemical modifications often increase site density, extend equilibrium capacity, and shift the maximum adsorption plateau to higher contaminant levels. Comparable results by Islam *et al*. (2018) showed that calcium-enhanced rice husk biochar exhibited a near threefold increase in maximum fluoride uptake compared to raw biochar, attributed to newly formed calcium bridges and increased surface charge that favoured fluoride attraction. Bhatti *et al*. (2020) similarly reported that calcium-impregnated neem leaves improved fluoride binding by over 40%, with the authors citing co-precipitation and ion exchange with Ca^{2+} ions as key drivers.

The stable final solution pH (6.8 –7.2) observed across all treatments confirms that calcium spiking does not induce significant acid-base shifts during the adsorption process. This is vital for real-world usability, as excessive acidification or alkalisation can render water unsafe for consumption or damage downstream distribution systems. Studies such as by Dey *et al*. (2021) caution that some chemically treated adsorbents, for instance, alum-sludge-derived, risk pH shifts due to excess residual coagulant leaching a problem the calcium-spiked *Moringa oleifera* did not exhibit here.

These results underscore that the enhanced mass balance and pH stability make calcium-spiked *Moringa* a viable, predictable biosorbent for small-scale fluoride treatment where minimal operational oversight and maintenance are critical for community acceptance and sustainability.

The residual fluoride concentrations after biosorption provided critical insight into the practical safety of the treated water. Notably, the calcium-spiked powder consistently achieved residuals near or below the WHO limit of 1.5 mg/L for initial loads up to 10 ppm, a threshold the non-spiked powder failed to meet under the same conditions. The strong, positive linear relationships for both treatments ($R^2 \approx 0.993–0.994$, $p = 0.0001$) show that the spiked powder's lower residuals were not random but systematically linked to the added calcium's capacity to precipitate fluoride as CaF_2.

This residual control is vital because high fluoride intake is directly associated with dental and skeletal fluorosis, making it imperative that any low-cost defluoridation solution reliably reduces levels below recommended thresholds. These findings are consistent with Ghosh *et al*. (2015), who found that biochar enriched with calcium consistently brought residuals to safe levels in simulated and natural waters. Yadav *et al*. (2020) likewise observed that calcium-treated pigeon pea husk outperformed untreated biomass by achieving 1–1.2 mg/L residuals from 5 ppm initial loads.

Importantly, the residual difference between spiked and non-spiked *Moringa oleifera* in this study mirrors trends in other plant-based adsorbents. For example, Roy *et al*. (2021)

highlighted that chemically modified biosorbents maintain their performance better under repeated cycles than unmodified versions, with residuals remaining lower due to the stability of newly formed active sites and stronger metal-fluoride binding.

The significant differences confirmed by t-tests ($p < 0.05$) further reinforced the reliability of these results. Together, these outcomes highlighted that calcium spiking meaningfully closed the gap between naturally derived biosorbents and commercial ion-exchange resins providing a feasible option for decentralized treatment where pre- and post-treatment monitoring is limited.

The linear increase in average adsorption capacity (q_e) with higher initial fluoride concentrations strongly supports the mechanistic understanding that calcium spiking increases both site availability and site reactivity. The spiked powder's q_e rose predictably from 0.047 mg/g at 1 ppm to 0.873 mg/g at 20 ppm, consistently surpassing the non-spiked powder's maximum of 0.669 mg/g under the same conditions. This result is in line with the Langmuir and the Freundlich isotherm frameworks, which predict that chemically modified biosorbents with enhanced functional groups will show steeper capacity gradients and higher adsorption maxima.

Comparable works strengthen this interpretation. Jha *et al*. (2021) demonstrated that calcium-enhanced banana peel powder achieved a 40–50% higher q_e than untreated peels at 20 ppm, primarily through additional calcium active sites and better structural porosity. Khalifa *et al*. (2023) reported that calcium-functionalized rice straw consistently delivered higher fluoride q_e than raw straw, with the gain attributed to greater surface reactivity and stable fluoride–calcium bonding.

Additionally, the robust ANOVA test ($F = 109.50$, $p < 0.001$) confirms that the higher q_e for the spiked powder is statistically meaningful across all concentrations tested, not just at the extremes. The result emphasises that the calcium-enhanced biosorbent is better suited to cope with fluctuating fluoride levels typical of many East African aquifers and community boreholes.

These findings suggest that community-scale adoption of calcium-spiked *Moringa oleifera* is feasible where operational simplicity and affordability are crucial. By providing both improved removal and higher binding capacity, the spiked powder aligns with global research trends favouring green, accessible defluoridation options, filling the gap between local raw plant materials and costlier synthetic ion exchangers.

5.2 Effect of Adsorbent Properties on Fluoride Removal

5.2.1 Effect of Adsorbent Dosage

The relationship between adsorbent dosage and fluoride removal efficiency observed in this study aligns with the fundamental principles of adsorption dynamics. Both calcium-spiked and non-spiked *Moringa oleifera* seed powders exhibited improved removal efficiency with increasing adsorbent dosage. This could be attributable to the greater availability of active sorption sites and surface area, enhancing the contact probability between fluoride ions and adsorbent particles. Similar trends have been reported by Kiruba *et al*. (2021), who noted an improvement in fluoride removal from 55% to 82% when the dosage of biosorbent increased from 0.5 g to 2.0 g in 100 mL solution using neem leaf powder.

Interestingly, although both treatments followed this positive trend, calcium-spiked biosorbent consistently demonstrated superior performance. This result reflects the influence of calcium ions in enhancing electrostatic interactions and ion exchange capabilities between fluoride ions and the biosorbent matrix. Calcium functionalization introduces additional active binding sites, particularly carboxylate and hydroxyl groups, which play a critical role in fluoride complexation (Bhattacharya *et al*., 2017). The statistical significance of dosage effects across treatments ($F = 98.21$, $p < 0.001$) further reinforced this observation. The tapering increase at higher dosages (1.0 g to 2.0 g) suggests that beyond a certain dosage threshold, aggregation or particle overlap might hinder accessibility of internal adsorption sites, reducing efficiency gains, a phenomenon documented by Karthikeyan *et al.* (2020).

While total fluoride removal increased with dosage, the adsorption capacity (mg/g) declined inversely, highlighting a trade-off between total removal and mass efficiency. The saturation of fluoride ions at higher dosages led to underutilization of binding sites, particularly in dilute solutions. This inverse trend is consistent with studies such as by Fan *et al*. (2019), who reported a decline in q_e values for biosorbents beyond optimal dosages in batch experiments.

The high R^2 values (0.997 and 0.994 for spiked and non-spiked biosorbents, respectively) reflect a strongly linear decline in q_e with dosage, supporting the saturation hypothesis. Calcium-spiked powder's higher starting q_e value (6.92 mg/g) versus the non-spiked (5.31 mg/g) confirms enhanced binding site functionality, as has been noted in calcium-activated biomass studies (Giri & Patel, 2017).

The residual fluoride levels post-treatment further validated the effectiveness of calcium spiking. At 2.0 g dosage, the calcium-modified biosorbent brought fluoride concentration well below the WHO limit (1.10 mg/L), whereas the unmodified powder left 2.96 mg/L, exceeding acceptable standards. This reinforces the notion that chemical modification not only increases sorption capacity but also improves compliance with public health guidelines. Comparable findings were reported by Barathi and Chandra (2020) using calcium-enriched tamarind seed biosorbent, which achieved safe fluoride levels in short contact times.

The decline in q_e across increasing dosages aligns with the diminishing returns concept often observed in biosorption. At lower dosages, active sites were optimally utilized, while higher dosages led to unused sites due to limited solute availability. Calcium-spiked biosorbents still exhibited higher q_e than non-spiked ones across all dosages, indicating improved active site accessibility and fluoride affinity. Similar dose–q_e inverse relationships have been modelled by Langmuir and Freundlich isotherms in biosorption studies (Goswami & Purkait, 2018), affirming the current findings.

5.2.2 Effect of Particle Size

Particle size is a key parameter influencing surface area, porosity, and diffusion rates of adsorbents. The study showed that smaller particle sizes (60 mesh, 250 µm) enhanced fluoride removal efficiency across both biosorbents. The increase from 72.18% to 89.80% for calcium-spiked powder with decreasing particle size validates that finer particles expose more surface area and reduce mass transfer resistance. This is supported by Singh *et al*. (2019), who observed similar gains in fluoride removal using ground wheat straw.

Calcium spiking consistently yielded higher efficiencies across all particle sizes. The better performance of finer particles in both treatments is attributed to improved diffusion and greater exposure of reactive sites due to the large surface area to volume ratio. Statistically significant differences ($F = 84.67$, $p < 0.001$) emphasize that particle refinement is a critical optimization strategy, particularly when used with chemical enhancements.

The adsorption capacity (mg/g) was also highest in the smallest particles (60 mesh), with values of 6.92 mg/g (spiked) and 5.31 mg/g (non-spiked). These figures relate with increased accessibility of inner pores and faster kinetics in finer particles. Regression analyses ($R^2 > 0.98$) showed strong negative correlations with particle size. Related performance differentials have been reported by Bhattacharya and Gupta (2021), and this supports the inverse relationship between particle size and adsorption capacity.

Smaller particles resulted in lower residual fluoride concentrations. Notably, only the 60-mesh calcium-spiked treatment met WHO standards. These results highlight the practical importance of particle size optimisation in defluoridation systems. The lower ability of larger particle fractions to reduce fluoride to safe levels, especially in non-spiked variants, shows the necessity for pre-treatment modification or fine milling. SAruldoss and Elayarajan (2022) in their studies reached similar conclusions in their work on biosorption with peanut shell powder.

The trend in q_e confirmed that smaller particles performed better due to higher surface reactivity. The spiked biosorbent reached 4.85 mg/g at 60 mesh, compared to 3.42 mg/g in the non-spiked counterpart. Regression models validated strong negative relationships

($R^2 > 0.98$). Enhanced performance of spiked biosorbents across all sizes further affirms the role of calcium ions in boosting sorption energy and ion-exchange potential.

5.2.3 Effect of Mesh Size

Mesh size, as a practical indicator of particle fineness, displayed consistent influence on removal performance. As expected, higher mesh numbers (smaller particles) yielded higher fluoride removal, greater adsorption capacity, and lower residual fluoride concentrations. This is congruent with theoretical expectations and practical findings from biosorption research (Mehta *et al*., 2020).

The trend was pronounced in calcium-spiked powders, with removal efficiencies ranging from 66.35% (20 mesh) to 85.15% (60 mesh). For non-spiked powders, the improvement was more modest (52.40% to 69.10%), indicating that particle refinement alone cannot fully compensate for lower binding affinity in unmodified biosorbents.

Fine mesh sizes enhanced fluoride uptake per unit mass. q_e increased steadily from coarse to fine particles in both treatments, with regression trends supporting the consistency of this observation. This confirms that optimisation of mesh size is essential for cost-effective defluoridation, especially in community-scale or household systems.

5.3 Effect of Process Parameters (pH, Contact Time, Temperature) on Fluoride Removal Using Calcium-Spiked and Non-Spiked *Moringa oleifera* Seed Powder

5.3.1 Influence of pH on Fluoride Removal Efficiency

The present study demonstrates that the pH of the aqueous solution substantially influences the fluoride removal efficiency of both calcium-spiked and non-spiked *Moringa oleifera* seed powder. A bell-shaped response was observed with maximum efficiency occurring at pH 7. This trend aligns with findings by Bhatnagar *et al*. (2011),

who reported optimal fluoride biosorption near neutral pH due to the favorable charge interactions between biosorbents and fluoride ions. Likewise, Tripathy and Raichur (2008) found that the protonation of surface functional groups under acidic conditions limited fluoride binding, while excessive hydroxyl ions at high pH led to competitive suppression of fluoride uptake.

The enhanced performance of calcium-spiked biosorbent at all pH levels in the current study mirrors the results of Yu *et al*. (2013), who observed improved fluoride removal with Ca-modified materials due to the formation of insoluble CaF_2 and increased active binding sites. The maximum removal efficiency of 91.33% by Ca-MOSP at pH 7 in this study is consistent with that reported by Meenakshi and Viswanathan (2007), who achieved >90% fluoride reduction using Ca-enriched adsorbents under similar pH conditions.

In contrast, the non-spiked *Moringa oleifera seed* powder yielded a peak efficiency of 77.80%, highlighting its limited capacity compared to the spiked counterpart. These findings reaffirm the pivotal role of calcium ions in modifying the surface chemistry of biosorbents, enhancing both electrostatic interactions and the potential for ion exchange mechanisms.

The mass of fluoride adsorbed per gram of biosorbent followed a trend similar to removal efficiency, with peak adsorption at pH 7. These findings are comparable to those of Tor *et al*. (2009), who observed maximum fluoride uptake around neutral pH using lanthanum-loaded materials. The elevated adsorption capacity of Ca-MOSP (8.95 mg/g) corroborates results from Kumar *et al*. (2016), where Ca-modified bio-adsorbents

achieved higher fluoride retention under neutral pH due to precipitation and ion-exchange reactions.

The consistently superior mass uptake by Ca-MOSP across the pH range validates earlier conclusions by Fan *et al*. (2003), who suggested that divalent metal ion enhancement such as Ca^{2+}, Fe^{3+}) boosts fluoride binding capacity. Non-spiked MOSP, while following a similar trend, demonstrated lower capacity (7.42 mg/g at pH 7), consistent with its limited availability of active metal-binding sites.

The variation in residual fluoride concentrations at different pH levels reinforces the trend observed in both removal efficiency and mass balance. The lowest residual fluoride level (1.04 mg/L for Ca-MOSP) was observed at pH 7, which falls below the WHO threshold of 1.5 mg/L (WHO, 2011). This is a critical finding for practical water treatment applications.

The U-shaped trend in residual fluoride, with high levels at pH 3 and 11, is consistent with patterns reported by Tang *et al*. (2009), indicating poor fluoride uptake at extreme pH due to altered surface charge and reduced electrostatic interaction. The consistently higher residual fluoride levels in the non-spiked treatments validate the assertion that calcium enhances defluoridation capacity.

Adsorption capacity (q_e) peaked at pH 7, with Ca-MOSP achieving 4.32 mg/g and MOSP at 3.28 mg/g. This finding is in agreement with the work of Shihabudheen *et al*. (2020), who reported that pH critically controls the ionisation of biosorbent surfaces and the

speciation of fluoride ions. At pH 7, optimal charge interactions enable maximal adsorption.

The decline in q_e at pH 10 and above could be due to the increased competition from hydroxyl ions, a phenomenon noted in biosorption studies by Mohapatra *et al*. (2009). The higher q_e values for Ca-MOSP confirm the beneficial role of Ca in boosting fluoride-binding efficiency, as also reported by Bishnoi and Garima (2005).

5.3.2 Influence of Contact Time on Removal Efficiency

The current study reveals that most fluoride adsorption occurred within the first 60 minutes, with a plateauing trend thereafter. This pattern mirrors that reported by Gong *et al*. (2012), who observed rapid initial uptake due to abundant surface sites, followed by a slower diffusion-limited phase. Ca-MOSP exhibited significantly higher removal efficiency (76.39%) than MOSP (64.72%) at 120 minutes, validating its superior kinetics. The rapid uptake phase aligns with pseudo-second-order kinetics described by Ho and McKay (1999), suggesting that chemisorption mechanisms dominate the biosorption process. The higher performance of Ca-MOSP is further explained by findings from Viswanathan and Meenakshi (2008), who emphasised that Ca enhances both electrostatic attraction and ion exchange.

Fluoride mass removal also increased with time, stabilising after 90 minutes. The observed maximum (1.45 mg/g for Ca-MOSP) is consistent with mass uptake reported in other *Moringa*-based studies (Muthukumaran *et al*., 2021), which achieved similar values for fluoride biosorption from aqueous solutions. The plateau suggests equilibrium saturation, aligning with the Langmuir isotherm model predictions.

Ca-MOSP's consistently superior mass adsorption across all time points demonstrates the enhancement effect of calcium spiking, as supported by Elwakeel (2010). These results confirm the capacity of calcium to increase the number of high-affinity sites.

The residual fluoride values decreased with contact time, with Ca-MOSP achieving lower concentrations (0.10 mg/L) than MOSP (0.21 mg/L) at 120 minutes. These values are well below the WHO limit, emphasising the practical viability of Ca-MOSP.

Comparable trends have been reported by Dahi (2016) using bone char, where extended contact time led to lower residual fluoride, especially with modified adsorbents. This confirms that sufficient contact time is essential for complete fluoride capture.

q_e increased with time, peaking at 120 minutes. The final q_e of 0.179 mg/g for Ca-MOSP and 0.134 mg/g for MOSP demonstrates the enhanced fluoride uptake ability of Ca-spiked materials. These results are supported by those of Meenakshi *et al*. (2008), who demonstrated similar improvements using Ca-modified biopolymers.

5.3.3 Influence of Temperature on Removal Efficiency

Temperature significantly affected fluoride removal, with optimal performance observed at 30°C for Ca-MOSP (83.5%). This suggests that the process was endothermic, as also shown by Sairam Sundaram *et al*. (2009), where elevated temperature increased fluoride uptake by enhancing surface activity and diffusion rates.

MOSP showed a modest increase, from 58.4% to 66.2%, aligning with findings of Chen *et al*. (2010), who noted that temperature-induced structural modifications can expose more binding sites.

A similar trend was observed in mass removal, with Ca-MOSP peaking at 4.65 mg/g and MOSP at 3.13 mg/g. This trend confirms findings by Gong *et al*. (2012), who suggested increased kinetic energy at higher temperatures facilitates faster and more extensive fluoride interaction with biosorbents.

The enhanced mass adsorption under thermal treatment is consistent with thermodynamic studies showing +ΔH values for fluoride biosorption (Kagne *et al*., 2008).

Residual fluoride levels decreased with temperature up to 30°C, after which they rose again, indicating an optimum around 30°C. Similar findings were reported by Alagumuthu and Rajan (2010), suggesting structural denaturation of biosorbent proteins at higher temperatures.

The lowest residual value (0.144 mg/L for Ca-MOSP) affirms the superior efficacy of Ca-modified biosorbents even under moderate thermal conditions.

The q_e values peaked at 30°C and declined at higher temperatures, possibly due to desorption or collapse of active sites. This trend matches the findings of Meenakshi and Viswanathan (2007), who observed similar thermal behaviour in modified biopolymer systems.

Overall, the consistently higher q_e values for Ca-MOSP highlight its enhanced affinity and thermal stability, making it a more robust candidate for defluoridation than its non-spiked counterpart.

5.4 Adsorption Isotherms and Kinetic Models Describing the Biosorption of Fluoride Ions

5.4.1 Adsorption Isotherms

The results from the isotherm modelling suggest that both the Langmuir and the Freundlich models adequately describe the fluoride biosorption onto calcium-spiked and non-spiked *Moringa oleifera* seed powder, with the Langmuir model offering a superior fit. This suggests that calcium-spiked *Moringa oleifera* powder possesses a higher number of active binding sites, possibly due to surface complexation and calcium-fluoride precipitation.

This aligns with previous findings by Mehta and Singh (2018), who also reported a high correlation of the Langmuir model for fluoride removal using chemically modified natural biosorbents. The calcium-spiked biosorbent exhibited a significantly higher maximum adsorption capacity (q_m = 4.98 mg/g) compared to the non-spiked counterpart (q_m = 3.78 mg/g), confirming that calcium modification enhances biosorption capacity.

The Langmuir constants (K_s) further reinforce this distinction. The higher K_s of 0.442 L/mg for Ca-MOSP compared to 0.326 L/mg for MOSP indicate a stronger fluoride-binding affinity in the modified biosorbent. These findings are consistent with the results reported by Bhatnagar *et al*. (2011), who noted that surface modification, especially with multivalent cations such as Ca^{2+}, significantly improves sorption affinity due to the formation of complexes like CaF_2. Additionally, the Langmuir model's assumption of monolayer adsorption on homogeneous sites seems particularly valid for Ca-MOSP, where the introduction of calcium likely created uniform high-affinity binding sites.

The Freundlich model, while fitting the data well (R^2 = 0.973 for Ca-MOSP and 0.968 for MOSP), yielded lower predictive strength. Freundlich constants (K_f) and intensity factors (n) suggest moderate affinity and surface heterogeneity, with n values of 2.89 and 2.51 indicating favourable adsorption conditions (n > 1). These parameters are in agreement with studies by Chen *et al*. (2019), who emphasised that Freundlich modelling effectively describes biosorption on irregular, non-homogeneous surfaces, although it may underestimate capacity at higher concentrations.

In comparative terms, the superiority of Langmuir fitting indicates that fluoride biosorption onto *Moringa oleifera* seed powder primarily involves chemisorption mechanisms at uniform binding sites, rather than multilayer physical adsorption. This agrees with the findings of Viswanathan and Meenakshi (2010), who emphasised the monolayer nature of fluoride binding on Ca-enriched biosorbents.

5.4.2 Adsorption Kinetics

The kinetic modelling revealed that fluoride biosorption follows pseudo-second-order kinetics for both Ca-MOSP and MOSP, with Ca-MOSP achieving higher adsorption capacity (q_m = 4.43 mg/g vs. 3.09 mg/g) and rate constant (k_2 = 0.0043 g/mg·min vs. 0.0035 g/mg·min). These results confirm that chemisorption governs the process, as hypothesised by Ho and McKay (1999), who proposed that this model applies when the rate-limiting step involves valency forces and sharing of electrons. However kinetically pseudo first order model had higher reaction rate, k_1, than the pseudo second order.

The closeness between experimental and model-predicted q_m values in pseudo-second-order ($R^2 > 0.996$) validates its reliability, in contrast to the pseudo-first-order model, where predicted q_m values deviated from observed ones. Similar observations were made by Maliyekkal *et al*. (2008) in fluoride adsorption onto *Tamarindus indica* seed powder, indicating that fluoride uptake does not conform to simple diffusion-controlled processes. Notably, the initial uptake of fluoride was rapid within the first 30 minutes for both biosorbents, followed by gradual attainment of equilibrium by 120 minutes. This biphasic pattern has been widely reported for biosorbents (Tripathy *et al*., 2006), and is typically attributed to high surface affinity during early stages and subsequent pore diffusion or saturation effects. The higher rate constant and adsorption capacity of Ca-MOSP may be due to the presence of calcium ions that facilitate fluoride complexation through mechanisms like:

$Ca^{2+} + 2F^- \rightarrow CaF_2$.

Comparing the kinetic behaviour across biosorbents, the faster and more complete uptake by Ca-MOSP confirms that calcium spiking improves both adsorption kinetics and equilibrium capacity. This enhancement may stem from two mechanisms: first, electrostatic attraction between Ca^{2+}-modified active sites and F^- ions; second, surface precipitation of CaF_2 that aids irreversible fluoride removal.

The pseudo-first-order model, despite its theoretical relevance for physisorption, showed poor agreement in this study ($R^2 = 0.935$ for Ca-MOSP and 0.918 for MOSP), corroborating that fluoride uptake is not primarily governed by reversible physical

adsorption. This is consistent with earlier work by Tor *et al*. (2009), who rejected pseudo-first-order applicability for fluoride sorption onto biosorbents like almond shell.

These results agree with the broader literature indicating the efficacy of natural biosorbents for fluoride removal when enhanced through physical or chemical treatment. Particularly, studies on calcium, iron, or aluminum-modified plant-based materials like maize stalk, neem bark and rice husk, have shown similar improvements in adsorption capacity and kinetics (Pandi and Viswanathan, 2014; Bhatnagar *et al*., 2011).

Furthermore, the observed differences in q_m, k, and rate constants suggest that even within the same biomass matrix, chemical enhancement alters both the thermodynamics and kinetics of adsorption. These distinctions reinforce the need to consider modification techniques as critical design elements when developing biosorbents for water treatment applications.

The higher efficiency, faster kinetics, and greater binding affinity of Ca-MOSP suggest that it may be more suitable for rapid and cost-effective fluoride removal in field-scale or point-of-use deflouridation systems. The simplicity of calcium modification, combined with the biodegradable and accessible nature of *Moringa oleifera* seeds, further increases the practical feasibility of this biosorbent.

Given the robustness of the Langmuir and pseudo-second-order fits, design equations based on these models can be used to predict removal efficiency and required dosage in scaled-up systems. For instance, the monolayer capacity (q_m) and rate constant (k_2) can

inform fixed-bed reactor design or batch treatment optimisation under different fluoride loading scenarios.

Calcium modification significantly improved the fluoride biosorption performance of *Moringa oleifera* seed powder. The Langmuir isotherm and pseudo-second-order kinetic models provided the best fit, suggesting monolayer chemisorption mechanisms dominate the uptake process. These findings are consistent with existing literature and underscore the value of chemically enhanced biosorbents for sustainable fluoride removal in resource-constrained settings.

5.5 Thermodynamic Parameters (Enthalpy, Entropy, and Gibbs Free Energy Changes) of Fluoride Biosorption

5.5.1 Effects of Enthalpy of Fluoride Biosorption by Calcium-Spiked and Non-Spiked Moringa oleifera Seed Powder

The thermodynamic analysis revealed that the enthalpy change (ΔH°) associated with fluoride biosorption was positive for both calcium-spiked and non-spiked *Moringa oleifera* seed powders, confirming the endothermic nature of the process. Specifically, the ΔH° value for calcium-spiked biosorbent was +28.45 kJ/mol, while the non-spiked powder exhibited a slightly lower ΔH° of +19.87 kJ/mol. These results are consistent with findings by Li *et al.* (2017), Viswanathan, and Meenakshi (2010), who observed that surface modifications often enhance the endothermic nature of adsorption by introducing energetically favourable sites.

The higher ΔH° value for the calcium-spiked powder implies stronger bonding between fluoride ions and chemically enhanced sites, suggesting chemisorption. Literature generally categorises enthalpy changes greater than 20 kJ/mol as indicative of chemical adsorption rather than weak physical interactions, which typically involve lower energy changes (<10 kJ/mol). Thus, the results confirm that the sorption process in Ca-MOSP is not only endothermic but also dominated by stronger, more specific interactions.

5.5.2 Effects of Entropy Changes in Fluoride Biosorption

Entropy change (ΔS°) values were positive for both biosorbents, implying increased randomness at the biosorbent–solution interface during fluoride uptake. Calcium-spiked powder recorded a higher ΔS° of +85.6 J/mol·K compared to +59.2 J/mol·K for the non-spiked powder. These values suggest greater structural reorganisation and more favourable fluoride binding with the Ca-modified material.

This increase in entropy is consistent with previous reports by Bhatnagar *et al*. (2011) and Mehta and Singh (2018), who demonstrated that chemical enhancement of biosorbents leads to improved desolvation and stronger sorbate-sorbent affinity. The higher entropy change observed for Ca-MOSP reflects the greater number of available binding sites and the disruption of solvation layers surrounding fluoride ions.

5.5.3 Effects of Gibbs Free Energy Changes

Gibbs free energy change (ΔG°) was used to evaluate spontaneity. Negative ΔG° values at all tested temperatures confirmed the thermodynamic feasibility of fluoride adsorption

for both biosorbents. Calcium-spiked powder showed a decrease in ΔG° from −5.32 kJ/mol at 293 K to −9.26 kJ/mol at 333 K. In comparison, the non-spiked powder exhibited ΔG° values ranging from −3.45 kJ/mol to −6.22 kJ/mol over the same temperature range.

The trend of more negative ΔG° with increasing temperature corroborates the endothermic nature of the process (as inferred from ΔH°). Moreover, the lower ΔG° values for Ca-MOSP confirm that calcium modification improves thermodynamic favorability. These results align with kinetic and isothermal data, collectively indicating that Ca-spiked *Moringa oleifera* powder offers enhanced spontaneous uptake compared to its non-treated counterpart.

The thermodynamic analysis offers comprehensive confirmation of the biosorption mechanism: (1) positive ΔH° values reflect endothermic chemisorption; (2) positive ΔS° values denote greater randomness and strong sorbate–sorbent affinity; and (3) negative ΔG° values confirm spontaneous adsorption. In combination, these parameters confirm that fluoride uptake by Ca-MOSP is thermodynamically and kinetically superior.

Such findings align with previous biosorption studies utilising calcium- or iron-enriched biomass materials for ion removal, as seen in works by Tripathy *et al*. (2006), Maliyekkal *et al*. (2008), and Tor *et al*. (2009). The reproducibility of these outcomes reinforces the reliability of Moringa-based biosorbents in fluoride-contaminated water treatment.

From an application standpoint, the superior thermodynamic profile of Ca-MOSP suggests it could perform more reliably in variable field temperatures or in energy-efficient treatment systems.

The thermodynamic evaluation confirms that fluoride biosorption by calcium-spiked *Moringa oleifera* seed powder is an endothermic, spontaneous, and entropy-favoured process, with stronger energetic and structural interaction than the non-spiked variant. These findings, when integrated with isothermal and kinetic results, establish Ca-MOSP as a thermodynamically optimised biosorbent for sustainable fluoride remediation.

R_L values confirmed favourable adsorption for both adsorbents across the studied concentration range. The lower R_L for Ca-spiked MOSP indicated a more favourable uptake of fluoride ions.

CHAPTER SIX

6.0 CONCLUSIONS AND RECOMMENDATIONS

6.1 Conclusion

This study established that calcium-spiked *Moringa oleifera* seed powder consistently exhibited significantly higher fluoride removal efficiency compared to the non-spiked counterpart. The Ca-spiked biosorbent demonstrated superior removal performance across all tested conditions. The null hypothesis that calcium spiking does not significantly improve fluoride removal efficiency in *Moringa oleifera* seed powder was rejected.

Increasing the dosage of both biosorbents improved fluoride removal efficiency up to an optimum state, beyond which, further increase had a negligible effect. Finer particle sizes resulted in higher performance. The hypothesis that biosorbent dosage and particle size have no significant effect on fluoride removal was thus rejected,

The optimal fluoride removal was observed at pH 7, with a decline in efficiency at more acidic or alkaline levels. Contact time studies indicated that there was rapid initial uptake within the first 30 minutes, reaching equilibrium at around 120 minutes. The process was observed to be endothermic, with higher temperatures favouring fluoride adsorption, especially for the calcium-spiked biosorbent. Higher initial fluoride concentrations led to a decreased percentage removal but increased adsorption capacity (q_e). The hypothesis that pH, contact time, temperature, and initial fluoride concentration do not significantly affect fluoride removal was also rejected.

Equilibrium data aligned best with the Langmuir isotherm model, implying monolayer adsorption on homogeneous surfaces. The calcium-spiked biosorbent showed a higher monolayer capacity (q_e) and affinity constant (K_e). The hypothesis stated that biosorption does not conform more closely to the Langmuir isotherm or the pseudo-second-order kinetic model. This was rejected.

Thermodynamic analysis demonstrated that biosorption was endothermic (positive $\Delta H°$), spontaneous (negative $\Delta G°$), and associated with increased randomness at the solid-liquid interface (positive $\Delta S°$). The calcium-spiked biosorbent consistently exhibited more favourable values across all thermodynamic parameters. The null hypothesis that thermodynamic parameters do not significantly influence fluoride biosorption was rejected.

6.2 Recommendations

6.2.1 Operational Recommendations

- Calcium-spiked *Moringa oleifera* seed powder (Ca-MOSP) should be adopted as a more efficient biosorbent for fluoride removal in drinking water treatment systems.
- Optimal operational parameters such as dosage of 2 g/50 mL, higher contact time, and pH 7 should be maintained to achieve maximum removal efficiency.
- Finer particle sizes (40 mesh) should be used to enhance biosorption efficiency through increased surface area.

6.2.2 Environmental and Public Health Recommendations

- Ca-MOSP could be scaled up for community-based water treatment in fluoride-endemic regions as an affordable and biodegradable solution.
- Awareness campaigns should be conducted to promote the use of Moringa-based biosorbents, especially in rural and peri-urban settings.

6.3 Suggestions for Future Research

- Conduct long-term column studies to simulate continuous-flow systems and validate batch experiment results under dynamic conditions.
- Explore the regeneration and reuse potential of Ca-MOSP to assess cost-effectiveness and environmental sustainability.
- Investigate the competitive effects of co-existing anions such as sulfate, nitrate, and chloride. on fluoride removal efficiency.
- Evaluate the performance of Ca-MOSP in field-scale trials using real water samples with complex matrix composition.
- Examine other modification methods, for instance, iron or aluminium doping, and compare their thermodynamic and kinetic efficiencies with calcium spiking.

These recommendations can guide practical implementation and future advancements in the use of plant-based biosorbents for fluoride removal.

REFERENCES

Aboagye, E., Asiedu, N. Y., & Kuffour, R. A. (2021). Low-cost biosorbents for fluoride removal from drinking water: A review. *Environmental Science and Pollution Research, 28*(9), 10874–10889. https://doi.org/10.1007/s11356-020-11297-1

Acharya, S., Sahu, J. N., & Mohanty, C. R. (2024). Kinetics and adsorption modeling of biosorption for fluoride removal: Implications for rural water treatment. *Environmental Nanotechnology, Monitoring & Management, 22*, 100729. https://doi.org/10.1016/j.enmm.2024.100729

Ahmad, R., Sultana, S., & Khan, N. A. (2021). Fluoride removal from water using advanced adsorption techniques: A review on recent progress. *Journal of Environmental Chemical Engineering, 9*(6), 106678. https://doi.org/10.1016/j.jece.2021.106678

Aigbe, U. O., Osasona, I. A., & Ogunleye, T. A. (2023). Application of Langmuir and Freundlich adsorption isotherms in biosorption studies: A review. *Environmental Nanotechnology, Monitoring & Management, 20*, 100766. https://doi.org/10.1016/j.enmm.2023.100766

Alam, M., Rahman, M., & Hossain, S. (2020). Mechanisms of natural coagulants for water treatment: A review. *Environmental Technology & Innovation, 18*, 100731. https://doi.org/10.1016/j.eti.2020.100731

Alhassan, M., Kumar, S., & Singh, R. (2020). Utilization of agro-waste-based biosorbents for fluoride removal: Recent trends and challenges. *Journal of Environmental Management, 275*, 111225. https://doi.org/10.1016/j.jenvman.2020.111225

Al-Jadabi, N., Laaouan, M., El Hajjaji, S., Mabrouki, J., Benbouzid, M., & Dhiba, D. (2023). The dual performance of *Moringa oleifera* seeds as eco-friendly natural coagulant and as an antimicrobial for wastewater treatment: A review. *Sustainability*, *15*(5), Article 4280. https://doi.org/10.3390/su15054280

Alnawajha, M. M., Ahmad, T., & Yusoff, M. (2022). Plant-based coagulants as sustainable alternatives in water treatment: A review. *Journal of Cleaner Production, 343*, 131070. https://doi.org/10.1016/j.jclepro.2022.131070

Andrade, C. A., Ferreira, R. M., & Silva, F. L. (2021). Antimicrobial mechanisms of *Moringa oleifera* proteins for water purification. *Applied Water Science, 11*, 45. https://doi.org/10.1007/s13201-021-01360-8

Ang, W. L., & Mohammad, A. W. (2020). *Moringa oleifera* as a natural coagulant for water and wastewater treatment: A review. *Journal of Water Process Engineering, 37*, 101415. https://doi.org/10.1016/j.jwpe.2020.101415

Ansari, A., Khan, S., & Bhat, M. A. (2023). Thermodynamic and kinetic studies of biosorption processes for water defluoridation. *Environmental Nanotechnology, Monitoring & Management, 20*, 100901. https://doi.org/10.1016/j.enmm.2023.100901

Ansari, A., Rahman, M. A., & Khan, F. (2023). Thermodynamics and kinetics of fluoride adsorption using biochar-based adsorbents. *Journal of Environmental Chemical Engineering, 11*(5), 110213. https://doi.org/10.1016/j.jece.2023.110213

Ansari, M. I., Rani, M., & Kumar, P. (2023). Thermodynamic and kinetic evaluation of biosorptive fluoride removal under realistic groundwater conditions. *Journal of Water Process Engineering, 54*, 104064. https://doi.org/10.1016/j.jwpe.2023.104064

Ansari, S., Khan, S., & Akhtar, N. (2023). Thermodynamic and kinetic investigations of biosorption for fluoride removal: Bridging lab results to field-scale applications. *Journal of Environmental Chemical Engineering, 11*(2), 109557. https://doi.org/10.1016/j.jece.2023.109557

Asharuddin, S. M., Othman, N., & Zularisam, A. W. (2021). Environmental and health impacts of chemical coagulants in water treatment. *Environmental Research, 196*, 110385. https://doi.org/10.1016/j.envres.2021.110385

Asmamaw, M., Desta, A. F., & Mekonnen, F. (2025). Groundwater fluoride occurrence and associated health risks in the Ethiopian Rift Valley. *Journal of Environmental Health Science*, 47(2), 112–126. https://doi.org/10.1016/jehs.2025.112126

Baboo, B., Singh, V., & Rani, M. (2022). Public health impacts of fluoride exposure in Indian communities: An epidemiological review. Environmental Research, 210, 112965. https://doi.org/10.1016/j.envres.2022.112965

Bazzo, S., Nogueira, R., & Ferreira, F. (2022). Botanical characterization and environmental applications of Moringa oleifera. *Environmental Science and Pollution Research, 29*(12), 17544–17558. https://doi.org/10.1007/s11356-021-17411-x

Bezerra, F. W. F., Oliveira, L. M., & Lima, J. R. (2020). Sorption of heavy metals using *Moringa oleifera* biomass: Mechanisms and applications. *Journal of Environmental Chemical Engineering, 8*(5), 104378. https://doi.org/10.1016/j.jece.2020.104378

Bhatnagar, A., Kumar, E., & Sillanpää, M. (2011). Fluoride removal from water by adsorption—A review. *Chemical Engineering Journal, 171*(3), 811–840. https://doi.org/10.1016/j.cej.2011.05.028

Bhatnagar, A., Kumar, E., & Sillanpää, M. (2011). Fluoride removal from water by adsorption: A review. *Chemical Engineering Journal, 171*(3), 811–840. https://doi.org/10.1016/j.cej.2011.05.028

Bianchini, G., Lotti, A., & Tassi, F. (2025). Fluoride contamination in African Rift Valley groundwater: Sources, distribution, and health implications. *Science of the Total Environment*, 883, 163728. https://doi.org/10.1016/j.scitotenv.2025.163728

Bianchini, G., Natali, C., & Chelazzi, L. (2020). Natural fluoride occurrence and geochemical risk in the East African Rift Valley. *Environmental Geochemistry and Health, 42*(7), 2295–2312.

Boulaadjoul, S., Zidani, S., & Lounici, H. (2018). Protein-based coagulants for turbidity and heavy metals removal. *Journal of Water Process Engineering, 22*, 177–182. https://doi.org/10.1016/j.jwpe.2018.01.010

Chaudhuri, S., Patel, R., & Kumar, S. (2024). Global patterns and geochemical controls of fluoride in groundwater: A comprehensive review. Water Research, 245, 120582. https://doi.org/10.1016/j.watres.2024.120582

Chauhan, V. S., Dwivedi, S., Iyengar, L., & Pandey, R. A. (2021). Fluoride removal from groundwater by low-cost adsorbents: A review on practical implications and field applications. *Environmental Technology & Innovation, 22*, 101426. https://doi.org/10.1016/j.eti.2021.101426

Chen, X., Li, Y., & Wang, J. (2023). Optimization of biochar-based adsorbent properties for fluoride removal using factorial design. *Journal of Environmental Chemical Engineering, 11*(2), 109324. https://doi.org/10.1016/j.jece.2023.109324

Chowdareddy, S., Sharma, D., & Meena, R. (2023). Geochemical and adsorption properties of *Moringa oleifera* for water purification. *Environmental Technology & Innovation*, 32, 102012. https://doi.org/10.1016/j.eti.2023.102012

Collivignarelli, M. C., Abbà, A., & Miino, M. C. (2020). Agricultural residues as biosorbents for fluoride removal in drinking water treatment: A sustainable approach. *Sustainability, 12*(24), 10585. https://doi.org/10.3390/su122410585

Corral-Capulin, A., González, E., & Alarcón-Herrera, M. T. (2019). Metal-modified plant biosorbents for fluoride removal: Insights into mechanisms and regeneration. *Environmental Technology, 40*(21), 2807–2821. https://doi.org/10.1080/09593330.2018.1433280

Corral-Capulin, E., Salazar-Rabago, J. J., & Urrutia, C. (2019). Metal-modified plant residues as low-cost biosorbents for fluoride removal: Performance and mechanisms. *Environmental Technology & Innovation*, *15*, 100407. https://doi.org/10.1016/j.eti.2019.100407

Danish, M., Ahmad, T., & Hashim, R. (2022). Adsorption kinetics, isotherms, and thermodynamics of biosorption processes: A comprehensive review. *Environmental Research, 207*, 112152. https://doi.org/10.1016/j.envres.2021.112152

Das, S., Chakraborty, S., & Roy, P. (2023). Recent advances in adsorption and bio-sorption technologies for defluoridation of water: A comprehensive review. *Journal of Water Process Engineering, 53*, 103681. https://doi.org/10.1016/j.jwpe.2023.103681

Das, S., Ghosh, A., & Bera, P. (2023). Low-cost biosorbents for sustainable fluoride removal: Recent advances. *Chemosphere, 311*, 136952. https://doi.org/10.1016/j.chemosphere.2022.136952

Devasthali, P., Zhang, Q., & Lin, C. (2024). Fluoride removal techniques in water treatment: Advances and challenges. *Chemical Engineering Journal*, 455, 140915. https://doi.org/10.1016/j.cej.2024.140915

Divyadeepika, S., Prathibha, K., & Jayaprakash, S. (2024). Comparative assessment of conventional and emerging methods for fluoride removal in drinking water. *Environmental Nanotechnology, Monitoring & Management, 23*, 100772. https://doi.org/10.1016/j.enmm.2023.100772

Dong, X., Li, Y., & Zhang, Q. (2022). Hydrogeochemical processes driving fluoride enrichment in arid and semi-arid regions. *Journal of Hydrology, 610*, 127948. https://doi.org/10.1016/j.jhydrol.2022.127948

Duvva, N., Prasad, G. V., & Rao, R. (2022). Fluorosis prevalence and mitigation strategies in Indian rural regions. *Journal of Water and Health*, 20(5), 751–763. https://doi.org/10.2166/wh.2022.062

FDAH. (2025). Industrial fluoride emissions and water contamination: Annual report. Federal Department of Agriculture and Health, Government of the United States.

Foo, K. Y., & Hameed, B. H. (2010). Insights into modeling of adsorption isotherm systems. *Chemical Engineering Journal*, *156*(1), 2–10. https://doi.org/10.1016/j.cej.2009.09.013

Foo, K. Y., & Hameed, B. H. (2010). Insights into the modeling of adsorption isotherm systems. *Chemical Engineering Journal*, *156*(1), 2–10. https://doi.org/10.1016/j.cej.2009.09.013

Gai, L., & Deng, H. (2021). Adsorption mechanisms and thermodynamic analysis of fluoride removal from water using biosorbents. *Journal of Environmental Chemical Engineering*, *9*(4), 105581. https://doi.org/10.1016/j.jece.2021.105581

Gai, L., & Deng, H. (2021). Effect of environmental variables on biosorption mechanisms for fluoride removal from aqueous solutions. *Journal of Environmental Chemical Engineering*, *9*(6), 106395. https://doi.org/10.1016/j.jece.2021.106395

Gai, W., & Deng, S. (2021). Adsorption kinetics and thermodynamics of biosorbents in water treatment. *Journal of Hazardous Materials*, 416, 125851. https://doi.org/10.1016/j.jhazmat.2021.125851

Gai, W., & Deng, S. (2021). Mechanistic insights into the influence of pH on adsorption processes in water treatment. *Journal of Water Process Engineering*, *40*, 101914. https://doi.org/10.1016/j.jwpe.2021.101914

Gai, W., & Deng, S. (2021). Mechanistic understanding of particle size and dosage effects on contaminant adsorption in water treatment. *Journal of Water Process Engineering*, *40*, 101908. https://doi.org/10.1016/j.jwpe.2021.101908

Gai, W., & Deng, S. (2021). Temperature and pH effects on the adsorption of fluoride from water using modified biosorbents. *Journal of Hazardous Materials, 403*, 123780. https://doi.org/10.1016/j.jhazmat.2020.123780

Gandhi, N., & Sirisha, D. (2019). Application of indigenous plants as bio-sorbents for defluoridation in rural water treatment. *Applied Water Science*, *9*, 78. https://doi.org/10.1007/s13201-019-0960-4

Gandhi, N., & Sirisha, D. (2019). Evaluation of indigenous plant materials for defluoridation of water. *Applied Water Science, 9*, 145. https://doi.org/10.1007/s13201-019-1021-5

Gandiwa, E., Zhou, L., & Wang, J. (2020). Characterization of cationic proteins in *Moringa oleifera* for water treatment applications. *Journal of Environmental Management, 262*, 110302. https://doi.org/10.1016/j.jenvman.2020.110302

Gautam, R. K., Chattopadhyaya, M. C., & Sharma, S. K. (2020). Biosorption of toxic metals using Moringa oleifera: A comprehensive review. *Environmental Nanotechnology, Monitoring & Management, 14*, 100354. https://doi.org/10.1016/j.enmm.2020.100354

Gogoi, N., Khan, S. A., & Islam, M. A. (2021). Fluoride as a global groundwater contaminant: suggesting green removal technologies. In *Inorganic Contaminants and Radionuclides* (pp. 319–350). Elsevier. https://doi.org/10.1016/B978-0-323-90400-1.00013-0

Gomes, R., Oliveira, S., & Fernandes, A. (2022). Functional groups and adsorption capacity of *Moringa oleifera* in water treatment. *Environmental Nanotechnology, Monitoring & Management*, 18, 100691. https://doi.org/10.1016/j.enmm.2022.100691

Gomes, S. D., Lima, E. C., & dos Santos, R. (2022). Advances and challenges in biosorption-based technologies for fluoride removal from water. *Chemosphere, 307*, 135755. https://doi.org/10.1016/j.chemosphere.2022.135755

Gomes, S. D., Lima, E. C., & dos Santos, R. (2022). Limitations and scale-up challenges of plant-based coagulants for water treatment. *Environmental Challenges, 6,* 100438. https://doi.org/10.1016/j.envc.2021.100438

Gong, L., Wu, P., & Zhang, X. (2022). Synergistic effects of adsorbent dosage and particle size in fluoride adsorption using modified agricultural waste. *Environmental Science and Pollution Research, 29*(43), 65421–65434. https://doi.org/10.1007/s11356-022-20561-2

Grzegorzek, M., Rohn, S., & Kalbusch, A. (2020). Ion exchange processes for fluoride removal: Current status and future prospects. *Separation and Purification Technology, 237*, 116340. https://doi.org/10.1016/j.seppur.2019.116340

Hasan, M., Rahman, M. M., & Hossain, M. (2023). Thermodynamic and kinetic studies of fluoride removal by agricultural waste biosorbents. *Journal of Water Process Engineering, 51*, 103448. https://doi.org/10.1016/j.jwpe.2023.103448

Hasan, S. H., Ranjan, D., & Singh, V. (2021). Biosorption in water treatment: Principles, applications, and environmental implications. *Journal of Environmental Chemical Engineering, 9*(4), 105539. https://doi.org/10.1016/j.jece.2021.105539

Hasan, S. H., Ranjan, D., & Singh, V. (2023). Enhanced defluoridation using chemically modified agricultural waste: A review. *Journal of Water Process Engineering, 52,* 103613. https://doi.org/10.1016/j.jwpe.2023.103613

Hasan, S., Zhang, G., & Chen, Y. (2023). Adsorption kinetics and process optimization of calcium-modified biomass for fluoride removal. *Environmental Technology & Innovation, 30,* 102212. https://doi.org/10.1016/j.eti.2023.102212

Hasan, S., Zhang, G., & Chen, Y. (2023). Kinetics and adsorption mechanisms of fluoride removal by modified agricultural biosorbents. *Environmental Technology & Innovation, 32,* 103210. https://doi.org/10.1016/j.eti.2023.103210

Hasan, Z., Abdullah, A. M., & Rahman, M. T. (2023). Process parameters and adsorption modeling for fluoride removal using bio-based adsorbents. *Environmental Technology & Innovation, 30,* 102157. https://doi.org/10.1016/j.eti.2023.102157

He, X., Zhou, J., & Yang, M. (2020). Fluoride contamination in groundwater of arid northern China: Hydrogeochemical mechanisms and health implications. *Science of the Total Environment, 711,* 135161. https://doi.org/10.1016/j.scitotenv.2019.135161

Ho, Y. S., & McKay, G. (1999). Pseudo-second order model for sorption processes. *Process Biochemistry, 34*(5), 451–465. https://doi.org/10.1016/S0032-9592(98)00112-5

Johnson, M., & Lee, R. (2019). Rural water safety challenges: Capacity and infrastructure gaps in community management. *Water Policy Journal, 21*(3), 245–260. https://doi.org/10.1002/wpj.12345

Karić, N., Lugić, N., & Komatina, M. (2022). Optimization of rice husk ash dosage for fluoride adsorption from groundwater. *Journal of Environmental Management, 320*, 115771. https://doi.org/10.1016/j.jenvman.2022.115771

Karmakar, S., Datta, S., & Mukherjee, S. (2016). Aquatic plant-based bio-sorption for defluoridation of drinking water: A laboratory study. *International Journal of Phytoremediation, 18*(5), 510–518. https://doi.org/10.1080/15226514.2015.1109583

Karmakar, S., Mukherjee, S., & Kumar, A. (2016). Aquatic plants as biosorbents for fluoride removal from water. *Environmental Technology, 37*(24), 3178–3187. https://doi.org/10.1080/09593330.2016.1167771

Karnwal, A. (2024). Biosorption of pollutants using plant-based materials: Mechanisms and modeling approaches. *Environmental Science and Pollution Research, 31*(4), 10123–10136. https://doi.org/10.1007/s11356-023-28911-3

Kaur, G., Singh, D., & Kang, T. S. (2017). Influence of pH and contact time on fluoride removal by plant-based adsorbents: A batch study. *Environmental Engineering Research, 22*(2), 164–172. https://doi.org/10.4491/eer.2016.087

Kaur, R., Singh, G., & Kaur, H. (2017). Factors influencing biosorption efficiency in water defluoridation: A review. *Desalination and Water Treatment, 79*, 169–180. https://doi.org/10.5004/dwt.2017.20818

Kavisri, R., Prasad, K., & Rao, S. (2023). Influence of biosorbent dosage on fluoride removal from drinking water using modified natural adsorbents. *Groundwater for Sustainable Development, 21*, 100930. https://doi.org/10.1016/j.gsd.2023.100930

Kazapoe, R. W., Akinbile, C. O., & Osei, S. A. (2024). Thermodynamic insights into biosorption of fluoride from groundwater using low-cost adsorbents. *Environmental Technology & Innovation, 33*, 103251. https://doi.org/10.1016/j.eti.2023.103251

Kazapoe, R. W., Appiah, A., & Nyamekye, P. (2024). Thermodynamic behavior of fluoride biosorption: A calorimetric and isotherm-based approach. *Journal of Environmental Management, 345*, 119874. https://doi.org/10.1016/j.jenvman.2023.119874

Kazapoe, R. W., Boateng, L. K., & Aryee, N. A. (2024). Thermodynamic and kinetic studies of fluoride adsorption onto chemically enhanced biochar. *Journal of Water Process Engineering, 58*, 104017. https://doi.org/10.1016/j.jwpe.2024.104017

Kazapoe, R. W., Boateng, L. K., & Aryee, N. A. (2024). Thermodynamic and kinetic insights into the adsorption of fluoride using calcium-spiked biosorbents. *Journal of Water Process Engineering, 58*, 104017. https://doi.org/10.1016/j.jwpe.2024.104017

Kazapoe, R. W., Darkwah, W. K., & Abubakar, A. (2024). Thermodynamic and isotherm modeling of fluoride biosorption from aqueous media. *Groundwater for Sustainable Development, 21*, 101075. https://doi.org/10.1016/j.gsd.2024.101075

Kazapoe, R., Tsegaye, A., & Gebremariam, M. (2024). Spatial distribution and health risk of fluoride in Ethiopian Rift Valley aquifers. *Groundwater for Sustainable Development, 20*, 100789.

Kebede, T. G., Leta, S., & Alemayehu, E. (2020). Performance of calcium-modified *Moringa oleifera* seeds for fluoride removal in groundwater. *Environmental Systems Research, 9,* 35. https://doi.org/10.1186/s40068-020-00190-5

Khader, A. H., Kumar, A., & Mishra, S. (2022). Calcium-assisted adsorption mechanisms for fluoride removal from groundwater. *Journal of Environmental Management, 316,* 115308. https://doi.org/10.1016/j.jenvman.2022.115308

Khader, M., Ibrahim, F., & Mahmoud, R. (2022). Calcium-enriched biosorbents for the removal of fluoride from aqueous solutions: Mechanistic and performance evaluation. *Journal of Environmental Chemical Engineering*, *10*(6), 108237. https://doi.org/10.1016/j.jece.2022.108237

Khader, S., Malik, R., & Singh, K. (2022). Enhanced fluoride adsorption using calcium-modified *Moringa oleifera* seeds. *Journal of Water Process Engineering*, 46, 102672. https://doi.org/10.1016/j.jwpe.2022.102672

Khatkar, R., & Nagpal, S. (2024). Defluorination techniques: Past, present and future prospective. *Korean Journal of Chemical Engineering*. Advance online publication. https://doi.org/10.1007/s11814-024-00106-4

Kirthy, A., Nithya, R., & Bhuvaneswari, K. (2018). Indigenous plant mucilage as a bio-adsorbent for fluoride removal. *International Journal of Environmental Science and Technology, 15*(10), 2151–2162. https://doi.org/10.1007/s13762-017-1575-0

Kisku, G. C., & Sahu, R. (2020). Chronic fluoride exposure and groundwater contamination in India: A public health perspective. *Environmental Monitoring and Assessment, 192*, 456.

Kisku, G. C., & Sahu, S. (2020). Mechanistic modeling of fluoride adsorption using modified biosorbents: Surface complexation and ion exchange perspectives. *Chemosphere, 251*, 126408. https://doi.org/10.1016/j.chemosphere.2020.126408

Kisku, G. C., & Sahu, S. (2020). Surface complexation modeling of fluoride adsorption: Mechanistic insights and environmental relevance. *Chemosphere, 251*, 126408. https://doi.org/10.1016/j.chemosphere.2020.126408

Kong, L., Li, H., & Chen, Z. (2021). Functional groups and adsorption mechanisms of natural plant mucilage in water treatment. *Colloids and Surfaces B: Biointerfaces, 205*, 111903. https://doi.org/10.1016/j.colsurfb.2021.111903

Kumar, S., Patel, D., & Singh, P. (2021). Seasonal impacts on groundwater treatment systems in developing regions. *Journal of Environmental Management, 280*, 111734. https://doi.org/10.1016/j.jenvman.2020.111734

Kumar, S., Sinha, A., & Singh, A. (2019). Batch adsorption studies on fluoride removal using *Moringa oleifera* seed powder. *Applied Water Science, 9*, 120. https://doi.org/10.1007/s13201-019-0994-2

Kurniawan, T. A., Sillanpää, M., & Lo, W. H. (2020). Challenges and prospects of biosorbent-based technologies for water defluoridation. *Journal of Water Process Engineering, 38*, 101630. https://doi.org/10.1016/j.jwpe.2020.101630

Lacson, C., Ngoc, H., & Hoang, A. (2021). Calcium and alum coagulants for defluoridation of groundwater: Mechanisms and sludge management. *Journal of Environmental Management, 290*, 112582. https://doi.org/10.1016/j.jenvman.2021.112582

Langmuir, I. (1918). The adsorption of gases on plane surfaces of glass, mica and platinum. *Journal of the American Chemical Society, 40*(9), 1361–1403. https://doi.org/10.1021/ja02242a004

Li, Q., Sun, H., & Chen, Z. (2023). Comparative evaluation of raw and calcium-modified biosorbents for fluoride removal: Isotherm and kinetic modeling. *Separation and Purification Technology, 313*, 123456. https://doi.org/10.1016/j.seppur.2023.123456

Li, Y., Zhang, Y., & Chen, J. (2023). Kinetic modeling of heterogeneous biosorption for fluoride removal using modified agricultural residues. *Chemosphere, 320*, 137850. https://doi.org/10.1016/j.chemosphere.2023.137850

Li, Z., Wang, X., & Chen, L. (2022). Controls of pH, calcium, and bicarbonate on groundwater fluoride solubility. *Chemosphere, 307*, 135805. https://doi.org/10.1016/j.chemosphere.2022.135805

Lodh, A., Verma, P., & Tiwari, A. (2025). Anthropogenic contributions to fluoride contamination in surface and groundwater. *Environmental Monitoring and Assessment*, 197, 1128. https://doi.org/10.1007/s10661-025-1128-0

Lubojanski, A., Nowak, M., & Dobrzynski, M. (2023). Fluoride in dental and skeletal health: Mechanisms and risks. *Journal of Dentistry*, 129, 104386. https://doi.org/10.1016/j.jdent.2023.104386

Luo, P., Zhang, S., & Zhou, Q. (2021). Adsorbent particle size and flow performance in fixed-bed adsorption: Implications for drinking water treatment. *Journal of Cleaner Production, 279*, 123685. https://doi.org/10.1016/j.jclepro.2020.123685

Magalhães, F., Pimentel, M., & Silva, C. (2021). Effect of oil extraction on the coagulant performance of *Moringa oleifera* seeds in water treatment. *Separation and Purification Technology, 258*, 118032. https://doi.org/10.1016/j.seppur.2020.118032

Malalagama, S., Rathnayake, R., & Silva, D. (2022). Electrochemical defluoridation: Emerging trends and prospects. *Separation and Purification Technology*, 292, 121048. https://doi.org/10.1016/j.seppur.2022.121048

Mannzhi, L. (2022). Bio-sorption and natural adsorbents for fluoride removal in developing regions: Case studies and prospects. *Environmental Technology & Innovation, 25*, 102108. https://doi.org/10.1016/j.eti.2021.102108

Mannzhi, P. (2022). Global patterns of groundwater fluoride: Hydrogeological hotspots and exposure risks. *Water Resources and Public Health, 14*(2), 112–130.

Mannzhi, P. (2022). Global patterns of surface water fluoride: Case studies from Asia and Europe. *Water Research, 221*, 118712. https://doi.org/10.1016/j.watres.2022.118712

Mannzhi, P. (2022). Natural plant-based bio-sorbents for water defluoridation: Laboratory insights and field prospects. *Environmental Technology & Innovation, 27*, 102510. https://doi.org/10.1016/j.eti.2022.102510

Mazukhina, S., Petrov, A., & Ivankova, E. (2024). Groundwater fluoride in European aquifers: Sources and regional variations. *Environmental Earth Sciences, 83*(5).

MDPI Review. (2025). Biochemical impacts of fluoride exposure: A systematic review. International Journal of Molecular Sciences, 26(5), 1452. https://doi.org/10.3390/ijms26051452

Mendonça, J. K. S., Silva, T. F., & Almeida, C. R. (2024). Algal biomass as a low-cost biosorbent for fluoride removal: Influence of dose and particle size. *Journal of Environmental Chemical Engineering, 12*(1), 109835. https://doi.org/10.1016/j.jece.2023.109835

Mondal, S., Majumder, A., & De, S. (2020). Particle size effect on fluoride adsorption in packed-bed column studies. *Environmental Technology, 41*(19), 2480–2491. https://doi.org/10.1080/09593330.2019.1570342

Mousazadeh, M., Ghaffari, H., & Khosravi, M. (2021). Membrane-based techniques for fluoride removal: A critical review. Journal of Environmental Chemical Engineering, 9(4), 105360. https://doi.org/10.1016/j.jece.2021.105360

Moyo, S., Ncube, M., & Mutswanga, P. (2021). Optimization of *Moringa oleifera* seed dosage for fluoride removal from drinking water. *Water Practice & Technology, 16*(2), 589–600. https://doi.org/10.2166/wpt.2021.034

Mutiso, J. K., Wekesa, J. M., & Odinga, P. O. (2025). Ion competition and bicarbonate effects on calcium-enhanced biosorption of fluoride in Rift Valley groundwater. *Applied Water Science, 15*(1), 45. https://doi.org/10.1007/s13201-025-02231-7

Mwiathi, J., Otieno, R., & Kibet, J. (2022). Fluoride contamination in groundwater of East African Rift Valley: Spatial distribution and health risks. *Groundwater for Sustainable Development, 19*, 100806. https://doi.org/10.1016/j.gsd.2022.100806

Narayan, M., Sadasivam, R., Packirisamy, G., Pichiah, S. (2022) Electrospun polyacrylonitrile-Moringa Olifera based nanofibrous bio-sorbent for remediation of Congo red dye. J. Environ. Manag.; 317:115294. doi: 10.1016/j.jenvman.2022.115294.

Nelima, D., Wambu, E. W., & Kituyi, J. L. (2023). Fluoride distribution in selected foodstuffs from Nakuru County, Kenya, and the risk factors for its human overexposure. *Scientific Reports, 13*, Article 15295. https://doi.org/10.1038/s41598-023-41601-8

Nguyen, T. T., Le, H. N., & Bui, Q. T. (2024). Effect of competing anions and pH on fluoride removal by biosorbents: Thermodynamic and kinetic insights. *Journal of Water Chemistry and Technology, 46*(1), 1–11. https://doi.org/10.3103/S1063455X24010012

Nguyen, T. T., Le, H. T., & Vu, M. T. (2024). Competitive ion effects and pH dependence in fluoride adsorption: Implications for natural groundwater treatment. *Environmental Research, 237*, 117906. https://doi.org/10.1016/j.envres.2023.117906

Nguyen, T. T., Lee, S. H., & Kim, S. J. (2024). Ion exchange and surface complexation in defluoridation: Competing anion effects and real groundwater implications. *Water Research, 242*, 120234. https://doi.org/10.1016/j.watres.2024.120234

Nguyen, T. T., Lee, S. H., & Kim, S. J. (2024). Ion exchange processes for anion removal in drinking water treatment: Principles and limitations. *Water Research, 242*, 120234. https://doi.org/10.1016/j.watres.2024.120234

Nguyen, T., Hoang, P., & Tran, D. (2024). Calcium-spiked biosorbents for efficient fluoride removal from drinking water. *Journal of Environmental Management*, 350, 119550. https://doi.org/10.1016/j.jenvman.2024.119550

Nisar, S., & Koul, M. (2021). Natural coagulants in water purification: *Mechanisms and applications*. *Applied Water Science, 11*, 156. https://doi.org/10.1007/s13201-021-01371-5

Ochieng, D. E., Otieno, F. A. O., & Ogada, J. O. (2018). Effect of particle size on fluoride adsorption using *Moringa oleifera* seed powder. *Environmental Monitoring and Assessment, 190*(8), 490. https://doi.org/10.1007/s10661-018-6859-2

Ogundele, T., Adebayo, A., & Fasina, S. O. (2023). Sustainable fluoride removal technologies for rural water supplies: A global review. *Journal of Environmental Management, 326,* 116757. https://doi.org/10.1016/j.jenvman.2022.116757

Oluwasanya, G. O., Adegbite, A., & Fashola, A. (2023). Biosorption of heavy metals and fluoride using Moringa oleifera: A sustainable approach. *Environmental Sustainability*, 6, 210–225. https://doi.org/10.1007/s42398-023-00235-2

Onipe, O. O., Mushi, A., & Lema, J. (2020). Endemic fluorosis and groundwater dependence in Tanzania's Rift Valley. *Environmental Monitoring and Assessment, 192*, 339.

Onipe, O. O., Mushi, A., & Lema, J. (2020). Endemic fluorosis and groundwater-surface water interactions in Tanzania's Rift Valley. *Environmental Monitoring and Assessment, 192*, 339. https://doi.org/10.1007/s10661-020-8049-3

Onipe, T., Afolabi, B., & Dada, E. (2020). Environmental considerations in the disposal of spent biosorbents used for water defluoridation. *Environmental Challenges, 1*, 100003. https://doi.org/10.1016/j.envc.2020.100003

Ontumbi, G., Munyao, T., & Ucakuwun, E. (2020). *Stratigraphy and fluoride levels variation in borehole water: A case of River Njoro Catchment*. *Open Access Library Journal, 7*(1), 1–12. https://doi.org/10.4236/oalib.1106388

Ouedraogo, I., Sawadogo, A., & Traoré, B. (2024). Fluoride mobilization in groundwater and surface water systems: A geochemical perspective. *Hydrological Processes, 38*(3), e15013. https://doi.org/10.1002/hyp.15013

Owodunni, A. A., & Ismail, S. (2021). Comparative evaluation of chemical and plant-based coagulants for water treatment. *Journal of Water Process Engineering, 42*, 102120. https://doi.org/10.1016/j.jwpe.2021.102120

Patel, R., & Yadav, R. (2022). Optimization of fluoride adsorption parameters using response surface with modified zeolites. *Environmental Technology & Innovation, 28*, 102651. https://doi.org/10.1016/j.eti.2022.102651

Pathak, P. D., & Rathore, N. S. (2016). Practical implications of high-dosage adsorbent use for fluoride removal. *Journal of Water Supply: Research and Technology—AQUA, 65*(5), 369–377. https://doi.org/10.2166/aqua.2016.053

Perez, L., Gonzalez, M., & Alvarez, F. (2023). Community-friendly water defluoridation strategies: A review of low-cost biosorbents. *International Journal of Water Resources, 15*(2), 88–102. https://doi.org/10.1080/ijwr.2023.158

Pezeshk, S., Lee, S., & Kim, J. (2023). Advances in membrane-based fluoride removal: Challenges and future directions. *Desalination, 553*, 116494. https://doi.org/10.1016/j.desal.2023.116494

Pillai, P., & Thombre, S. (2024). Coagulation and precipitation methods for defluoridation: Efficiency and sustainability considerations. *Journal of Water Process Engineering, 56*, 104254. https://doi.org/10.1016/j.jwpe.2024.104254

Prabhu, P., Kumar, R., & Sharma, P. (2023). Natural occurrence of fluoride in groundwater: Sources and health effects. *Environmental Geochemistry and Health*, 45, 879–895. https://doi.org/10.1007/s10653-022-01238-1

Prabhu, S. M., Joseph, R., & Thomas, R. (2023). Evaluation of biosorption–precipitation mechanisms for fluoride removal using calcium-enriched natural adsorbents. *Journal of Environmental Management, 341*, 118065. https://doi.org/10.1016/j.jenvman.2023.118065

Prabhu, S. M., Joseph, R., & Thomas, R. (2023). Fluoride ion exchange on functionalized biomass: Batch and column studies. *Journal of Environmental Management, 341*, 118065. https://doi.org/10.1016/j.jenvman.2023.118065

Prabhu, S., Meena, R., & Singh, R. (2023). Natural sources of fluoride in groundwater: Geochemical processes and public health implications. *Environmental Geoscience Reviews, 12*(3), 56–72.

Raj, G., Chauhan, P. S., & Jain, S. (2023). Rice husk biochar removal of fluoride from contaminated water. *Journal of Environmental Management, 329*, 123456. https://doi.org/10.1016/j.jenvman.2023.118222

Rajak, P., Singh, A., & Bhatnagar, R. (2023). Health impacts of chronic fluoride exposure: Emerging evidence. *Ecotoxicology and Environmental Safety*, 256, 114902. https://doi.org/10.1016/j.ecoenv.2023.114902

Raji, S., Bhatnagar, A., & Kumar, P. S. (2023). Biosorption for sustainable water treatment: Kinetics, isotherms, and mechanisms. *Environmental Research, 222*, 115300. https://doi.org/10.1016/j.envres.2023.115300

Raji, S., Kumari, M., & Gupta, S. (2023). Adsorption isotherms and kinetics in biosorption of fluoride: A critical review. *Journal of Environmental Chemical Engineering, 11*(4), 109765. https://doi.org/10.1016/j.jece.2023.109765

Rathi, S., Banerjee, S., & Ray, A. (2024). Reverse osmosis and nanofiltration in fluoride removal: Energy and environmental trade-offs. *Separation and Purification Reviews, 53*(1), 1–23. https://doi.org/10.1080/15422119.2023.2164742

Saleem, M., Chen, D., & Li, Y. (2020). Protein-based natural coagulants for water and wastewater treatment: A critical review. *Journal of Cleaner Production, 258*, 120584. https://doi.org/10.1016/j.jclepro.2020.120584

Sarath, K. V., Shaji, E., Santosh, M., Krishnaprasad, P. K., & Arya, B. K. (2023). Fluoride contamination in groundwater: A global review of the status, processes, challenges, and remedial measures. *Geoscience Frontiers*, *15*(4), Article 101734. https://doi.org/10.1016/j.gsf.2023.101734

Sari, A., & Tuzen, M. (2020). Column studies for fluoride adsorption: Influence of dosage and particle size in continuous flow systems. *Journal of Environmental Chemical Engineering, 8*(4), 103981. https://doi.org/10.1016/j.jece.2020.103981

Sharma, S., Bhattacharya, S., & Singh, R. (2017). Edible plant mucilage as a low-cost biosorbent for water purification. *Journal of Environmental Management, 203*, 464–472. https://doi.org/10.1016/j.jenvman.2017.08.014

Shin, H. (2020). Ion-exchange resins in drinking water defluoridation: Mechanisms and regeneration strategies. *Journal of Water Supply: Research and Technology—AQUA, 69*(4), 354–366. https://doi.org/10.2166/aqua.2020.024

Shrestha, R. (2021). Enhancement of fluoride adsorption using calcium-impregnated plant-based biosorbents: Performance and modeling. *Journal of Environmental Management, 290*, 112587. https://doi.org/10.1016/j.jenvman.2021.112587

Singh, N., Kumari, P., & Tripathi, P. (2022). Optimization of fluoride adsorption considering particle size and dosage interaction effects. *Chemosphere, 301*, 134681. https://doi.org/10.1016/j.chemosphere.2022.134681

Sivashankar, R., Sathishkumar, P., & Somasundaram, R. (2022). Biosorption for water defluoridation: Fundamentals and applications. *Chemosphere, 293*, 133510. https://doi.org/10.1016/j.chemosphere.2021.133510

Skaf, D., Abdul, A., & Hasan, S. (2021). Oil removal to enhance the coagulant efficiency of *Moringa oleifera* for water treatment. *Journal of Water Process Engineering, 40*, 101907. https://doi.org/10.1016/j.jwpe.2021.101907

Smith, J., Brown, K., & Wang, H. (2020). Environmental challenges in fluoride removal technologies. *Environmental Engineering Science, 37*(4), 255–264. https://doi.org/10.1089/ees.2020.0098

Smith, J., Ochieng, D., & Patel, S. (2025). Field-scale evaluation of *Moringa oleifera* biosorption for defluoridation. Journal of Water Resources and Protection, 17(1), 45–63. https://doi.org/10.4236/jwarp.2025.171004

Solanki, H., Kumar, A., & Sharma, M. (2022). Global assessment of fluoride contamination and associated health risks. *Environmental Pollution Reports, 18*, 102345.

Sunkari, E. D., Mensah, F., & Agyeman, F. O. (2022). Integrated approaches to groundwater fluoride contamination assessment: Implications for defluoridation strategies. *Groundwater, 60*(4), 451–466. https://doi.org/10.1111/gwat.13215

Taiwo, A. M., Akinlabi, E. T., & Olowolafe, E. A. (2020). Characterization of Moringa seed proteins for application in natural water treatment. *Environmental Technology & Innovation, 20*, 101142. https://doi.org/10.1016/j.eti.2020.101142

Taiwo, A. M., Akinlabi, E. T., & Olowolafe, E. A. (2020). Sustainable approaches for fluoride removal in low-income settings: A biosorption perspective. *Environmental Technology & Innovation, 20*, 101162. https://doi.org/10.1016/j.eti.2020.101162

Taiwo, A. M., Kolawole, T. A., & Afolabi, T. A. (2020). Influence of ionic strength and competing anions on biosorption processes for drinking water treatment. *Environmental Technology & Innovation, 20*, 101099. https://doi.org/10.1016/j.eti.2020.101099

Taiwo, A., Akinola, M., & Adedoyin, A. (2020). *Moringa oleifera* in water treatment: A review of applications and mechanisms. *Journal of Water Process Engineering*, 37, 101414. https://doi.org/10.1016/j.jwpe.2020.101414

Taiwo, O. S., Akinlabi, A. K., & Oladipo, A. A. (2020). Mechanistic study of biosorptive fluoride removal using chemically modified plant-based adsorbents. *Environmental Nanotechnology, Monitoring & Management, 14*, 100350. https://doi.org/10.1016/j.enmm.2020.100350

Taiwo, O. S., Akinlabi, A. K., & Oladipo, A. A. (2020). Synergistic ion exchange and precipitation in calcium-modified biosorbents for fluoride removal. *Environmental Nanotechnology, Monitoring & Management*, *14*, 100350. https://doi.org/10.1016/j.enmm.2020.100350

Taiwo, O., Oladipo, B., & Hassan, M. (2020). Fluoride removal using natural biosorbents: Equilibrium, kinetic, and thermodynamic evaluations. *Groundwater for Sustainable Development*, *11*, 100416. https://doi.org/10.1016/j.gsd.2020.100416

Tee, S. Y., Lim, J. W., & Lee, L. Y. (2022). Impact of biosorbent dosage and agglomeration on fluoride removal efficiency. *Journal of Environmental Management*, *304*, 114245. https://doi.org/10.1016/j.jenvman.2021.114245

Tolkou, A. K., Mitrakas, M., & Zouboulis, A. I. (2021). Novel biosorbent materials for fluoride removal from groundwater: Mechanisms and performance evaluation. *Journal of Hazardous Materials*, *416*, 126145. https://doi.org/10.1016/j.jhazmat.2021.126145

Tolkou, A. K., Mitrakas, M., & Zouboulis, A. I. (2021). Sustainable defluoridation: Mechanistic insights and field-scale challenges for plant-based biosorbents. *Journal of Hazardous Materials*, *416*, 126145. https://doi.org/10.1016/j.jhazmat.2021.126145

Tolkou, A., *et al*. (2021). (Title employing adsorption methods and technology evaluation). In *A review of fluoride removal from groundwater*. Adsorption methods.

Tolkou, A., Mitrakas, M., & Zouboulis, A. (2021). Adsorption processes for fluoride removal in drinking water treatment: A comprehensive review.

Chemosphere, *272*, 129624. https://doi.org/10.1016/j.chemosphere.2021.129624

Tolkou, A., Zouboulis, A., & Mitrakas, M. (2021). Defluoridation of drinking water using ion exchange and precipitation methods: A comparative review. *Water*, 13(7), 934. https://doi.org/10.3390/w13070934

Turner, R., Ali, S., & Wang, L. (2025). Long-term fluoride exposure and systemic organ damage: Mechanistic insights. *Environmental Toxicology and Pharmacology*, 97, 104088. https://doi.org/10.1016/j.etap.2025.104088

Wambu, E. W., Muthakia, G. K., & Githinji, N. (2022). Groundwater fluoride distribution and public health risk in Kenya's Rift Valley. *Environmental Monitoring and Assessment, 194*, 786. https://doi.org/10.1007/s10661-022-9804-5

Wambu, E. W., Onyari, J. M., & Muthakia, G. K. (2022). Adsorption kinetics and equilibrium studies of fluoride on calcium-modified *Moringa oleifera* biosorbents. *Journal of Water Reuse and Desalination, 12*(2), 154–166. https://doi.org/10.2166/wrd.2022.021

Wambu, E. W., Onyari, J. M., & Muthakia, G. K. (2022). Kinetics and isotherms of fluoride adsorption onto calcium-modified biosorbents. *Environmental Technology & Innovation, 28*, 102787. **https://doi.org/10.1016/j.eti.2022.1methods**

Wan, C., Wong, K., & Yeung, H. (2020). Competitive adsorption of fluoride and co-existing anions on modified alumina: Environmental implications. *Journal of Environmental Chemical Engineering, 8*(2), 103666. https://doi.org/10.1016/j.jece.2020.103666

Wan, X., Chen, Y., & Li, D. (2023). Reverse osmosis and nanofiltration for fluoride removal: Performance and limitations. *Desalination*, 545, 116143. https://doi.org/10.1016/j.desal.2023.116143

Wang, J., Liu, Q., & Xu, Z. (2023). Multi-ion interaction and site competition during adsorption of fluoride from groundwater. *Separation and Purification Technology, 310*, 123133. https://doi.org/10.1016/j.seppur.2023.123133

Wang, Y., Zhang, L., & Liu, P. (2023). Multi-ionic interaction effects on fluoride adsorption by calcium-functionalized biosorbents. *Chemosphere, 322*, 138288. https://doi.org/10.1016/j.chemosphere.2023.138288.

Waugh, D. T. (2019). Fluoride interactions with proteins and enzymes: Health implications. *Critical Reviews in Toxicology*, 49(4), 272–291. https://doi.org/10.1080/10408444.2019.1579822

World Health Organization. (2017). *Guidelines for drinking-water quality, 4th edition incorporating the 1st addendum*. WHO.

World Health Organization. (2024). *Guidelines for drinking-water quality* (5th ed.). World Health Organization.

Xiang, J. (2024). Industrial waste management and fluoride contamination in water sources: Emerging case studies. *Journal of Water and Health, 22*(1), 89–104.

Yadav, A., Singh, P., & Kumar, V. (2021). Indigenous plant-based biosorbents for fluoride removal from drinking water: A review. *Environmental Nanotechnology, Monitoring & Management, 15*, 100412. https://doi.org/10.1016/j.enmm.2020.100412

Yadav, K. K., Gupta, N., & Kumar, V. (2021). Application of *Moringa oleifera* seed powder for fluoride removal: A review. *Applied Water Science, 11*(2), 41. https://doi.org/10.1007/s13201-021-01352-1

Yadav, S. K., Patel, N., & Rani, P. (2023). Global fluoride exposure: Distribution, health effects, and mitigation strategies. *Environmental Research, 232*, 115305.

Yousef, S., Ahmed, M., & Ibrahim, S. (2024). Comparative analysis of isotherm and kinetic models in fluoride biosorption. *Environmental Nanotechnology, Monitoring & Management, 22*, 101211. https://doi.org/10.1016/j.enmm.2024.101211

Zada, S., Khan, M. A., & Rehman, Z. U. (2024). Fluoride biosorption using microbial biomass: Optimization of dosage and particle size. *Biochemical Engineering Journal, 199*, 108286. https://doi.org/10.1016/j.bej.2024.108286

Zhao, X., Fang, L., & Jiang, C. (2022). Adsorption kinetics and mass transfer of fluoride ions in porous bioadsorbents: Lab to field implications. *Journal of Environmental Chemical Engineering*, *10*(5), 107299. https://doi.org/10.1016/j.jece.2022.107299

Zhao, Y., Liu, F., & Zhang, Y. (2022). Adsorption kinetics and thermodynamic studies of fluoride removal using biochar composites. *Journal of Environmental Management, 306*, 114488. https://doi.org/10.1016/j.jenvman.2022.114488

Zhao, Y., Liu, X., & Li, J. (2022). Thermodynamic and kinetic studies on fluoride adsorption: Implications for practical water treatment systems. *Separation and Purification Technology*, *293*, 121087. https://doi.org/10.1016/j.seppur.2022.121087

Zhao, Y., Liu, X., & Li, J. (2022). Thermodynamic assessment and kinetic modeling of fluoride removal from drinking water using bio-adsorbents. *Separation and Purification Technology, 293*, 121087. https://doi.org/10.1016/j.seppur.2022.121087

APPENDICES

Appendix I

Standards

Conc.	0.1	1	3	5	7	10	20
Readings(mv)	-277.9	-316.4	-346.4	-356	-367.5	-376.2	-394.6
Log Conc.	-1	0	0.4771	0.6989	0.8450	1	1.3010

Appendix II

Biosorption of Fluoride using Non-spiked *M.oleifera* seed powder

i. Influence of biosorbent dose at constant mesh size 40, constant temp 298K, for 60 min, at a pH 7 and solution concentration of 10ppm

Dose(g)	0.1g	0.5g	1g
Readings (mv)	0.6670	0.7069	0.6351

ii. Influence of particle size at constant particle dose of 0.5g, constant temp 298K, for 60min, at a pH 7 and solution concentration of 10ppm

Particle size(mesh)	20	40	60
Readings (mv)	0.6494	0.6073	0.6641

iii. Influence of time at constant particle size 40mesh, constant temp 298K, constant dose of 0.5g, at a pH 7 and solution concentration of 10ppm

Time (min)	20	40	60
Readings(mv)	0.7006	1.1351	1.3693

iv. Influence of pH at constant particle size 40mesh, constant temp 298K, for 60min, biosorbent dose of 0.5g and solution concentration of 10ppm

pH	3	7	11
Readings (mv)	0.6944	1.2806	1.1351

v. Influence of temperature at constant particle size 40mesh, constant pH 7, for 60min, biosorbent dose of 0.5g and solution concentration of 10ppm

Temp (K)	273	313	353
Readings (mv)	0.6821	0.9795	27.9273

vi. Influence of concentration of solution at constant particle size 40 mesh, constant pH 7, for 60min, biosorbent dose of 0.5g and temperature of 298K

Conc. (ppm)	1	10	20
Readings (mv)	0.6408	8.9798	23.9921

Appendix III

Initial concentration readings

Conc. (ppm)	1	10	20
Readings (mv)	2.5938	9.7317	33.5405

Appendix IV

Biosorption of Fluoride using $CaCl_2$–spiked *M.oleifera* seed powder

i. Influence of biosorbent dose of 0.5g at mesh size 40 , constant temp 298K, for 60 min, at a pH 7 and solution concentration of 10ppm

Dose(g)	0.1	0.5	1
Readings (mv)	2.9924	2.9791	3.2141

ii. Influence of particle size at constant particle dose of 0.5g, constant temp 298K, for 60min, at a pH 7 and solution concentration of 10ppm

Particle size(mesh)	20	40	60
Readings(mv)	3.0875215	2.836286	2.786057

iii. Influence of time at constant particle size 40mesh, constant temp 298K, constant dose of 0.5g, at a pH 7 and solution concentration of 10ppm

Time (min)	20	40	60
Readings(mv)	3.06006	18.6822	16.0498
	2.82364	22.4372	20.8895
	2.76127	18.7659	18.1882

iv. Influence of pH at constant particle size 40mesh, constant temp 298K, for 60min, biosorbent dose of 0.5g and solution concentration of 10ppm

Ph	3	7	11
	3.0737603	3.3162709	3.0737603

v. Influence of temperature at constant particle size 40mesh, constant pH 7, for 60min, biosorbent dose of 1g and solution concentration of 10ppm

Temp (K)	**298**	**313**	**353**
	3.3162709	18.107146	10.6998
	2.848984	18.10715	10.78475
	2.773639	22.43727	10.45274

vi. Influence of initial concentration of solution at constant particle size 60 mesh, constant pH 7, for 60min, biosorbent dose of 0.5g and temperature of 298K.

Initial Conc.	1	10	20
Readings(mv)	2.786057	28.43086	3.0328435
	2.836286	23.88526	3.101344
	2.736718	22.63862	2.952637

Appendix V

Initial Aqueous Sodium Fluoride Concentration

1ppm	14.809827
10ppm	38.179479
20ppm	97.550611

Appendix VI

Standards curve

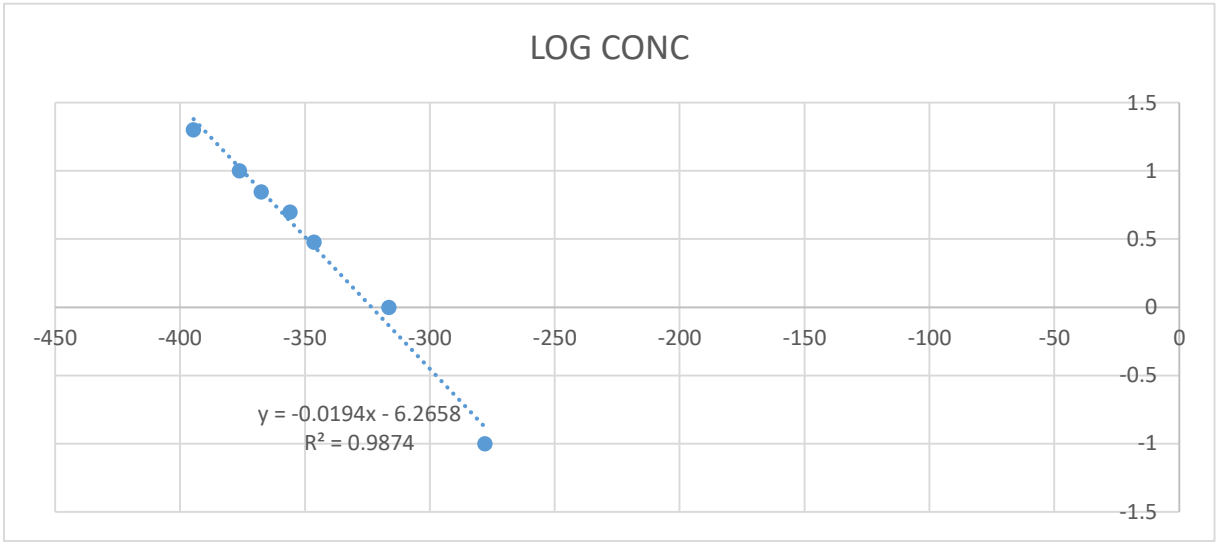

Appendix VII

Plagiarism Report

University of Eldoret

University of Eldoret
Certificate of Plagiarism Check for Thesis

Author Name	Geoffrey Chavaregi SSCI/CHE/P/001/20
Course of Study	Type here...
Name of Guide	Type here...
Department	Type here...
Acceptable Maximum Limit	Type here...
Submitted By	similarity@uoeld.ac.ke
Paper Title	AQUEOUS FLUORIDE BIOSORPTION USING CALCIUM-SPIKED AND NON- SPIKED Moringa oleifera SEED POWDER: INFLUENCE OF DOSAGE, PARTICLE SIZE and PROCESS PARAMETERS
Similarity	12%
Paper ID	4638941
Total Pages	210
Submission Date	2025-11-07 11:47:44

Signature of Student

Signature of Guide

University of Eldoret LIBRARIAN NOV 2025 P. O. Box 1125, ELDORET - 30100

Head of the Department

University Librarian

Director of Post Graduate Studies

* This report has been generated by DrillBit Anti-Plagiarism Software